

Title	INTERACTIONS BETWEEN MULTIPLE OSCILLATORS IN THE BIOLOGICAL RHYTHMS
Author(s)	Kawato, Mitsuo
Citation	大阪大学, 1981, 博士論文
Version Type	VoR
URL	https://hdl.handle.net/11094/2742
rights	
Note	

Osaka University Knowledge Archive : OUKA

<https://ir.library.osaka-u.ac.jp/>

Osaka University

INTERACTIONS BETWEEN MULTIPLE OSCILLATORS
IN THE BIOLOGICAL RHYTHMS

Mitsuo KAWATO

INTERACTIONS BETWEEN MULTIPLE OSCILLATORS
IN THE BIOLOGICAL RHYTHMS

A Thesis

Submitted to the Faculty
of Engineering Science

of

Osaka University

by

Mitsuo KAWATO

February 1980

ACKNOWLEDGMENTS

I wish to express my appreciation to Prof. R. Suzuki for his guidance during my research. I wish to acknowledge and extend my sincere appreciation to the department of Biophysical Engineering for the support given me in the pursuit of the thesis. They all helped me to finish my writing and keep my sanity. I should like to express my gratitude to Dr. S. Sato, Dr. K. Kobayashi and Dr. O. Sueda for many helpful comments. I am more than grateful to two, great American scientists, Pr. C. S. Pittendrigh and Pr. A. T. Winfree for their enthusiastic encouragement and constructive criticism of the biological formulation in Chapters 1 and 2.

TABLE OF CONTENTS

CHAPTER

0 - INTRODUCTION

1 - TRANSIENT AND STEADY STATE PHASE RESPONSE CURVES OF BIOLOGICAL OSCILLATORS

- 1.1 Introduction
- 1.2 Definition of Phase Response Curves
- 1.3 Mathematical Formulation of PRC and PTC
- 1.4 Topological Properties of PRC and PTC
- 1.5 Applications of Theoretical Results to Neurobiology
- 1.6 Drosophila's PTC and Inner Structures of its Circadian Oscillator
- 1.7 Two-oscillator Model for Drosophila's PTC
- 1.8 Notes for Phase Response Curves

2 - TWO COUPLED NEURAL OSCILLATORS AS A MODEL OF THE CIRCADIAN PACEMAKER

- 2.1 Introduction
- 2.2 Assumptions and Descriptions of the General Model
- 2.3 Analysis of the General Two-oscillator model
- 2.4 Two coupled Neural Oscillator Model
- 2.5 Primary and Secondary Bifurcations of the Neural Model
- 2.6 Discussion and Conclusions

3 - SYNERGISM AND ANTAGONISM OF NEURONS CAUSED BY AN ELECTRICAL SYNAPSE

- 3.1 Introduction
- 3.2 A General Model System consisting of Two Neurons electrically coupled
- 3.3 Stability of a Perfect In-phase Solution and the Existence of an Anti-phase Solution
- 3.4 Two BVP Model Neurons coupled by Diffusion
- 3.5 Primary Bifurcation
- 3.6 Computation of Secondary Bifurcation by Perturbation Method
- 3.7 Bifurcation Diagram of Two BVP Neurons
- 3.8 Discussions

BIBLIOGRAPHY

CHAPTER 0
INTRODUCTION

The failure of statistical-mechanical ideas to make much headway in biology has some bearing on the notions of reductionism which are prevalent in biology. For statistical mechanics is one of the rare examples of a successful reductionist theory in physics; it allows us to explain phenomena at a higher dynamical level (the gas level, say) in terms of dynamical events at a lower level (the molecular level). The current postulate of reductionism in biology is that all biological phenomena are ultimately explainable in molecular terms, which means in particular that we must be able to pass both upward and downward from any biological level to any other biological level. Statistical mechanics allows such a transition in physics between a particular pair of levels. The lack of success of these studies (e.g. between the molecular and the epigenetic level; between the neural and behavioral level; between the population level and what may be called the biotic level) may indicate that the implementation of reductionism between pairs of biological levels is, at the very least, a far more challenging problem than the more sanguine postulants of reductionism has believed (Rosen, 1970). Many important aspects of biological activity are certain to be refractory to reductionist techniques, and must be treated holistically and relationally (Rosen, 1968).

In this thesis we develop a phenomenological and holistic approach to the problem of biological rhythms. In some sense it is similar to thermodynamics rather than statistical mechanics. We lean on topology and dynamical system theory, which has been developed dramatically in these two decades.

There are many biological oscillators at various biological levels. Circadian oscillators, biochemical oscillators, pacemaker neurons, bursting neurons and the neural networks which discharge periodic outputs are used as

examples. We do not try to study biochemical or molecular mechanism of these oscillators. Rather we examine interactions between multiple oscillators, hierarchical structures of oscillators and the synchronization effect of external forces. Interactions between biological oscillators can be classified into three categories according to their temporal structure. Each of three is studied in the following chapter.

Chapter 1 (Instantaneous Interaction). The duration of interaction is much shorter than the periods of oscillators. In other words, an internal state variable of the oscillator is chopped into the output by a very narrow window of the amplitude. Interaction through chemical synapses is an example.

Chapter 3 (Diffusion Interaction). Interactions are diffusions of some internal state variables of the oscillator. Temporal structure of interactions is uniform. Interaction through electrical synapses is an example.

Chapter 2 (Intermediate Interaction). In chapter 2 we examine the interaction which is neither instantaneous nor diffusion. Almost all interactions in biology may belong to this category.

CHAPTER 1

TRANSIENT AND STEADY STATE PHASE RESPONSE CURVES OF BIOLOGICAL OSCILLATORS

1. 1. Introduction

The analysis of phase shifts resulting from discrete perturbation of biological rhythms was developed and exploited by Pittendrigh and Bruce (1957) and by Perkel and co-workers (1964). By these methods, they achieved important insights into the entrainment behavior of circadian and neural rhythms, respectively. A phase response curve is a plot of a phase shift against the phase when the perturbation is applied. Phase response curves have been measured on various biological oscillators (e.g. circadian pacemakers, biochemical oscillators (Winfree, 1975), pacemaking neurons, bursting neurons (Pinsker, 1977) and human finger tapping neural networks (Yamanishi, Kawato and Suzuki, 1979)).

There are two kinds of phase response curves according to as we measure the phase shifts immediately or long after the perturbation. The former is the first transient phase response curve and the latter is the steady state phase response curve. The steady state phase response curves are utilized for studying entrainment behavior of biological oscillators by external forces or studying synchronization of the oscillators which interact with each other. Winfree (1970) pointed out that two different types of steady state phase response curves (i.e. Type 0 curve and Type 1 curve) were measured in the phase resetting experiments of circadian rhythms. Especially, he got the Type 0 curve in response to strong perturbation and got the Type 1 curve in response to weak perturbation for the Drosophila eclosion rhythm. Moreover he found that the medium perturbation which was applied at an appropriate phase stopped the oscillation. Winfree (1967, 1970, 1973a) and Pavlidis (1973) defined the phase response curves mathematically and explained

the two types of steady state phase response curves in a simple, special two-dimensional dynamical system. We define the phase response curves in a general way, and explain the difference between the two types by the homotopy theory in sections 1.2 and 1.3 (Kawato and Suzuki, 1978). We also prove that if a Type 0 curve is obtained at a certain magnitude of perturbation, there exists at least one lower magnitude for which the phase response curve is not defined.

By the way, can we examine the inner structure of a biological oscillator by measurement of its phase response curve? If it is possible, the quite phenomenological phase resetting experiment can tell us about inner structures. The steady state phase response curves are continuous and have naive properties. On the other hand, the transient phase response curves are sometimes discontinuous and have complex properties. So, the steady state phase response curves are easier to study than the transient phase response curves. We examine whether or not we can obtain some informations or restrictions about the model equations which describe a biological oscillator using only its steady state and transient phase response curves. For an arbitrary limit cycle oscillator we can obtain an arbitrary steady state phase response curve by choosing a perturbed cycle appropriately. So, the steady state phase response curve alone does not determine the describing equations although every part of the phase response curve can be informative about stages of the cycle. We must compare both kinds of phase response curves to get some information about inner structures. In sections 1.6 and 1.7 we study the phase response curves of Drosophila which were measured by Pittendrigh & Minis (1964) and prove that its circadian oscillator is not a single oscillator with two variables. Moreover we show that a two limit cycle oscillator model can simulate the Drosophila's phase response curves (Kawato, 1981a).

1. 2 Definition of phase response curves

Let us consider the biological oscillator which periodically causes some reference event (e.g. emergence of fruitflies Drosophila, spikes of pace-making neurons) with a period τ (see Fig. 1). At the time of reference event we set the phase θ zero. In the phase resetting experiment we apply the perturbation, which lasts for duration T and ends at the phase $\theta=\phi$ ($T<\tau$). This phase ϕ is called an old phase. In consequence of the perturbation, the i -th reference event after the perturbation advances or delays compared with the i -th reference event in the unperturbed case. We express this delay or advance by phase and call it the i -th phase shift, $\Delta\phi_i$, where $\Delta\phi_i$ is positive for the phase advance. If the oscillator is stable, its period returns to τ after a long duration. So, $\Delta\phi_i$ has its limit $\Delta\phi=\lim_{i\rightarrow\infty} \Delta\phi_i$. We call $\Delta\phi$ a phase shift. Both $\Delta\phi_i$ and $\Delta\phi$ depend on the old phase ϕ . The i -th phase shift and the phase shift as functions of the old phase, $\Delta\phi_i(\phi)$ and $\Delta\phi(\phi)$, are called the i -th transient phase response curve (transient PRC) and the steady state phase response curve (steady state PRC) respectively. Next, we define the i -th transient phase transition curve (transient PTC), $\phi_i^*(\phi)$, and the steady state phase transition curve (steady state PTC), $\phi'(\phi)$, as follows.

$$\begin{aligned}\phi_i^*(\phi) &= \phi + \Delta\phi_i(\phi) && (\text{mod } 1) \\ \phi'(\phi) &= \phi + \Delta\phi(\phi) && (\text{mod } 1)\end{aligned}\tag{1}$$

ϕ' is the "new" phase caused by an application of the perturbation at the old phase ϕ .

CONTROL SYSTEM

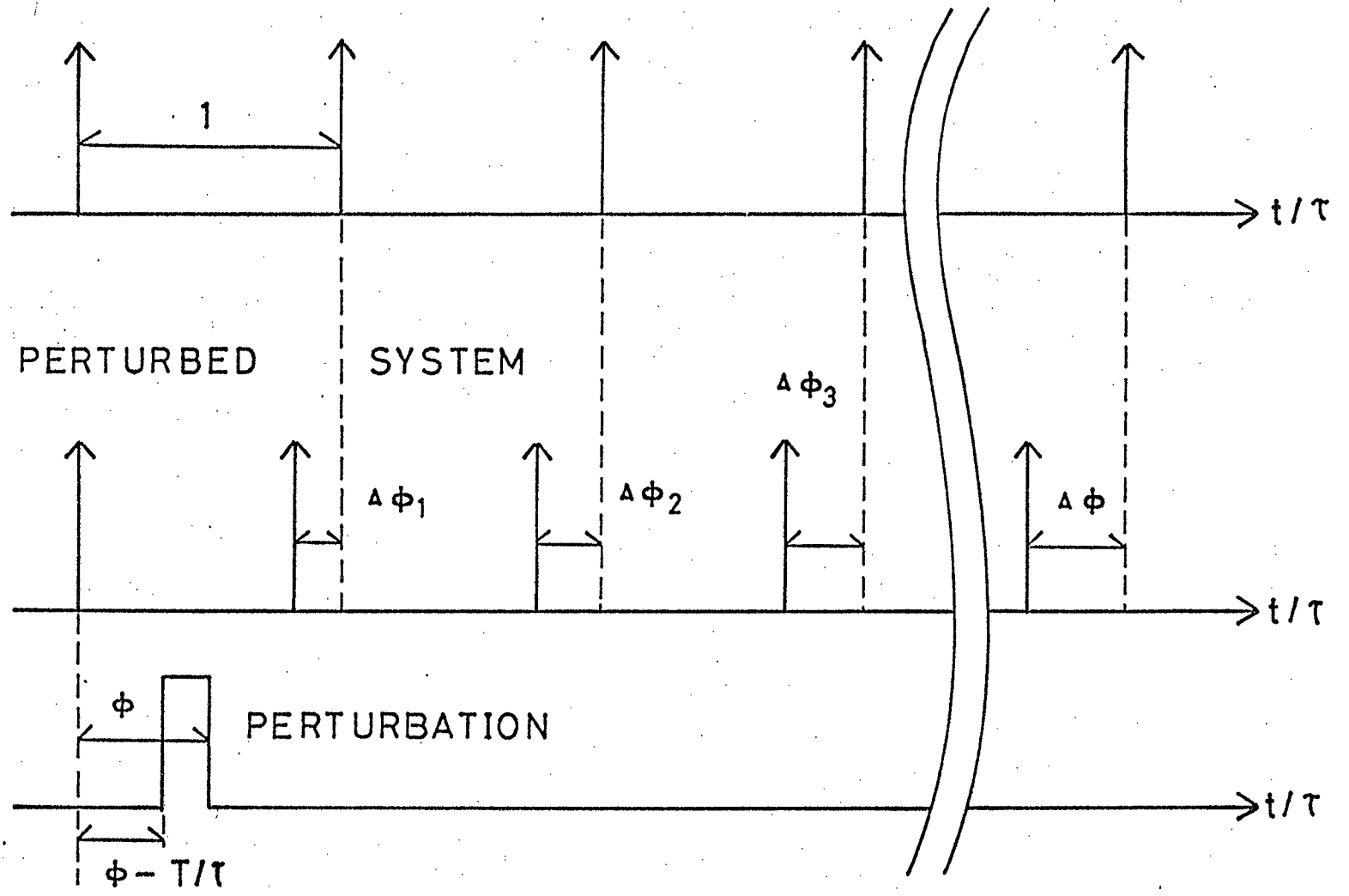


Fig. 1

1.3 Mathematical formulation of PRC and PTC

We redefine PRC and PTC within the framework of dynamical system theory. Our formulation is an extension of those by Winfree (1967, 1970, 1973a) and Pavlidis (1973). We assume that the oscillator in its free running state can be described by the following system of ordinary differential equations (2) on a smooth n -dimensional manifold M or be described by its equivalent flow $\Psi_0: M \times \mathbb{R} \rightarrow M$.

$$\frac{dx}{dt} = F(x, 0) \quad (2) \quad ; \Psi_0(x, t),$$

where x is the n -dimensional vector which represents the inner state of the oscillator. We assume that the oscillation is stable against noise and perturbation. Moreover we assume the structural stability of the system (2). So, the flow Ψ_0 is assumed to have an elementary (hyperbolic) stable limit cycle γ with a period τ . Let θ denote the Poincaré map of the limit cycle γ . The eigenvalues of $D\theta_x$, first partial derivatives of θ at x on γ are often called the characteristic multipliers of γ . One says that γ is an elementary (or hyperbolic) limit cycle if there are no characteristic multipliers of absolute value one.

Next, the oscillator under the perturbation of magnitude μ is described by the following equation (3) or its equivalent flow $\Psi_\mu: M \times \mathbb{R} \rightarrow M$.

$$\frac{dx}{dt} = F(x, \mu) \quad (3) \quad ; \Psi_\mu(x, t),$$

where μ is magnitude of the perturbation. We assume that $F(x, \mu)$ satisfies appropriate regularity conditions with respect to (x, μ) . Note that (3) coincides with (2) when μ is zero. We assume that the perturbation lasts for

duration T and ends at the old phase ϕ .

Definition 1. 1. If S is an arbitrary subset of M , then the stable set of S , denoted $W^S(S)$, is defined as follows.

$$W^S(S) = \{x \in M; \lim_{t \rightarrow \infty} \text{dis}(\Psi_0(x, t), \Psi_0(S, t)) = 0\},$$

where $\Psi_0(S, t) = \{\Psi_0(y, t); y \in S\}$. The distance dis is the distance function for some metric on M . If the stable set is also a manifold, it is called a stable manifold.

Definition 1. 2. Let a phase map $\theta: \gamma \rightarrow S^1$ be a homeomorphism such that for each $x \in \gamma$, $\theta(\Psi_0(x, t)) = \theta(x) + t/\tau \pmod{1}$, where S^1 is a circle of length 1. We set $\theta = 0$ at the time of the reference event.

The eventual phase map $\theta_e: W^S(\gamma) \rightarrow S^1$ can now be defined as follows.

Definition 1. 3. For an arbitrary $y \in W^S(\gamma)$, $\theta_e(y) = \theta(x)$ for x such that $x \in \gamma$ and $y \in W^S(x)$. That is $\lim_{t \rightarrow \infty} \text{dis}(\Psi_0(y, t), \Psi_0(x, t)) = 0$.

θ_e is a natural extension of θ . The existence of θ_e is not trivial. It exists because γ is an elementary stable limit cycle. See Hirsh and Smale (1974) for the proof of existence. From the definition, for arbitrary $x \in \gamma$, $W^S(x) = \{y \in M; \theta_e(y) = \theta(x)\}$. The following theorem regarding the stable set of each point x on γ is well known (Guckenheimer, 1975). The stable manifold of each point x on γ was originally called "isochron" by Winfree (1967).

Theorem 1. 0. The stable set $W^S(x)$ of each $x \in \gamma$ is i) a cross section of γ ,
ii) a manifold diffeomorphic to euclidean space. Moreover, the union of the
stable manifolds $W^S(x)$, $x \in \gamma$, is an open neighborhood of γ and the stable
manifold of γ .

Definition 1. 4. An event surface ES is an $(n-1)$ -dimensional cross section
of the flow in M , and is defined as follows. When the state point of (2)
crosses ES, the reference event is triggered.

In phase resetting experiments we define some reference point in the cycle
of an oscillator and determine phase of the oscillator by that special refer-
ence event. So, one who is doing experiments determines the event surface
ES. For example, let us assume that concentration of a chemical substance
has three peaks during one cycle of a biochemical oscillator. If we choose
some medium threshold for the concentration, there are six crossings of the
threshold during one cycle. Once we select the first upper crossing of the
threshold for the reference, we can easily extend this definition from limit
cycle (free running oscillation) to other orbits (perturbed oscillations).
So, event surface ES corresponds to measurement of the time by the man who
does experiments.

The crucial property of ES here is that it cuts the limit cycle γ only
once. For example, let us consider the Drosophila case. We assume that the
circadian oscillator controls the eclosion and it emits the gating signal
once in its period τ . When we describe the oscillator by a system of ordinary
differential equations, free running oscillation corresponds to a limit
cycle γ . Because the oscillator emits the signal only once in its cycle,
the event occurs only at one point of γ . Along other trajectories than the

limit cycle γ (that is, if free running oscillation is perturbed by some light or temperature stimulus) the event still occurs if these trajectories are sufficiently close to the limit cycle γ . The points on these trajectories where the event occurs constitute the event surface ES. So, ES cuts the limit cycle γ only once. ES may seem to be artificial. However, ES is essential to the formulation of the transient PRC because it corresponds to measurement of the time when the reference event occurs.

From Definitions 1.1 and 1.4, ES and γ meet only once at the point of phase zero $\theta^{-1}(0)$. Both ES and $W^S(\theta^{-1}(0))$ are $(n-1)$ -dimensional curved surfaces and both meet γ at $\theta^{-1}(0)$. ES and $W^S(\theta^{-1}(0))$ meet at $\theta^{-1}(0)$. But of course ES and $W^S(\theta^{-1}(0))$ are not the same. Let us illustrate ES and $W^S(\theta^{-1}(0))$ for FitzHugh's (1961) BVP equation which is a model of a pacemaking neuron.

$$\begin{aligned} dx/dt &= C(y+x-x^3/3), \\ dy/dt &= -(x-A+By)/C, \\ 0 < B < 1, \quad C > 0, \quad B < C^2, \end{aligned} \tag{4}$$

where x corresponds to membrane potential and y to refractoriness. For some parameter region (4) has a stable limit cycle (Hadelier et al., 1976). If we choose maximal excitation as the reference event, ES is a set of points for which $dx/dt=0$ and $d^2x/dt^2 > 0$ (maximum of the membrane potential). So, ES is the left part of the curve $y=-x+x^2/3$ to the equilibrium point (see the solid line in Fig. 2). The broken line in Fig. 2 is the stable manifold of $\theta^{-1}(0)$, $W^S(\theta^{-1}(0))$ obtained by computer simulation. Fig. 2 is the phase plane of the BVP model (4). (x_e, y_e) is the unstable equilibrium point. The chain line is the limit cycle γ . The parameter values $A=0.1$, $B=0.75$ and $C=1.0$ are chosen.

In this case both ES and $W^S(\theta^{-1}(0))$ are 1-dimensional surfaces (i.e. curves) as M is 2-dimensional.

$C(\phi, \mu): S^1 \times R^+ \rightarrow M$ is defined as follows. Here $R^+ = [0, \infty)$.

Definition 1. 5. $C(\phi, \mu) = \Psi_\mu^{-1}(\theta^{-1}(\phi - T/\tau), T)$. C_μ is the range of C for fixed μ , that is $C_\mu = \{C(\phi, \mu); \phi \in S^1\}$.

$C(\phi, \mu)$ is the state point at the end of the perturbation of magnitude μ which starts at the phase $\phi - T/\tau$. C_μ is a set of state points at the ending of perturbation. C_μ is a simple closed arc in M because of continuity of the solution of (3) with respect to initial conditions and because of the uniqueness of solutions to (3). We call C_μ a perturbed cycle.

Definition 1. 6. The timing sequence of an old phase ϕ is defined as the sequence of times $\{t_i(\phi)\}$ ($i=1, 2, \dots$) such that $\Psi_0(C(\phi, \mu), t_i(\phi)) \in ES$. Here $t_i(\phi) \geq 0$ and $t_{i+1}(\phi) > t_i(\phi)$.

$t_i(\phi)$ is the time elapsed from the end of perturbation to the i -th reference event when the perturbation is applied at the old phase ϕ . If $C(\phi, \mu) \in W^S(\gamma)$, then $\lim_{i \rightarrow \infty} (t_{i+1}(\phi) - t_i(\phi)) = \tau$.

Definition 1. 7. If $C \in W^S(\gamma)$, then the i -th transient PRC, $\Delta\phi_i(\phi): S^1 \rightarrow S^1$ and the i -th transient PTC, $\phi'_i(\phi): S^1 \rightarrow S^1$ are defined as follows

$$\begin{aligned} \Delta\phi_i(\phi) &= 1 - \phi - t_i(\phi)/\tau && \pmod{1} \\ \phi'_i(\phi) &= 1 - t_i(\phi)/\tau && \pmod{1} \end{aligned} \tag{5}$$

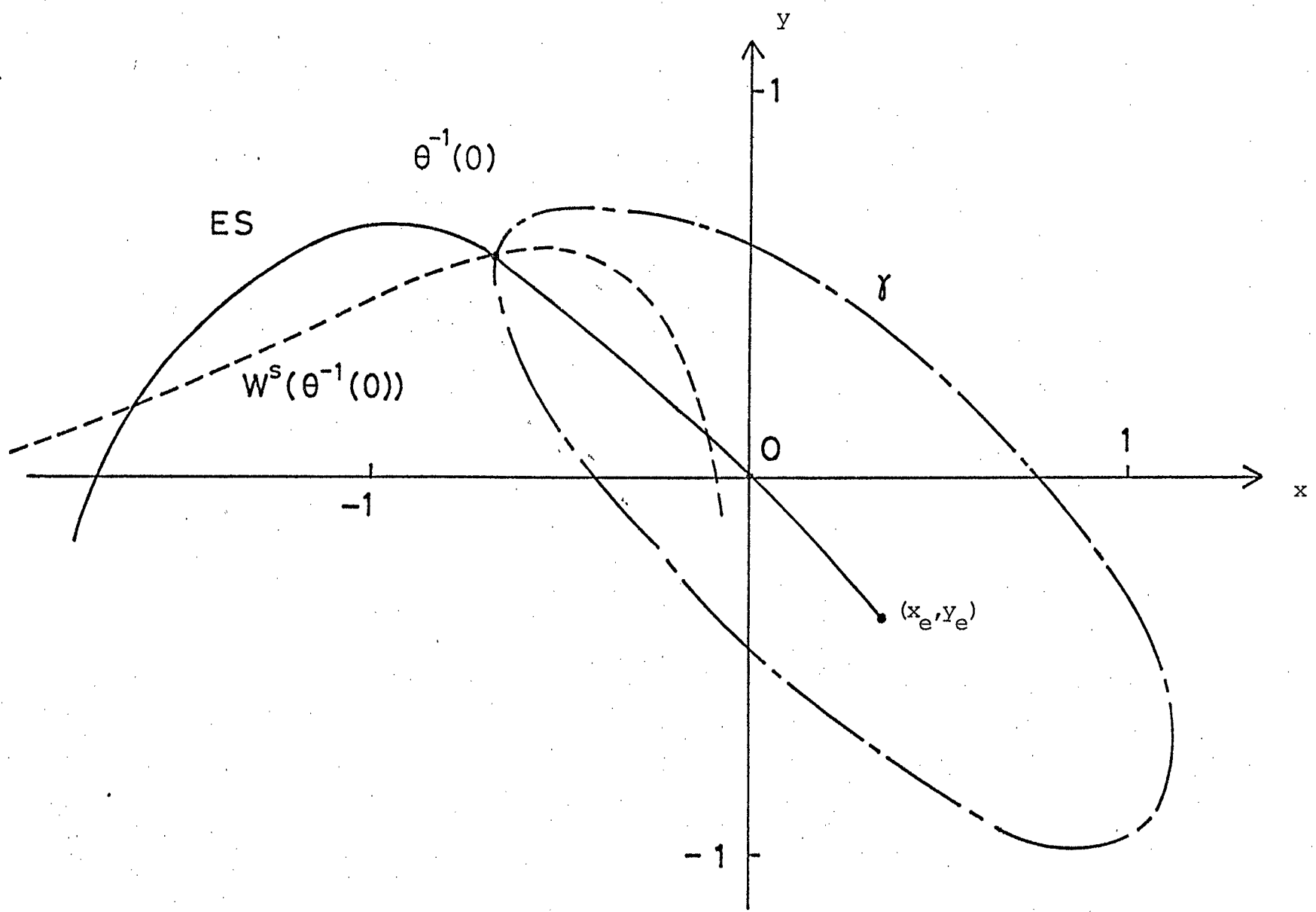


Fig. 2

Definition 1. 8. If $C \in W_{\mu}^S(\gamma)$, then the steady state PTC, $\phi'(\phi): S^1 \rightarrow S^1$ is defined as follows.

$$\phi'(\phi) = \theta_e(C(\phi, \mu)).$$

Clearly Definition 1.8 is compatible with Definition 1.7, that is $\lim_{i \rightarrow \infty} \phi_i'(\phi) = \phi'(\phi)$. The new phase ϕ' as a function of both the old phase ϕ and the stimulus magnitude μ , i.e. $\phi'(\phi, \mu) = \theta_e(C(\phi, \mu))$, is called the phase transition surface (PTS). The term "surface" implies that the magnitude of the stimulus is also varied.

1. 4 Topological properties of PRC and PTC

In this section, we examine general, topological properties of steady state and transient PTCs. Winfree (1970) classified steady state PTCs and PRCs into two types according to their average slopes. The PTC with an average slope of unity and the corresponding PRC with an average slope of zero are called Type 1. The PTC with an average slope of zero and the corresponding PRC with an average slope of minus one are called Type 0 (see Fig. 3). We can prove the following topological properties of the steady state PTC using Definition 1.8 and Theorem 1.0.

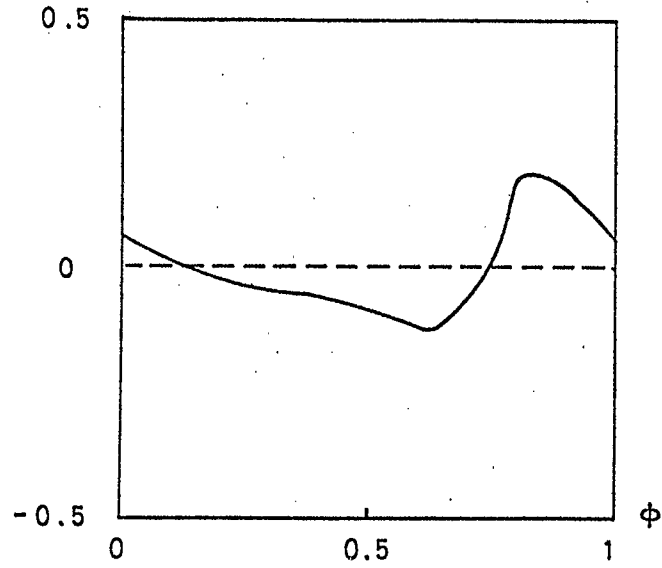
Lemma 1. 1. *The steady state PTC, $\phi'(\phi)$ is a continuous function.*

Proof. From Definition 1.2, θ^{-1} is continuous. The regularity of (3) guarantees the continuity of Ψ_{μ} . From Theorem 1.0 we can show that θ_e is a continuous function at the sufficiently small neighborhood of γ , $U(\gamma)$. For

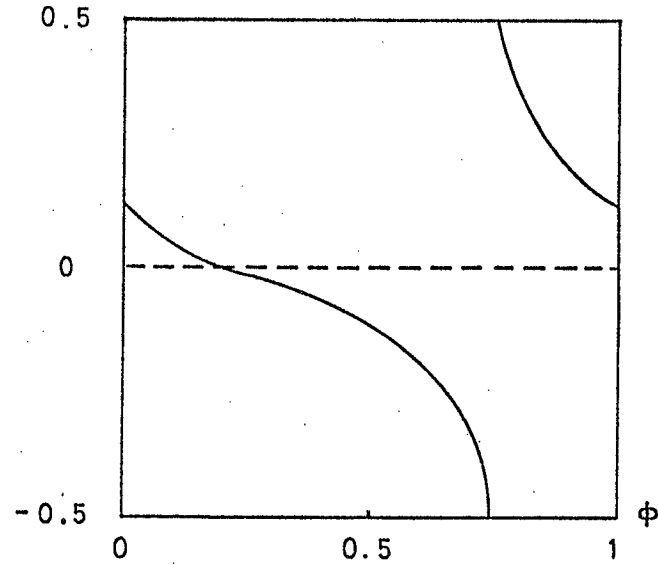
WEAK PERTURBATION

STRONG PERTURBATION

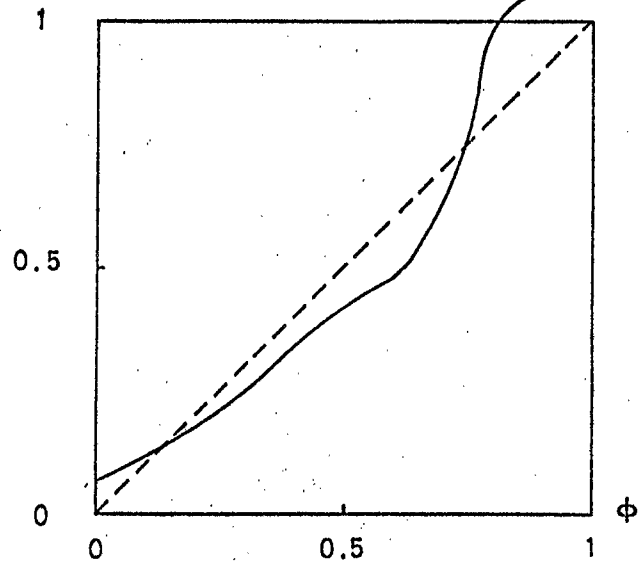
$\Delta\phi$ TYPE 1 PRC



$\Delta\phi$ TYPE 0 PRC



ϕ' TYPE 1 PTC



ϕ' TYPE 0 PTC

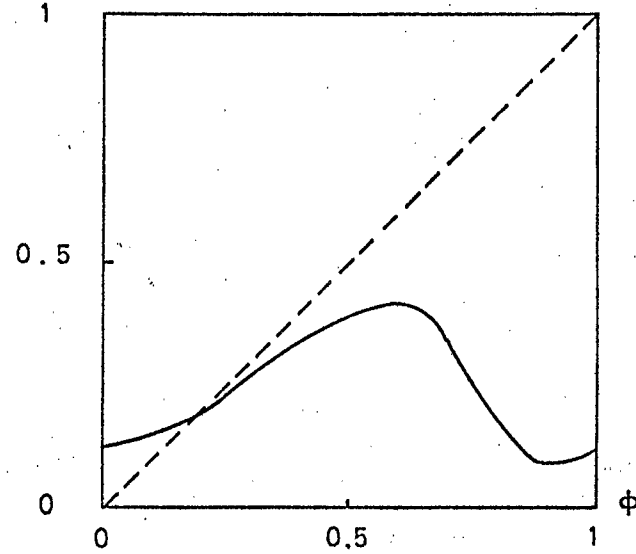


Fig. 3

an arbitrary $y \in W^S(\gamma)$, $\notin U(\gamma)$, there exists $s > 0$ such that $\Psi_0(y, s) \in U(\gamma)$ because γ is an asymptotically stable limit cycle. Here the equation $\theta_e(y) = \theta_e(\Psi_0(y, s)) - s/\tau \pmod{1}$ holds. Because $\Psi_0(x, s): M \rightarrow M$ is continuous, $\theta_e(x)$ is continuous in $W^S(\gamma)$. Because $\phi'(\phi) = \theta_e(\Psi_\mu(\theta_e^{-1}(\phi - T/\tau), T))$, we completed the proof.

Theorem 1.1. 1) If and only if C_μ is homotopic to γ in $W^S(\gamma)$, then the steady state PTC, $\phi'(\phi)$ for the stimulus magnitude μ is Type 1. 2) If and only if C_μ is homotopic to a constant mapping in $W^S(\gamma)$, then $\phi'(\phi)$ for μ is Type 0.

Proof. Because the steady state PTC depends on the stimulus magnitude μ , we express it explicitly as follows, $\phi'(\phi, \mu) = \theta_e(C(\phi, \mu)): S^1 \times R^+ \rightarrow S^1$.

Let us prove the sufficient condition of the first half 1). $\phi'(\phi, 0) = \phi$, $\gamma = C_0$. For convenience, we write $C(\phi, \mu)$ instead of C_μ . Because of the assumption there exists a homotopy $G: S^1 \times I \rightarrow W^S(\gamma)$; $G(\phi, 0) = C(\phi, 0)$, $G(\phi, 1) = C(\phi, \mu)$ and for fixed $v \in I = [0, 1]$, $G(\phi, v)$ is a closed path in $W^S(\gamma)$. For each $v \in I$, we define a continuous function $H(\phi, v): S^1 \rightarrow S^1$ as we have defined a PTC in Definition 1.7. That is, $H(\phi, v) = \theta_e(G(\phi, v))$. Because G and θ_e are continuous, H is a homotopy between $\phi'(\phi, 0)$ and $\phi'(\phi, \mu)$. That is, $H: S^1 \times I \rightarrow S^1$; $H(\phi, 0) = \phi$, $H(\phi, 1) = \phi'(\phi, \mu)$. This implies that $\phi'(\phi, \mu)$ is homotopic to the Type 1; $\phi'(\phi, 0) = \phi$. So, $\phi'(\phi, \mu)$ is Type 1. The proof of the sufficient condition of 2) is similar.

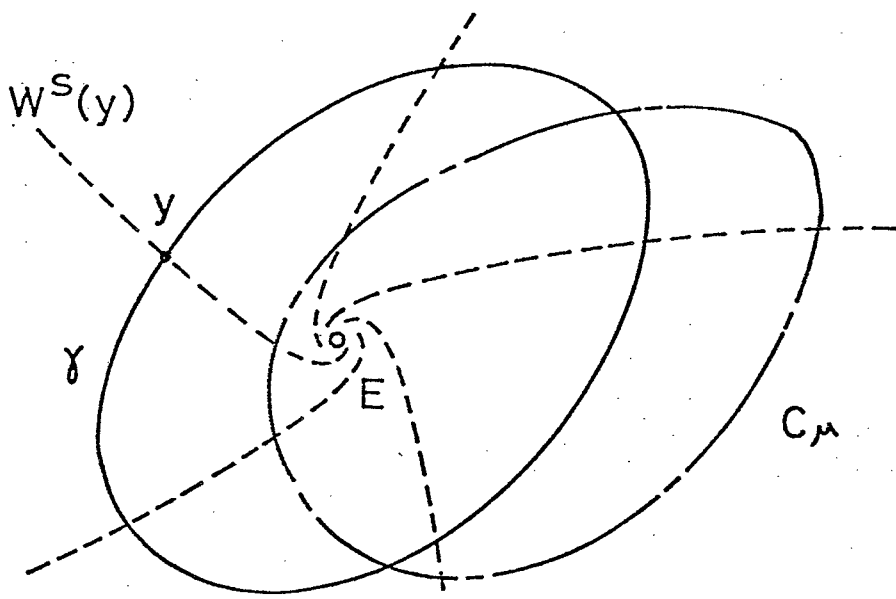
For the proof of the necessary conditions we must prove the fact that γ is a deformation retract of $W^S(\gamma)$. Theorem 1.0 guarantees the existence of smooth and sufficiently small neighborhood $U(\gamma)$ of γ whose boundary integral curves of (2) cross transversally and inwardly. γ is a deformation retract of $U(\gamma)$. The rest to be proved is that $U(\gamma)$ is a deformation retract of $W^S(\gamma)$. Because γ is asymptotically orbitally stable, for every $y \in W^S(\gamma)$, $\notin U(\gamma)$

there exists continuous $T(y) > 0$ such that $\Psi_0(y, T(y))$ is on the boundary of $U(\gamma)$. We define a homotopy $\{r_v\}: W^S(\gamma) \times I \rightarrow W^S(\gamma)$: If $y \in U(\gamma)$ then $r_v(y) = y$ and if $y \notin U(\gamma)$ then $r_v(y) = \Psi_0(y, vT(y))$. Because both $T(y)$ and Ψ_0 are continuous and $r_0(y) = y$, $r_1: W^S(\gamma) \rightarrow U(\gamma)$, r_v is the required retraction. It follows that $W^S(\gamma)$ is homotopy equivalent to γ . So, the fundamental group of $W^S(\gamma)$ is isomorphic to the integer group Z and its generator is a closed path $C(\phi, 0)$. If $C(\phi, \mu)$ is in $W^S(\gamma)$, then $C(\phi, \mu) \approx nC(\phi, 0)$ ($n=0, \pm 1, \pm 2, \dots$). If $C(\phi, \mu)$ is homotopic to $nC(\phi, 0)$ we can prove that the corresponding PTC is Type n (i.e. with an average slope of n) by similar discussion to the proof of the sufficient conditions. Since all types of PTCs have been listed up, we completed the proof of the necessary conditions.

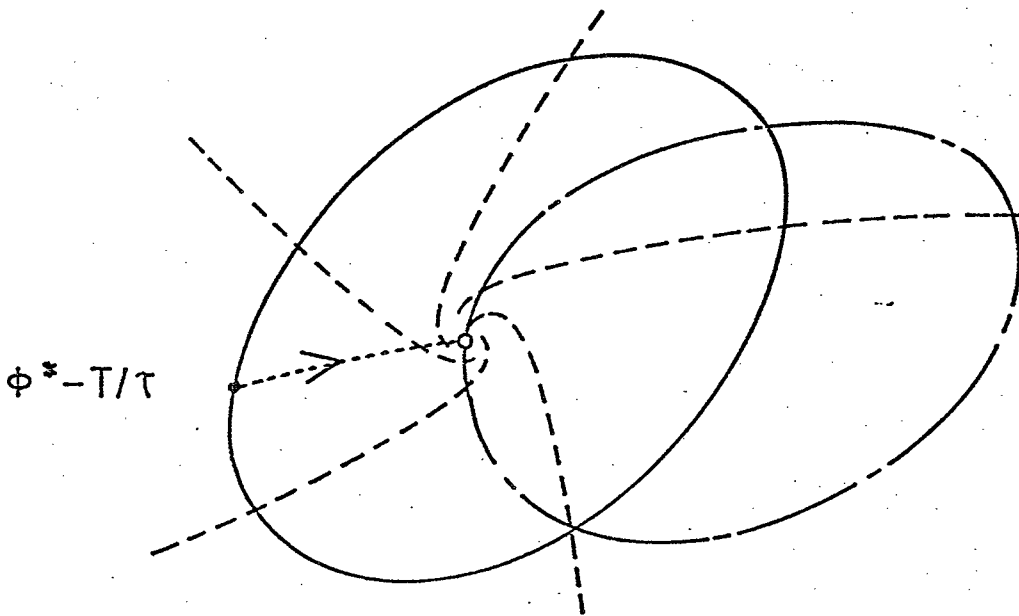
Theorem 1. 2. If there exists a stimulus magnitude μ_0 such that the corresponding steady state PTC is Type 0, then there exists at least one μ^ ($0 < \mu^* < \mu_0$) such that C_{μ^*} is not contained in $W^S(\gamma)$, in other words the PTC for this magnitude μ^* cannot be defined. That is, when we apply the perturbation of magnitude μ^* at an appropriate phase to the oscillator, it does not return to the unperturbed cycle.*

Proof. We prove the theorem by contradiction. We assume that for all μ ; $0 < \mu < \mu_0$, $C_\mu \subset W^S(\gamma)$. Since $\phi'(\phi, \mu)$ is continuous with respect to (ϕ, μ) because of continuity of $\Psi_\mu(x, t)$ with respect to (μ, x) , we can define a homotopy $J(\phi, v): S^1 \times I \rightarrow S^1$ as follows. $J(\phi, v) = \phi'(\phi, v\mu_0)$; $J(\phi, 0) = \phi'(\phi, 0) = \phi$, $J(\phi, 1) = \phi'(\phi, \mu_0)$. This implies that $\phi'(\phi, 0)$ is homotopic to $\phi'(\phi, \mu_0)$ but $\phi'(\phi, 0)$ is Type 1 and $\phi'(\phi, \mu_0)$ is Type 0. This is a contradiction.

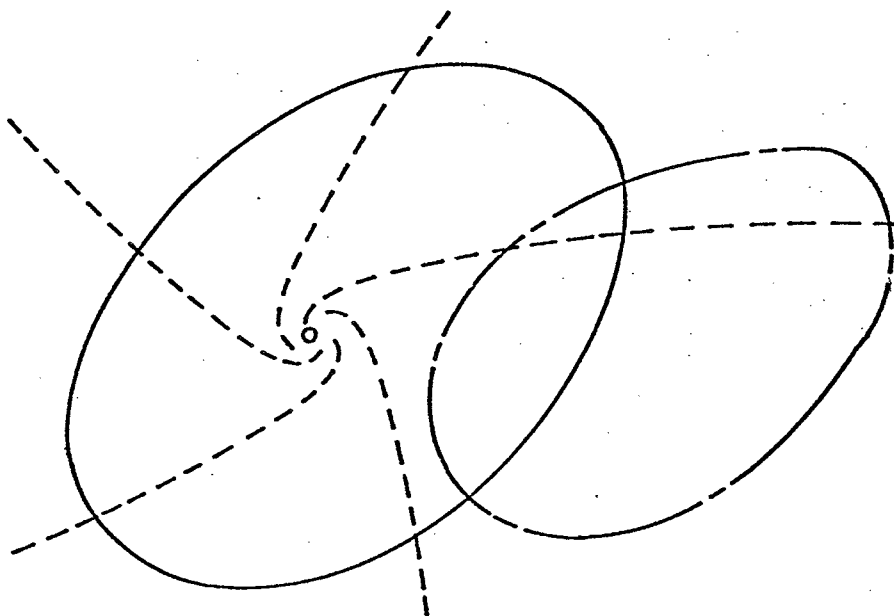
For the understanding of the discussion in the following sections, we explain intuitive meanings of Theorems 1.1 and 1.2 in a simple two-dimensional



a TYPE 1 (WEAK PERTURBATION)



b STOP (MEDIUM PERTURBATION)



c TYPE 0 (STRONG PERTURBATION)

dynamical system. Let us assume that the phase space of (2) is R^2 , (2) has an unstable equilibrium point E and a stable limit cycle γ which surrounds E and there is no other periodic solution or equilibrium point (see Fig. 4). Stable manifolds of five points on γ are drawn by broken lines. A stable manifold of a point on γ is a curve and all stable manifolds concentrate on E . When C_μ is close to γ and surrounds E (i.e. C_μ is homotopic to γ) in the case of the weak perturbation, then the PTC is Type 1 because C_μ crosses every stable manifold of $x \in \gamma$, $W^S(x)$ (see Fig. 4a). In Fig. 4 the closed curve of chain is the set of points perturbed from γ , C_μ . On the other hand, if C_μ is far apart from γ and does not go around the confluence of stable manifolds E (i.e. C_μ is homotopic to a constant mapping in $W^S(\gamma)$), then the PTC is Type 0 because all of new phases values ϕ' fall within a limited range (see Fig. 4c). If C_μ , which is perturbed from γ by a medium perturbation, exactly contains the equilibrium point E , then the PTC cannot be defined for this magnitude of perturbation. Especially in this case, the perturbation of this magnitude which begins at the phase $\phi^* - T/\tau$ in Fig. 4b stops the oscillation. The dotted line in Fig. 4b is the orbit of the system (3) starting from the point $\theta^{-1}(\phi^* - T/\tau)$.

Proposition 1. 1. Let us assume that $C_\mu \subset W^S(\gamma)$, that is the steady state PTC exists and is continuous. If there exists the old phase ξ such that $C(\xi, \mu) \in ES$, then the i -th transient PTC, $\phi'_i(\phi)$ is discontinuous at $\phi = \xi$.

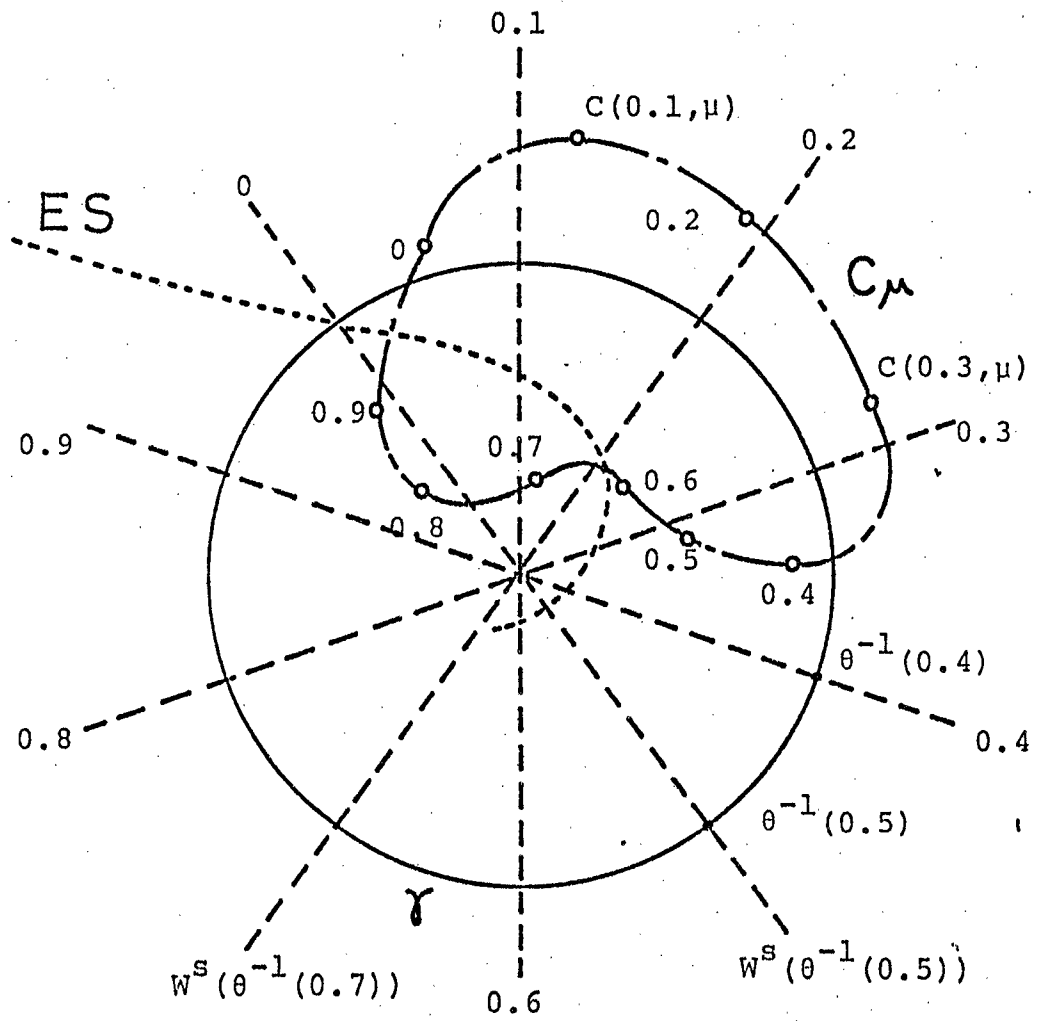
Proof. We can assume that ES is transverse to C_μ at $C(\xi, \mu)$ in generic cases. We assume that $[F(C(\xi, \mu), 0), dC(\xi, \mu)/d\phi] > 0$ where $[,]$ is the inner product. In this case $\lim_{\phi \rightarrow \xi + 0} t_1(\phi) = 0$ and $\lim_{\phi \rightarrow \xi - 0} t_1(\phi) > 0$ hold. If the inner product is negative, then $\lim_{\phi \rightarrow \xi + 0} t_1(\phi) = 0$ and $\lim_{\phi \rightarrow \xi - 0} t_1(\phi) > 0$. Since we can treat

the latter case similar to the former case, we only study the former. There exists $z \in \gamma$ such that $C(\xi, \mu) \in W^S(z)$. Since for any subset S , $W^S(\Psi_0(S, t)) = \Psi_0(W^S(S), t)$ holds, $\Psi_0(C(\xi, \mu), k\tau) \in W^S(z)$ ($k=1, 2, \dots$). Since $W^S(z)$ does not correspond to ES, $\Psi_0(C(\xi, \mu), k\tau) \notin ES$ in generic cases, that is $\lim_{\phi \rightarrow \xi+0} t_1(\phi) \neq k\tau$. Consequently $\phi'_1(\phi) = 1 - t_1(\phi)/\tau \pmod{1}$ is discontinuous at $\phi = \xi$. Similarly we can show that all $\phi'_i(\phi)$ ($i=1, 2, \dots$) have their discontinuity at $\phi = \xi$.

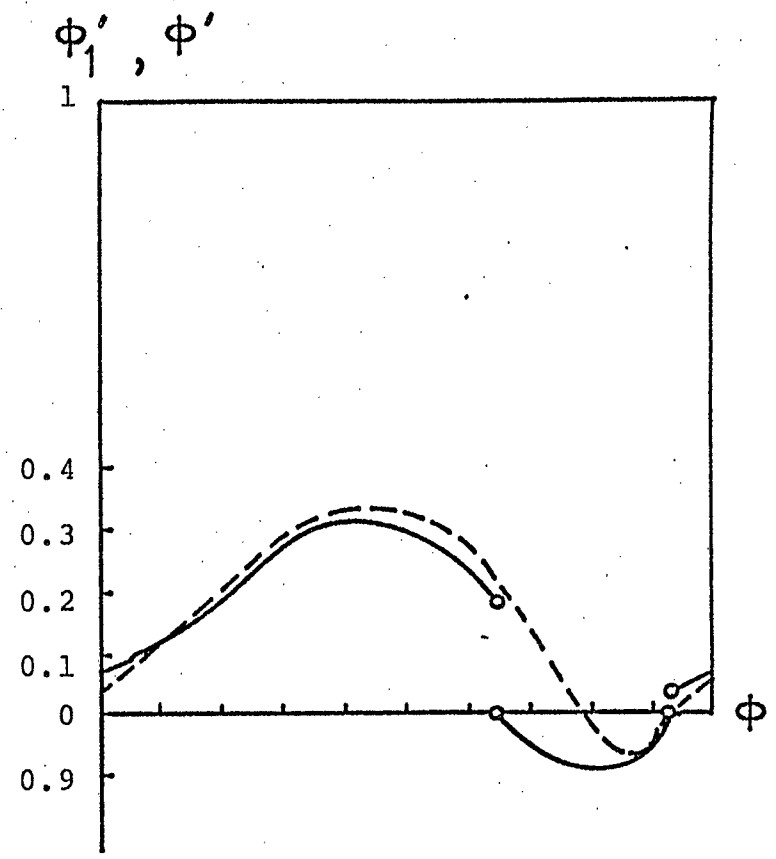
From Lemma 1.1 we know that the steady state PTC $\phi'(\phi)$ is a continuous function of ϕ . The discontinuity in Proposition 1.1 tends to zero as i goes to infinity. In Fig. 5a a simple two dimensional dynamical system is illustrated. In Fig. 5b, the steady state PTC (broken line) and the first transient PTC (solid line) are shown. For example, the dynamical system; $dr/dt = r(1-r^2)$, $d\theta/dt = 1$ in the polar coordinates (r, θ) has a limit cycle and stable manifolds such like those in this figure. The solid, closed path is the limit cycle γ . The broken lines are 10 stable manifolds of 10 points on γ . For example, abbreviation 0.1 denotes the stable manifold of a point of phase 0.1 on γ , $W^S(\theta^{-1}(0.1))$. The dotted curve is the event surface ES. The chain, closed curve is the set of points perturbed from γ , C_μ . For example, abbreviation 0.5 indicates the point which is perturbed from the point of phase 0.5 on γ , $C(0.5, \mu) = \Psi_0(\theta^{-1}(0.5), T)$. The first transient PTC is discontinuous as an example of Proposition 1.1. We call this discontinuity of the transient PTC the first kind of discontinuity.

Let $\partial(ES)$ denote the boundary of ES. Existence of $t > 0$ and ξ such that $\Psi_0(C(\xi, \mu), t) \in \partial(ES)$ is another reason of discontinuity of $\phi'_i(\phi)$ (for i such that $t_1(\xi) > t$) at $\phi = \xi$. We call this the second kind of discontinuity.

For many biological oscillators ES may be a smooth and connected surface. In this case if $A = \{\Psi_0(C(\phi, \mu), t_1(\phi)); \phi \in S^1\}$ is a closed arc in ES and if the



a DYNAMICAL SYSTEM



b STEADY STATE AND TRANSIENT PTCs

Fig. 5

Poincaré map θ of A in ES with image in ES associated with γ and $\theta^{-1}(0)$ can be defined then $\phi'_2(\phi)$ is continuous. Similarly if the k -th iteration of θ for A , $\theta^k(A)$ can be defined, $\phi'_{k+1}(\phi)$ is continuous.

1. 5 Applications of theoretical results to neurobiology

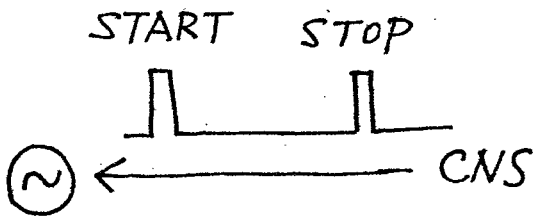
Some neural oscillators must be switched on and off by the central nervous system (CNS). In these controls two modes are possible. The one mode is a phasic control (P) and the other is a tonic control of an oscillator (T). In case of the phasic control, the starting signal and the stopping signal from the CNS to the oscillator are phasic signals. In the tonic control the CNS must keep sending a pulse train to the oscillator to maintain its oscillation or to keep it in the resting state. We can decide whether a certain neural oscillator is controlled under the phasic mode or under the tonic mode by examining the PTS of that oscillator. We define a singular set SS of stimulus magnitude and the old phase as follows. $SS = \{(\mu, \phi) \in \mathbb{R}^+ \times S^1 : C(\phi, \mu) \in W^S(\gamma)\}$. SS may be a point or may be a (un)connected domain(s). In the former case, Winfree called SS as a singular axis. In case of P, SS of PTS is a domain with finite extension, and in case of T it is a point (see Fig. 6a and b). For simplicity we explain these two modes of controls in the two dimensional dynamical system (see Fig. 6c). In the case of the phasic control, the state point is on the stable equilibrium point E in the resting state. It is driven out of the inside of an unstable limit cycle γ_2 by the starting signals from the CNS, and it keeps rounding along a stable limit cycle γ_1 until it is driven into the inside of γ_2 by the stopping signals from the CNS. CNS can switch on and off the oscillator quickly. The period of the oscillation is inherent in the oscillator, and stable

Fig. 6

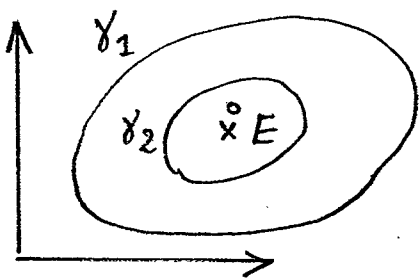
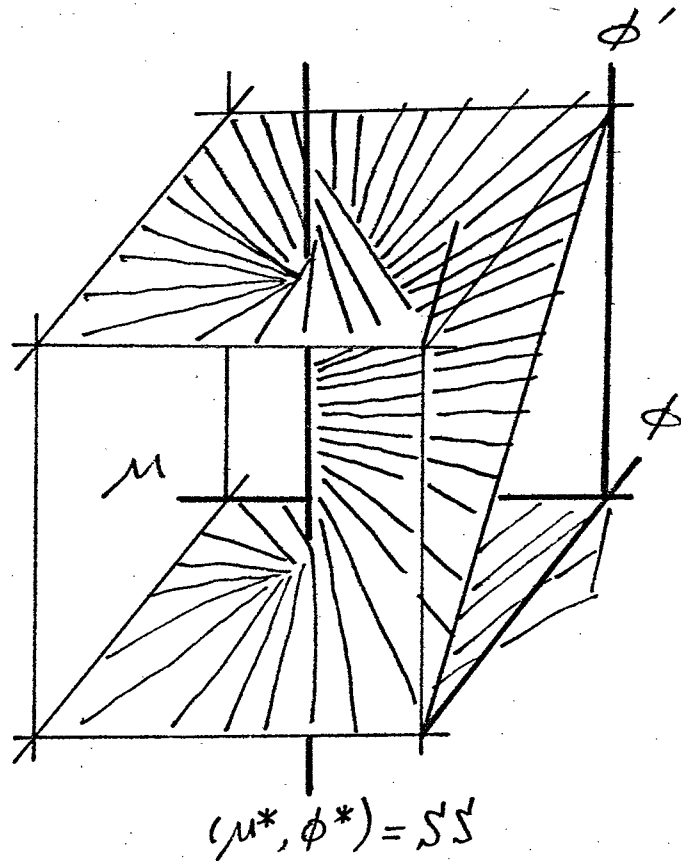
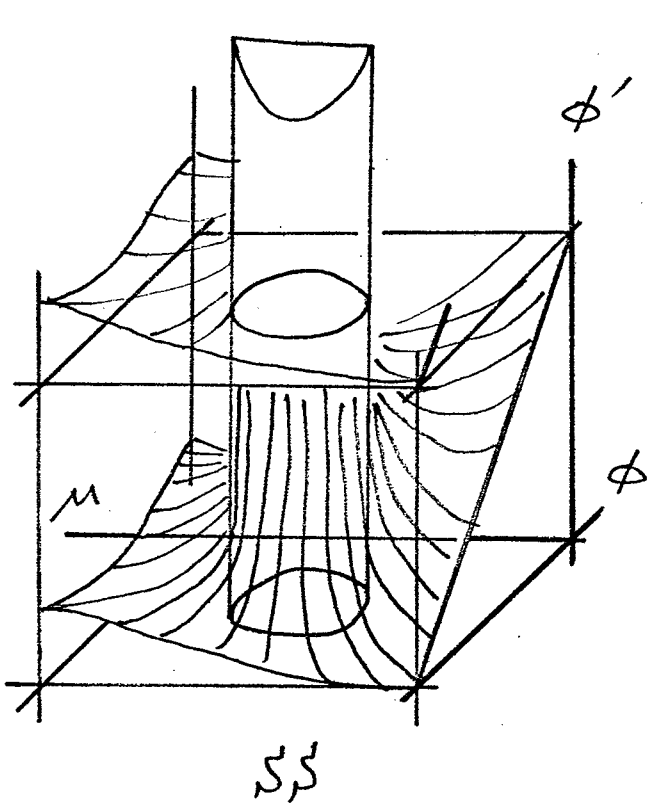
PHASIC CONTROL

TONIC CONTROL

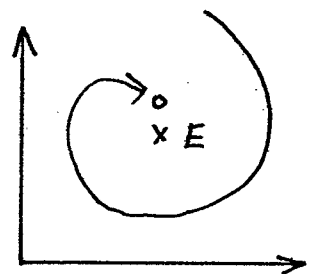
a.



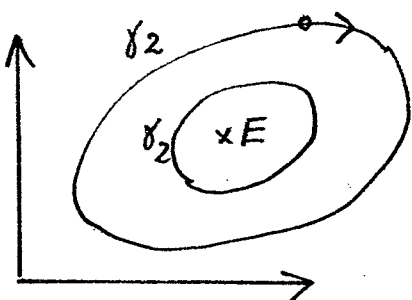
b.



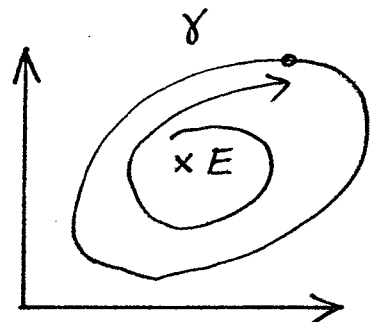
RESTING



c.



OSCILLATING



1. 6 Drosophila's PTC and inner structures of its circadian oscillator

We have mathematically formulated PRC and PTC and clarified their topological properties. All steady state PRC which were measured in biology are either Type 0 or Type 1. We can get any steady state PRC (Type 0 and Type 1) for an arbitrary dynamical system (2) with an elementary stable limit cycle if only the closed path C_{μ}^S is appropriately chosen in $W^S(\gamma)$. So, the steady state phase response curve alone imposes no restrictions on the equations which describe the oscillator although every part of the phase response curve can be informative about stages of the cycle. We must compare the transient PTCs with the steady state PTC in order to study the inner structure.

Pittendrigh and Bruce (1959) measured the transient and steady state PRCs of Drosophila's emergence rhythms. They used a 15 minutes light pulse as a perturbation. Fig. 7 is the first transient PTC (solid line) and the steady state PTC (broken line) which are redrawn from Pittendrigh (1965). The abscissa is the old phase ϕ multiplied by 24. The ordinate is either the first transient new phase ϕ'_1 or the steady state new phase ϕ' multiplied by 24. The transient PTCs almost converge to the steady state PTC for $i=6$ in this case. The reference event is emergence of fruitflies. The first transient PTC has a big discontinuity at $\phi=15.5/24$. It seems to be continuous at all other phases. Hereafter fractional phases such as $\phi=3/24$ or $17.5/24$ will be used frequently because Pittendrigh used the subjective circadian time (SCT) scale in their original drawings. Pittendrigh proposed a two-oscillator (Master-Slave) model of the circadian pacemaker of Drosophila to account for the transient resetting pattern. His model is composed of the light-sensitive master oscillator and the slave oscillator which directly controls the emergence (see Fig. 8). The model has been examined by many kinds of experiments and now its validity has been established. However,

$24 \cdot \phi_1', 24 \cdot \phi'$

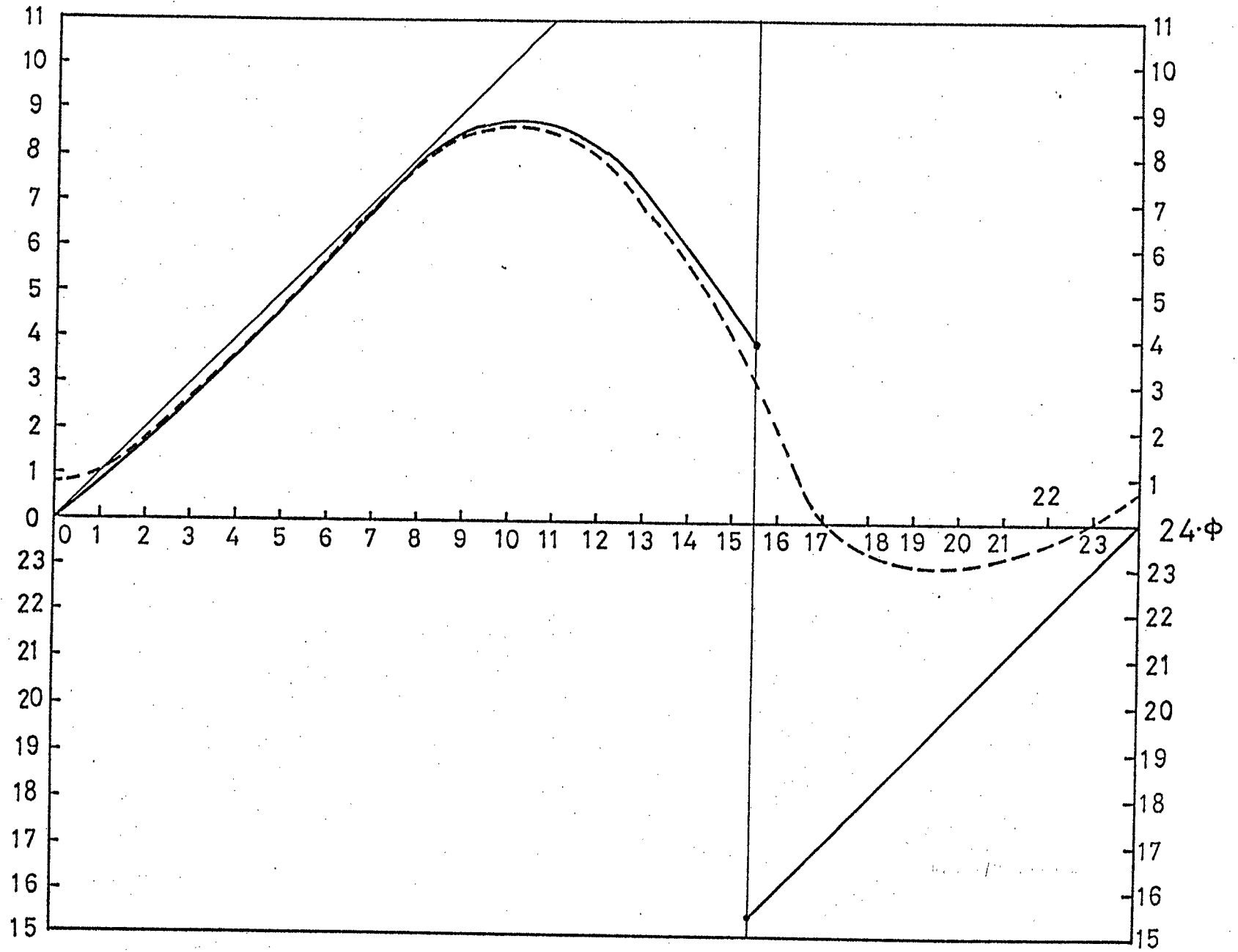


Fig. 7

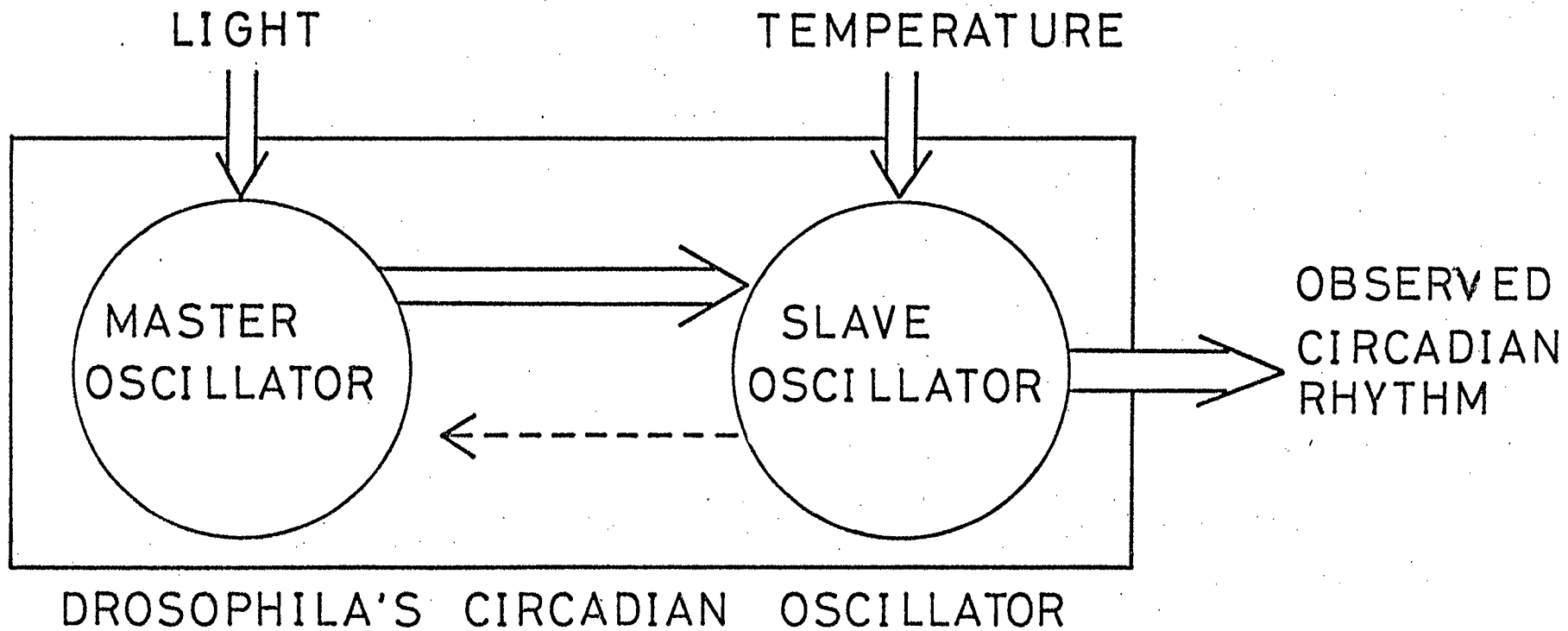


Fig. 8

here we would like to study the problem using only PTCs.

As shown in the preceding sections we cannot conclude that the system is composed of two oscillators on account of the discontinuity of the transient PTC. For example, the simple two-variable dynamical system in Fig. 5 has a discontinuous transient PTC. We can prove, however, the following Theorem 1.3 which tells us something about the inner structures of the *Drosophila*'s oscillator since the transient PTC in Fig. 7 has the big discontinuity of the second kind.

Theorem 1. 3. The first transient and steady state PTCs of Drosophila cannot be explained by a single oscillator with two variables. In other words, the circadian oscillator of Drosophila does not consist of a single oscillator of two degrees of freedom.

Proof. We prove the theorem by reductio ad absurdum. We assume that *Drosophila*'s circadian pacemaker is a single oscillator which is described by a two dimensional dynamical system (2) in the free-running state.

The first transient PTC in Fig. 7 shows $\phi'_1(0/24)=0/24$. When the light pulse is applied at phase $\phi=0/24$, the emergence of flies occurs immediately and irrelevantly to the perturbation. Because this means that $t_1(0/24)=0$, C_μ crosses ES (Event Surface: a set of points where the emergence occurs in this case) at $C(0/24,\mu)$. If $t_1(\phi)$ is a continuous function of ϕ for $\phi \in J$, then $\{\Psi_0(C(\phi,\mu), t_1(\phi)); \phi \in J\}$ is a continuous curve in ES, where J is an interval in $S^1=[0,1]$. $\phi'_1(\phi)$ is continuous for $\phi \in (15.5/24, 0/24] \cup [0/24, 15.5/24) = J_1 \cup J_2$. Consequently, $\{\Psi_0(C(\phi,\mu), t_1(\phi)); \phi \in J_1 \cup J_2\}$ is a connected subset of the one-dimensional ES. Let $\{\Psi_0(C(\phi,\mu), t_1(\phi)); \phi \in J_1\}$ be denoted by ES₁. If ES crosses C_μ at $C(\xi,\mu)$, either $t_1(\xi-0)$ or $t_1(\xi+0)$ must be 0. That is either

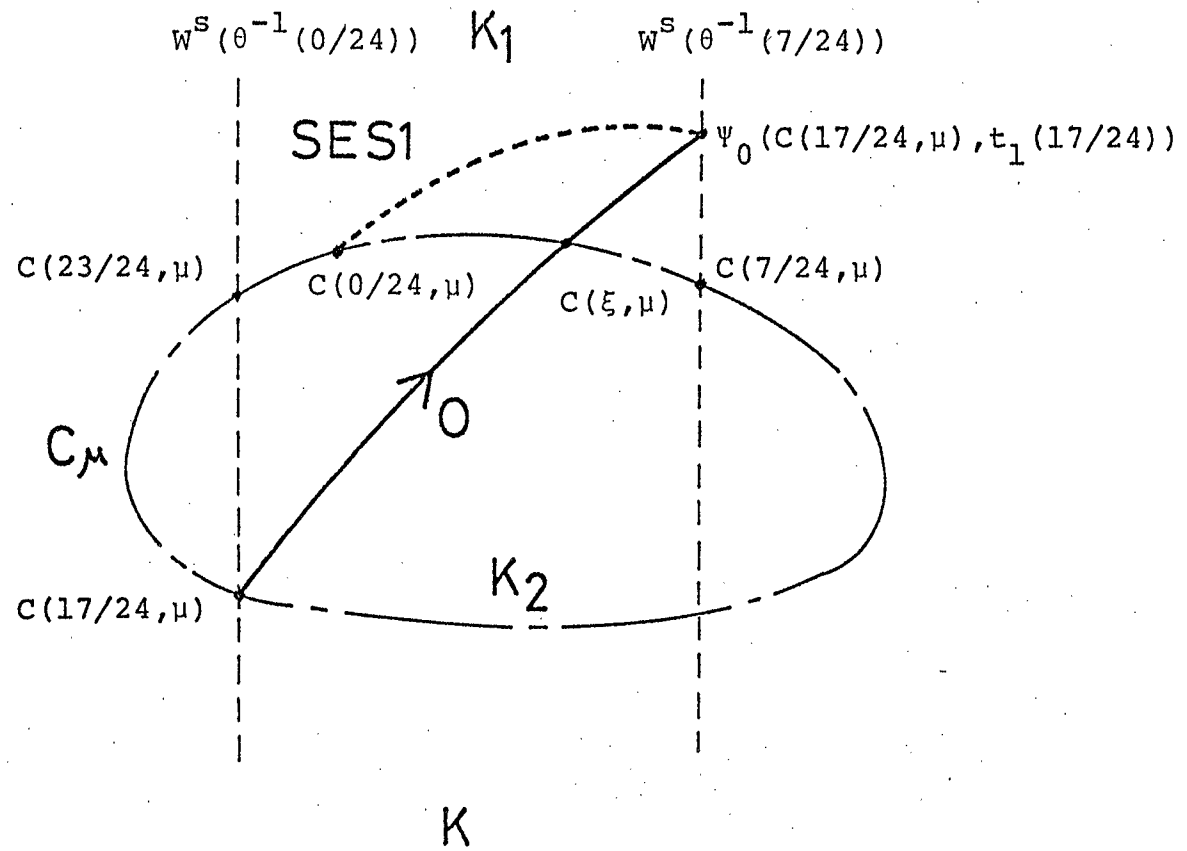


Fig. 9

$\phi'_1(\xi-0)$ or $\phi'_1(\xi+0)$ must be 0. As Fig. 7 shows, $\phi'_1(\phi)$ has its zero point only at $\phi=0$. ES crosses C_μ only once. ES1 has its endpoint $\Psi_0(C(0/24,\mu), t_1(0/24)) = \Psi_0(C(0/24,\mu), 0) = C(0/24,\mu)$ on C_μ . Since C_μ is a simple closed path in two-dimensional M , ES1 must be either inside or outside C_μ . Let us consider the two cases separately.

(Case I) The case that ES1 is inside C_μ . Since $\phi'_1(16/24) = 16/24$, $t_1(16/24) = 8\text{hr}$ (in subjective circadian time). Because $\phi'(16/24) = 2/24$, $\Psi_0(C(16/24,\mu), 8) \in \Psi_0(W^S(\theta^{-1}(2/24)), 8) = W^S(\theta^{-1}(10/24))$. $\Psi_0(C(16/24,\mu), t_1(16/24))$ is on ES1. Because the range of $\phi'(\phi)$ is $[23/24, 8.5/24]$, C_μ is contained in the set $\bigcup_{23/24 \leq \phi \leq 8.5/24} W^S(\theta^{-1}(\phi))$. The point $\Psi_0(C(16/24,\mu), t_1(16/24))$ is outside C_μ . This is contradiction.

(Case II) The case that ES1 is outside C_μ . Because of Theorem 1.0, the set $K = \{W^S(\theta^{-1}(\phi)); 0/24 \leq \phi \leq 7/24\}$ is divided into two subsets K_1 and K_2 by a part of C_μ , $\{C(\phi,\mu); 23/24 \leq \phi \leq 7/24\}$. $K_1 \cup K_2 \cup \{C(\phi,\mu); 23/24 \leq \phi \leq 7/24\} = K$. $K_1 \cap K_2 = \{\phi\}$. K_2 contains a part of the interior of C_μ (see Fig. 9). The subset of ES1, SES1 is defined as $SES1 = \{\Psi_0(C(\phi,\mu), t_1(\phi)); 17/24 \leq \phi \leq 0/24\}$. $\Psi_0(C(\phi,\mu), t_1(\phi))$ is on $W^S(\theta^{-1}(\phi'(\phi) + t_1(\phi)/\tau)) = W^S(\theta^{-1}(\phi'(\phi) - \phi'_1(\phi)))$. $\phi'(\phi) - \phi'_1(\phi)$ is a decreasing function of ϕ for $17/24 \leq \phi \leq 0/24$. $\Psi_0(C(17/24,\mu), t_1(17/24)) \in W^S(\theta^{-1}(7/24))$ (for, $\phi'_1(17/24) = 17/24$, $t_1(17/24) = 7\text{hr}$ (in subjective circadian time), $\phi'(17/24) = 0/24$). Consequently SES1 is contained in K , moreover it is contained in K_1 because of the assumption. The orbit $O = \{\Psi_0(C(17/24,\mu), t); 0 \leq t \leq t_1(17/24)\}$ is contained in K because of commutability of Ψ_0 and W^S . One endpoint of O , $C(17/24,\mu)$ is in K_2 , another endpoint of O , $\Psi_0(C(17/24,\mu), t_1(17/24))$ is in K_1 . So, O must cross $\{C(\phi,\mu); 23/24 \leq \phi \leq 7/24\}$ at some point $C(\xi,\mu)$. This implies that $t_1(\xi) = t_1(17/24) - \tau \cdot \phi'(\xi)$. That is $\phi'(\xi) = \phi'_1(\xi) + 7/24 \pmod{1}$ for $23/24 \leq \xi \leq 7/24$. This is a contradiction (see Fig. 7). Fig. 9 is an illustration of the proof in Case II. The closed path of chain is a set of points

perturbed from γ, C_μ . The left broken line is $W^S(\theta^{-1}(0/24))$. The right broken line is $W^S(\theta^{-1}(7/24))$. The region between these two lines is $K = \{W^S(\theta^{-1}(\phi)); 0/24 \leq \phi \leq 7/24\}$. K is divided into two regions K_1 (upper) and K_2 (lower) by a part of C_μ , $\{C(\phi, \mu); 23/24 \leq \phi \leq 7/24\}$. The dotted curve is a part of the event surface, SES1. The bold and solid curve is a orbit of (2) starting from the point $C(17/24, \mu)$.

Here, C_μ crosses ES at $C(0/24, \mu)$. So, the transient PTCs are discontinuous at $\phi=0/24$ from Proposition 1.1. But, in this case the phase shift at the old phase $\phi=0/24$, $\Delta\phi(0/24)$, is very small. Consequently, discontinuity of the first kind at $\phi=0/24$ is very small. But rigorously $\phi'_1(0/24-0)=0$ and $\phi'_1(0/24+0)>0$. Note that we used continuity of $\phi'_1(\phi)$ for only the interval J_1 safely. Our proof does not depend on the minute values of PTCs. For example, if $\phi'(16/24)=1.5/24$, our proof is valid as before. The reason is that we used only rough and topological properties of the measured PTCs in the proof.

1. 7 Two-oscillator model for Drosophila's PTC

The assumption that the phase space is two dimensional is essential in the proof of Theorem 1.3. A single oscillator with three variables can have both transient and steady state PTCs of Drosophila if we choose the appropriate flows Ψ_0, Ψ_μ and the appropriate event surface ES very skillfully. However, construction of such artificial and unnatural dynamical system does not seem to contribute to understanding. Mathematically speaking, there is no difference between two-oscillator models and one-oscillator models because the two-oscillator system which has a stable limit cycle is itself a single limit cycle oscillator. So, we must choose between the models on the basis

of their biological and physical utility. We tried to develop a one-oscillator model with three variables in order to simulate the transient resetting pattern before we adopted two-oscillator interpretation. However, such a one-oscillator model is hard to understand and does not seem to contribute to understanding and designing new experiments of the circadian oscillator. In this section we mathematically formulate Pittendrigh's two oscillator (Master-Slave) model (see Fig. 8) as generally as possible. Then we examine whether it can explain *Drosophila*'s PTCs or not. We assume that the master oscillator and the slave oscillator are described by the following two dynamical systems (6) and (7) with two degrees of freedom when they are uncoupled and the fly is in DD condition.

$$\begin{aligned} dp/dt &= f(p, q) \\ dq/dt &= g(p, q) \end{aligned} \tag{6}$$

$$\begin{aligned} dr/dt &= h(r, s) \\ ds/dt &= i(r, s) \end{aligned} \tag{7}$$

The system (6) has an elementary stable limit cycle γ_M of a period τ_M . The system (7) has an elementary stable limit cycle γ_S of a period τ_S . Because the slave oscillator controls the emergence, the system (7) has an event surface (event curve in this case) in its phase plane. We denote it ES_S . The experimental fact that the convergence of the advancing phase shifts takes as long as 6 cycles implies that the connection from the master oscillator to the slave oscillator is weak. Winfree (1973b) showed that the state point of fly's clock does not revert toward the limit cycle for several days after a weak pulse (Two-pulse experiment). His weak pulse is in some sense close to his singular stimulation (T^*, S^*) (Winfree, 1970). On

the other hand both Winfree (1973b) and Pittendrigh (1974) showed that the state point immediately returns to γ after a strong pulse (for example, 15 minutes light pulse). Because we examine the PRC for 15 minutes light pulse in this chapter, from the two pulse experiment we can assume that there is no feedback from the slave oscillator to the master oscillator. So, when the fly is in DD we can describe the system of two coupled oscillators as follows.

$$\begin{aligned}
 dp/dt &= f(p, q) \\
 dq/dt &= g(p, q) \\
 dr/dt &= h(r, s) + \epsilon \cdot a(p, q, r, s) \\
 ds/dt &= i(r, s) + \epsilon \cdot b(p, q, r, s),
 \end{aligned}
 \tag{8}$$

where ϵ is a very small parameter. The two-pulse experiment shows that the stability of the limit cycle of the master oscillator, γ_M , can be considered to be very strong. Note that "stability strength of a limit cycle oscillator" cannot be independent of the strength of stimulus. Because every limit cycle oscillator in R^n can be stopped by an appropriate stimulus as Winfree first pointed out (1970) and we rigorously proved, every oscillator is weak for this stimulus. The state point, which is perturbed from γ_M , returns quickly to γ_M . So, we may consider the phase of the master oscillator, η , as only one state variable of the master oscillator. Then we can reduce (8) to the following equation.

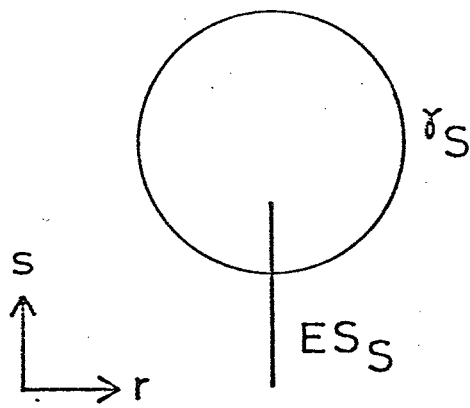
$$\begin{aligned}
 d\eta/dt &= 1/\tau_M \\
 dr/dt &= h(r, s) + \epsilon \cdot c(\eta, r, s) \\
 ds/dt &= i(r, s) + \epsilon \cdot d(\eta, r, s),
 \end{aligned}
 \tag{9}$$

where $\eta \in S^1$. The system (9) has the two-dimensional invariant torus which is close to $S^1 \times \gamma_S$ in its three dimensional phase space $(\eta, r, s) = S^1 \times R^2$ (Levinson, 1950). The circadian rhythm of *Drosophila* persists in DD. So, the master oscillator synchronizes the slave oscillator in DD condition. In our model, this fact implies that the system (9) has a stable limit cycle γ with a period of τ_M on the invariant torus. A stable manifold of a point on γ whose η -coordinate is α , is a set, $\{(\eta, r, s); \eta = \alpha\}$. Because we assume that the slave oscillator is insensitive to the light pulse and duration of perturbation (15 minutes) is very short compared with the period of oscillation, the state point (η, r, s) of (9) is perturbed to $(\eta + \Delta\phi(\eta), r, s) = (\phi'(\eta), r, s)$ by the light pulse, where $\Delta\phi(\eta)$ and $\phi'(\eta)$ are the steady state PRC and PTC of *Drosophila*. That is, the light pulse has no immediate influence on the slave oscillator. The event surface of the two coupled oscillators, i.e. (9), is close to $S^1 \times ES_S$, because ε in (9) is small.

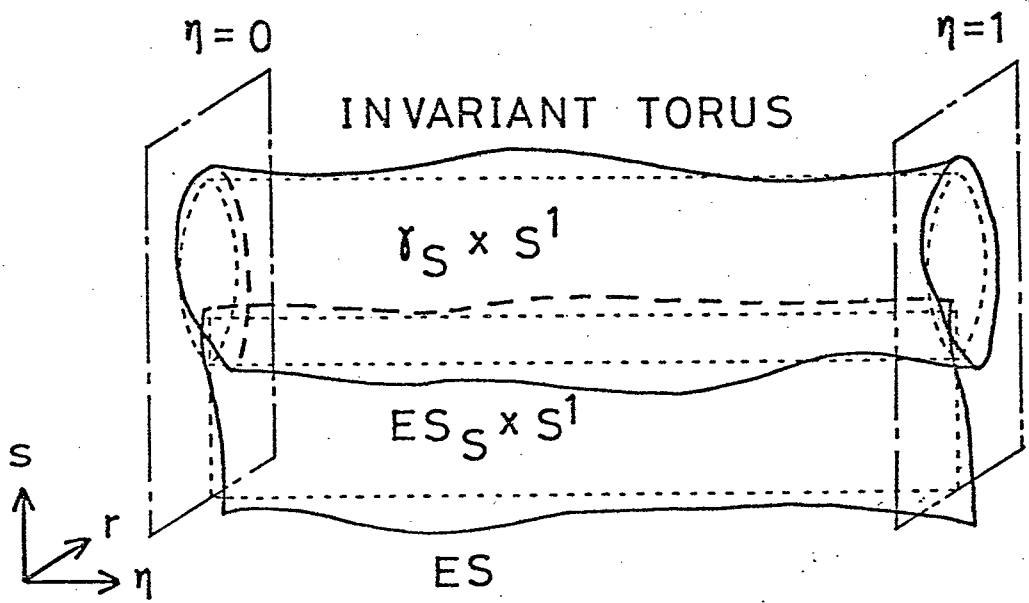
Let us illustrate the invariant torus, the event surface ES , the limit cycle γ and the set of points perturbed from γ , C_μ of the system (9) in Fig. 10. Fig 10.a is the phase plane of (7). For simplicity of the illustration, we assume that the limit cycle of the slave oscillator (7), γ_S is a circle and its event surface, ES_S is a semi-infinite line. Of course this assumption is not essential to the following development. In Fig.10b we draw the three dimensional phase space of (9). The abscissa is η . The vertical plane is the (r, s) -plane whose η coordinate is constant. Since η is the phase, we identify the right vertical plane $\{(\eta, r, s); \eta = 1\}$ with the left vertical plane $\{(\eta, r, s); \eta = 0\}$. The cylinder and the vertical plane, which are drawn with dotted lines, are $\gamma_S \times S^1$ and $ES_S \times S^1$ respectively. From Levinson's Theorem (1950) there exists invariant torus which is close to $\gamma_S \times S^1$ in the phase space. We figure it with bold and solid lines. The event surface of (9), which is close to $ES_S \times S^1$, is also drawn with bold and solid lines. The

Fig. 10

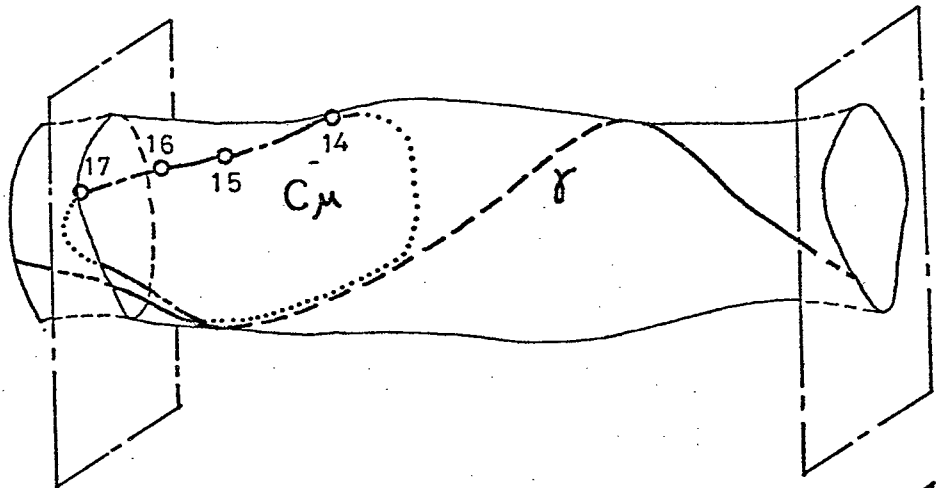
a



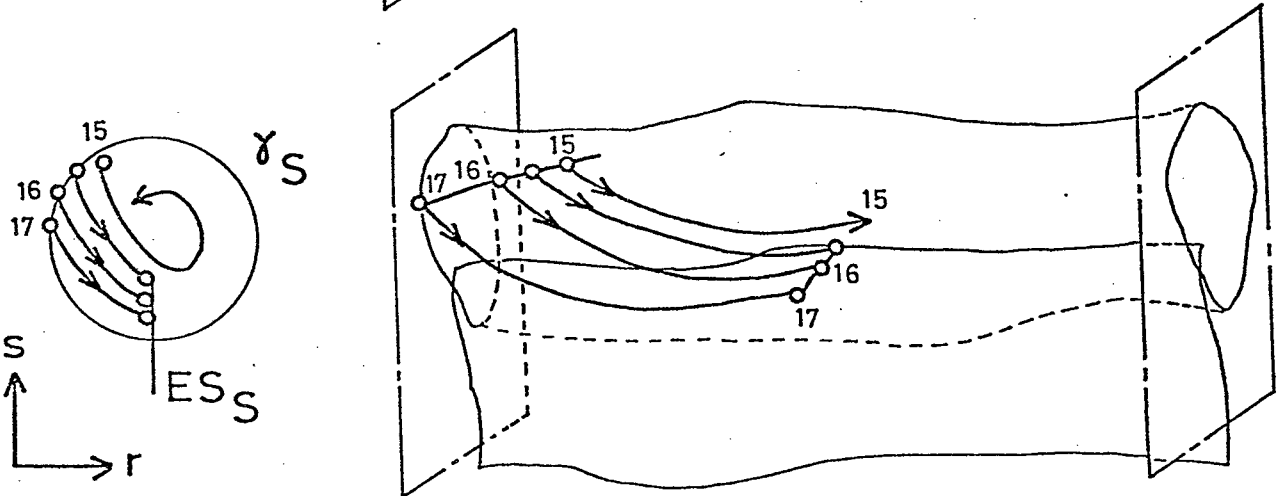
b



c



d



invariant torus and ES in Fig. 10b are drawn arbitrarily as an example.

In Fig. 10c the limit cycle γ is drawn with a solid line and a broken line (hidden part). γ coils itself round the invariant torus. γ is expressed as a set $\{\theta^{-1}(\phi); \phi \in S^1\}$. In this case the map θ^{-1} can be expressed as follows in the (η, r, s) -coordinates. $\theta^{-1} = (\theta_{\eta}^{-1}, \theta_r^{-1}, \theta_s^{-1})$. The light pulse does not change (r, s) -coordinates. The stable manifold of $\theta^{-1}(\phi)$, $W^s(\theta^{-1}(\phi))$ is the set $\{(\eta, r, s); \eta = \theta_{\eta}^{-1}(\phi)\}$. Consequently, if we neglect the short duration of perturbation, C_{μ} is a set $\{(\phi'(\theta_{\eta}^{-1}(\phi)), \theta_r^{-1}(\phi), \theta_s^{-1}(\phi)); \phi \in S^1\}$. It can be determined from γ and the steady state PTC $\phi'(\phi)$. Since ϵ is small, C_{μ} is nearly on the invariant torus (see Fig. 10c, a chain line and a dotted line for a hidden part). In Fig. 10d we show how the big discontinuity of the first transient PTC occurs. Four orbits of (9) starting from four points on C_{μ} , $C(15/24, \mu)$, $C(15.5/24, \mu)$, $C(16/24, \mu)$ and $C(17/24, \mu)$ are shown. The left diagram is its projection on (r, s) -plane. The orbit which starts from $C(15.5/24, \mu)$ crosses the boundary of ES. This is the second kind of discontinuity. Consequently, a quite general Master-Slave model is consistent with the *Drosophila*'s PTCs.

Pittendrigh, Bruce and Kaus (1958) and Kaus (1976) explained the transients measured by Pittendrigh using one oscillator and a linear oscillator. In section 1.6 we proved that at least 3rd variable is necessary for modelling the fly clock using the data of transients. The two references cited above explained the real data using a specific model. The section 1.6 imposes restrictions on the possible model of *Drosophila*'s clock using the experimental data. These two approaches are opposite in their directions and supplement each other. In this section we adopt a two-oscillator interpretation which consists of two loosely coupled limit cycle oscillators and explained the big discontinuity in the transient phase response curve. Our

model is different from those of the two references cited above in the second (slave) oscillator and our discussion is purely analytical and topological.

1. 8 Notes for phase response curves

We studied the properties of the human finger tapping neural network psychologically using PTC. We assume that an oscillatory neural network controls the human finger tapping (Yamanishi, Kawato and Suzuki, 1979). Two kinds of experiments were performed. In the first experiment, we showed that the PTC was available to estimate the degree of functional interaction between the finger tapping neural network and that which controls another task. Three tasks (rapid key-pushing, rapid voicing and pattern discrimination) were chosen as the perturbation of the phase resetting experiment. Analyzing shapes of PTCs, it was found that the interaction with the key-pushing network was the largest, and that with the pattern recognition network was the smallest of the three. In the second experiment, we modified the first task as perturbation of the phase resetting experiments to investigate further the interactions between the left and the right hand motor systems. Consequently the following results were revealed. First, shapes of PTCs are very different according as subject's experiences of finger tapping. Second, the type of PTC for some subjects changes from Type 0 to Type 1 by learning. Third, the PTC tends to become Type 0 for shorter tapping periods. Fourth, neither changes of motor loads (the necessary force to push the key) nor an alternation of the tapping hand and the key-pushing hand affects the shape of PTCs. In the paper (Yamanishi, Kawato and Suzuki, 1980), we investigate the control mechanism of the coordinated finger tapping by both hands. First, the subjects were instructed to coordinate the finger tapping by both hands so as to keep the phase difference between two hands constant. The performance

was evaluated by a systematic error and a standard deviation of phase differences. Second, we propose two coupled neural oscillators as a model for the coordinated finger tapping. Dynamical behavior of the model system is analyzed by using phase transition curves which were measured on one hand finger tapping in the previous experiment. Prediction by the model is in good agreement with the results of the experiments. Therefore, it is suggested that the neural mechanism which controls the coordinated finger tapping may be composed of a coupled system of two neural oscillators each of which controls the right and the left finger tapping respectively.

A skeleton photoperiod consists of two short pulses which are applied on the circadian oscillator at times corresponding to the beginning and to the end of a continuous light stimulus. To study several problems in entrainment of circadian rhythms by skeleton photoperiods, we develop a simple, diagrammatic solution of the steady state entrainment making use of phase transition curves which are directly gotten from phase response curves (Kawato and Suzuki, 1981). The graphical method is simple and systematic to study entrainment by light cycles with various day lengths. As the method is also intuitive, we can easily examine three problems. (1) In *Drosophila* the phase relation (ψ) between rhythm and light cycle is a continuous function of day length of skeleton photoperiods up to about 12 hours, but a marked discontinuity (ψ -jump) sets in between 13 and 14 hours. By the diagrammatic method we find that ψ -jump is mathematically a bifurcation phenomenon. (2) The action of photoperiods up to about 12 hours is fully simulated by two 15-minute skeleton pulses. Do 3-minute skeleton pulses imitate the complete photoperiods? We find that pulse width is arbitrary to some extent. (3) Why skeleton photoperiods up to about 12 hours are good models of complete photoperiods? The reason is the small amplitude and the nearly symmetrical form of phase response curves in the subjective

day.

CHAPTER 2

TWO COUPLED NEURAL OSCILLATORS AS A MODEL OF THE CIRCADIAN PACEMAKER

2.1 Introduction

There is much experimental evidence to suggest that two coupled oscillators may constitute the circadian pacemaker system. Two coupled oscillators were originally proposed to account for transient resetting patterns in the circadian rhythm of *Drosophila* (Pittendrigh and Bruce, 1959). Many phenomena (e.g. the transient resetting patterns, the two-pulse experiment, the rhythm splitting results, the spontaneous disappearance of rhythmicity and its reappearance, the non-monotonic transients) have been explained by the two-oscillator model. But most of these are not decisive evidence for the two-oscillator system. For example, the transient period of phase response curves can be explained by a simple one oscillator (Kawato and Suzuki, 1978; Kawato, 1981a). The most compelling evidence for the two-oscillator system in vertebrates is the occurrence of "splitting" of free-running activity rhythms into two distinct components. These two components typically run for a number of cycles with different frequencies before locking on to the stable condition where they are 180° anti-phase to one another. "Splitting" was first encountered as a response of the arctic ground squirrel free-running in constant light (Pittendrigh, 1960). Splitting occurs frequently in the golden hamster exposed to constant bright light (Pittendrigh, 1974; Pittendrigh and Daan, 1976). Hoffman (1971) reported that the splitting phenomenon was even more reproducible in the small diurnal primate *Tupaia*. In *Tupaia* rhythm splitting was induced by a drop in light intensity. Moreover it is not the magnitude of the step down in light intensity that initiates splitting, but rather the reduction of illumination below a certain level. A free-running

period of the splitting rhythm is longer than that of the single rhythm.

Hoffman found an evident hysteresis phenomenon. A single pattern of circadian activity persisted for increase of the light intensity. If the illumination was reduced below a certain level (about 1 or 0.1 lux depending on individuals), the rhythm split into two components. A further reduction in light intensity did not essentially change this pattern. When the light intensity was again increased fusion of two components took place. But higher intensities (about 100 lux) were necessary in order to fuse the two components. So, it is easier to maintain the single pattern or the split pattern than to initiate them.

Winfree (1967) proposed populations of coupled oscillators as a model for circadian rhythms. He found a splitting-like phenomenon on the behavior of 71 nearly identical electronic oscillators, each weakly interacting with all the others. Pavlidis (1973) has suggested a scheme of elastic coupling whereby two stable periodic solutions can be obtained by coupling n oscillators. In one solution, all units oscillate in synchrony and in phase. In another solution the oscillators form two groups with opposite phase. The former may correspond to a single pattern of locomotor activity and the latter may correspond to a splitting pattern. However, his proof of stability is incomplete. Mathematical analysis of many oscillators, each interacting with all the others, seems to be difficult.

A model for circadian pacemakers consisting of two coupled oscillators has been proposed in qualitative terms by Pittendrigh (1974). Pavlidis (1978) summarized the major properties of coupled oscillators which relate to circadian rhythms in a non-mathematical way. Daan and Berde (1978) developed and expanded the phenomenological model proposed by Pittendrigh using an explicit quantitative structure. Their algorithm is based on two

oscillators defined entirely in terms of their time course (period length, phase and phase shifts). They assumed that the interaction between two oscillators is by instantaneous resets similar to Pavlidis' (1973) analysis of firefly synchronization. Their model system can simulate several qualitative features in the experimental data. However, first their assumption of instantaneous resets seems to be unnatural. For example, if the multiple circadian pacemakers are tonic pacemaking neurons, the interaction between them can be treated as instantaneous resets. However, if they are bursting neurons, it cannot be. Anyway, the continuous representation of the coupling by the system of differential equations includes the representation of instantaneous resets. Second, it is dangerous to use phase response curves in the study of mutual synchronization without evidence that a state point of one oscillator returns quickly to its limit cycle after perturbation by another oscillator. So we study the two limit cycle oscillators which interact with each other in a continuous manner. In this framework we must use differential equation models.

If we assume that the circadian pacemaker of Tupaia is composed of two coupled oscillators and the coupled system is described by a system of ordinary differential equations, Hoffman's experiment is interpreted as follows. At the high intensity of illumination (>100 lux) the only stable solution of the coupled system is the in-phase solution where the two components are in phase and create a single pattern of activity. At the low intensity of illumination (<1 or 0.1 lux) the only stable solution is the anti-phase solution where the two components are 180° out of phase and create a splitting pattern. At the medium intensity (1 or 0.1 lux $<$ light intensity <100 lux) the coupled system has two stable solutions, the in-phase solution and the anti-phase solution (see Fig. 11). Which of the two

solutions is actually realized depends on the initial condition, i.e. the initial phase difference between the two oscillators. At the high intensity the anti-phase solution may be unstable or may not exist. Similarly the in-phase solution may be unstable or may not exist at the low intensity. We study whether the two interacting limit-cycle oscillators exhibit such behavior as in Fig. 11.

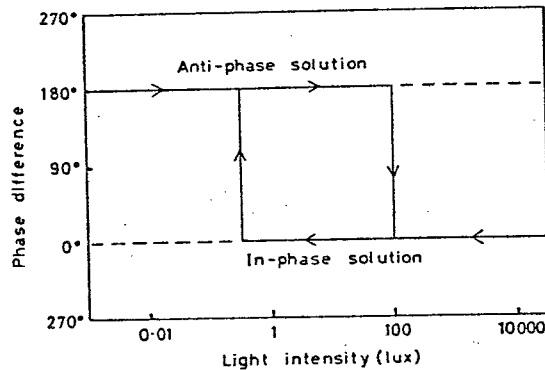


FIG.11 Stable phase difference between the two oscillators of *Tupaia* as a function of the light intensity. A solid line is a stable phase relationship. A dashed line is either an unstable phase difference or non-existence of the phase difference. This figure shows a remarkable hysteresis phenomenon.

2. 2 Assumptions and descriptions of the general model

There have been several mathematical works on the two limit cycle oscillators, which are coupled to each other. Ruelle has generally considered a synchronization effect between two interacting oscillating systems. When the two system are nearly identical, the interaction between the two systems make their periods equal. One may then wonder about the phase difference between the two synchronized oscillators. In general, there may be several phases corresponding to different solutions of the coupled system. If there

is only one solution then, by symmetry, the phase difference must be either 0° or 180° (Ruelle, 1973). Linkens (1977) studied two van der Pol oscillators coupled with a parallel RLC network as a model for intestinal electrical rhythms by the method of harmonic balance. He found that one region in the RLC parameter space give the two stable solutions, the in-phase and the anti-phase solutions, and another parameter region gives only the stable in-phase solution. So, he has proved the simultaneous stability of the two alternative solutions. However, his model is inappropriate for coupled circadian oscillators. Firstly, in neural or circadian modelling we must not think of "condensers" or "coils" in equivalent circuit format. Instead the coupling terms can be rates of change, i.e. 1st or 2nd derivatives terms. However, we do not know what physiological (neural or hormonal etc.) mechanism corresponds to "condenser-" or "coil-" coupling between constituent circadian oscillators. Secondly, there is no evidence that the constituent oscillator is a weakly non-linear oscillator. Thirdly and most conclusively, the anti-phase solution cannot be achieved by changing only the parameter because the in-phase solution is always stable. This is not in agreement with Hoffman's experiment.

By computer simulation, in the system consisting of two Brusselators coupled by diffusion Tyson and Kauffman (1975) found the two stable non-uniform periodic solutions, where the two oscillators oscillate asynchronously with small phase difference. In the same system Ashkenaji and Othmer (1978) proved the coexistence of the stable non-uniform periodic solutions and the stable in-phase solution by the method of the secondary bifurcation. However, their non-uniform solution is quite different from the anti-phase solution. As far as the phase difference is concerned, the non-uniform solution is almost the same with the in-phase solution because the phase differences between the two oscillators in the non-uniform solutions is

almost 0° .

We studied two BVP-model neurons coupled by diffusion as a model of electrotonically coupled neurons (Kawato, Sokabe and Suzuki, 1979). We showed the simultaneous stability of the two alternative solutions (in-phase and anti-phase) by the theory of Hopf bifurcation and computer simulation. Recently we proved it analytically by the method of secondary bifurcation (Kawato, 1981b). But again the diffusion coupled model is inappropriate for a circadian pacemaker because the in-phase solution is always stable whenever the anti-phase solution is stable.

We assume the following five points about the two oscillator system.

- (i) The two oscillators are identical.
- (ii) The coupling between the two oscillators is symmetrical.
- (iii) The coupling is weak.
- (iv) One oscillator in a resting state does not affect another oscillator.
- (v) With changing some environmental parameter Hopf bifurcation occurs in the differential equation which describes the single uncoupled oscillator.

Assumptions (i) and (ii) seem to be too restrictive, but they can be weakened to "nearly identical" and "nearly symmetrical" by discussion of structural stability. Assumption (iii) is reasonable because it took several days for the 180° phase difference to be achieved after the first signs of a split was observed in Hoffman's experiment.

For many animals it was revealed that anatomical loci of circadian pacemakers are parts of central nervous systems (e.g. the lobula region of the optic lobes for cockroaches, Nishiitsutsuji-Uwo and Pittendrigh, 1968; Page, Caldarola and Pittendrigh, 1977; suprachiasmatic nucleus (SCN) of the hypothalamus for rodents, Moore and Eichler, 1972; Ibuka and Kawamura, 1975; Inouye and Kawamura, 1979; midbrain for moths, Truman, 1971). Hudson and

Lickey (1977) found that the phase difference between bilateral ocular circadian pacemakers of *Aplysia* which was released into very dim LL or DD for 29-62 days came to be 180°. Inhibitory neural connections are known to exist between the eyes. In rodents Inouye (pers. comm.) found that the phase difference between the bilateral SCN is not 0° in a few cases by recording multiple unit activity. Recently the direct synaptic connections between bilateral SCN have been found. Consequently, we suppose that the interactions between two constituent circadian pacemakers are long-range. Because the diffusion coupling between neural oscillators (electrotonic coupling, intercellular communication through gap junction etc.) must be short-range, we consider that the diffusion coupling may be unnatural. In the case of long-range interactions by axons and chemical synapses, one neural oscillator in a resting state does not affect another oscillator [assumption (iv)].

As assumption (v) is critical, we must explain it in detail. In many animals an overt circadian rhythm can be discerned in DD but it is not discernible (or it soon damps out) in LL. There may be many interpretations for the damp out of the overt rhythmicity, but we assume that the oscillations of the two constituent oscillators really damp out. Our assumption is as follows. The differential equation which describes the single uncoupled oscillator has a stable equilibrium point in one environmental condition (e.g. LL). The stable equilibrium corresponds to the damp out of the oscillation. With changing some environmental factor the equilibrium point becomes unstable and a stable limit cycle appears via Hopf bifurcation. The limit cycle corresponds to the regular oscillation in another environmental condition (e.g. DD).

Each of our two oscillators (designated 1 and 2) is described by the following nth order differential equation, when the oscillators are un-

coupled.

$$\text{Oscillator 1} \quad \frac{dx_1}{dt} = f(x_1, \mu) \quad (2.1)$$

$$\text{Oscillator 2} \quad \frac{dx_2}{dt} = f(x_2, \mu) \quad (2.2)$$

x_1 and x_2 are n-dimensional vectors and represent state variables of the oscillator 1 and 2 respectively. f is an n-dimensional non-linear vector function and is common for the two oscillators because of assumption (i). μ is a scalar parameter, which represents some environmental factor such as a light intensity or an ambient temperature. $f(x, \mu)$ has an appropriate regularity with respect to μ . The pacemaker system comprising the two coupled oscillators is described by the following equation because of assumption (ii).

$$\begin{aligned} \frac{dx_1}{dt} &= f(x_1, \mu) + g(x_1, x_2, \nu), \\ \frac{dx_2}{dt} &= f(x_2, \mu) + g(x_2, x_1, \nu), \end{aligned} \quad (2.3)$$

g is an n-dimensional non-linear function, which depends on an environmental parameter ν . g represents the coupling between the two oscillators. It has an appropriate regularity with respect to ν . As both f and g contain environmental parameters, our model does not specify whether the effect of light or temperature in free-running conditions is on the two oscillators or on their coupling.

2.3 Analysis of the general two-oscillator model

In this section by the method of Hopf bifurcation we study whether the general

two oscillator system (2.3) has the two stable solutions (in-phase and anti-phase). Without loss of generality we can assume that an origin is an equilibrium point of (2.1) [i.e. of (2.2)], that is, $f(0,\mu)=0$ for all μ . Further we assume that it is stable for $\mu < 0$ and unstable for $\mu > 0$. Assumption (v) implies that a stable limit cycle appears for $\mu > 0$ via a supercritical bifurcation from the origin at $\mu=0$ in (2.1) [i.e. in (2.2)]. Assumptions (iii) and (iv) are expressed as follows:

$$(iii) \quad g(\xi, \eta, \nu) = \delta \cdot h(\xi, \eta, \nu) \quad (2.4)$$

$$(iv) \quad g(\xi, 0, \nu) = 0 \quad (2.5)$$

where δ is a small positive number and $h(\xi, \eta, \nu)$ is a C^1 -function (1-times continuously differentiable).

$$\partial g(\xi, \eta, \nu) / \partial \xi \big|_{(0,0,\nu)} = 0. \quad (2.6)$$

We can evaluate another derivative of g as follows because of (2.4.).

$$\partial g(\xi, \eta, \nu) / \partial \eta \big|_{(0,0,\nu)} = \delta \cdot D(\nu), \quad (2.7)$$

where $D(\nu) = \partial h(\xi, \eta, \nu) / \partial \eta \big|_{(0,0,\nu)}$ is an $n \times n$ matrix depending on the parameter ν .

Let $df(0,\mu)$ be a linearization matrix (i.e. Jacobian matrix); $df(0,\mu) = \partial f^j(0,\mu) / \partial \xi^k$ of $f(\xi,\mu)$ around $(0,\mu)$. From assumption (v), $df(0,\mu)$ has two distinct, complex conjugate eigenvalues $\lambda(\mu)$ and $\overline{\lambda(\mu)}$ such that $\text{Re} \lambda(\mu) \geq 0$ for $\mu \geq 0$. As both $f(0,\mu)$ and $g(0,0,\nu)$ are zero, the origin is an equilibrium point of (2.3). We investigate the in-phase and anti-phase solutions of (2.3) by making a change of co-ordinates as $z = (x_1 + x_2) / 2$ and $w = (x_1 - x_2) / 2$. z

is a mean of states of the two oscillators and w is their difference. In the new co-ordinates (2.3) becomes

$$\begin{aligned} dz/dt &= [df(0, \mu) + \delta \cdot D(v)] \cdot z + R_1(z, w, \mu, v) \\ dw/dt &= [df(0, \mu) - \delta \cdot D(v)] \cdot w + R_2(z, w, \mu, v), \end{aligned} \quad (2.8)$$

because of (2.6) and (2.7). Here, R_1 and R_2 contain only higher order terms than the second order. Because the periodic solution which bifurcates from the origin of (2.3) is unique, it is either the in-phase or the anti-phase solution, as Ruelle has pointed out (1973). Because z is the mean, the in-phase solution bifurcates from the origin when the matrix $[df(0, \mu) + \delta \cdot D(v)]$ becomes unstable.

Let us denote the n eigenvalues of $df(0, \mu)$ by $[\lambda(\mu), \overline{\lambda(\mu)}, \lambda_3(\mu), \lambda_4(\mu), \dots, \lambda_n(\mu)]$. Note that $\text{Re} \lambda_i(\mu) < 0$ ($i=3, \dots, n$) for small μ . Similarly denote n eigenvalues of $[df(0, \mu) + \delta \cdot D(v)]$ and those of $[df(0, \mu) - \delta \cdot D(v)]$ by $[\zeta(\mu), \overline{\zeta(\mu)}, \zeta_3(\mu), \dots, \zeta_n(\mu)]$ and $[\gamma(\mu), \overline{\gamma(\mu)}, \gamma_3(\mu), \dots, \gamma_n(\mu)]$ respectively. Because an eigenvalue is a continuous function of elements of matrices and δ is small, $\zeta(\mu)$ and $\gamma(\mu)$ correspond to $\lambda(\mu)$ and are close to it. Similarly $\zeta_i(\mu)$ and $\gamma_i(\mu)$ are close to $\lambda_i(\mu)$ ($i=3, \dots, n$). Note that $\text{Re} \zeta_i(\mu) < 0$ and $\text{Re} \gamma_i(\mu) < 0$ ($i=3, \dots, n$) for small μ . $\zeta(\mu)$ and $\gamma(\mu)$ can be expressed as follows:

$$\begin{aligned} \zeta(\mu) &= [\text{Re} \lambda(\mu) + \alpha(\delta, \mu, v)] + i [\text{Im} \lambda(\mu) + \beta(\delta, \mu, v)], \\ \gamma(\mu) &= [\text{Re} \lambda(\mu) + \alpha(-\delta, \mu, v)] + i [\text{Im} \lambda(\mu) + \beta(-\delta, \mu, v)], \end{aligned}$$

where $\alpha(\delta, \mu, v)$ and $\beta(\delta, \mu, v)$ are analytic real functions of δ and go to zero as δ goes to zero.

Theorem 2. 1. (Case I). If $\partial\alpha(\delta,\mu,\nu)/\partial\delta|_{(0,0,\nu)} > 0$, with increasing μ , first the in-phase solution bifurcates at negative μ_I . It is stable if the bifurcation is supercritical. Second the unstable anti-phase solution bifurcates at positive μ_A .

Theorem 2. 2. (Case II). If $\partial\alpha(\delta,\mu,\nu)/\partial\delta|_{(0,0,\nu)} < 0$, first the anti-phase solution bifurcates at negative μ_A and next the in-phase solution bifurcates at positive μ_I . The anti-phase solution is stable if the bifurcation is supercritical. The in-phase solution is always unstable near the bifurcation point ($\mu \sim \mu_I$) regardless of its direction of bifurcation.

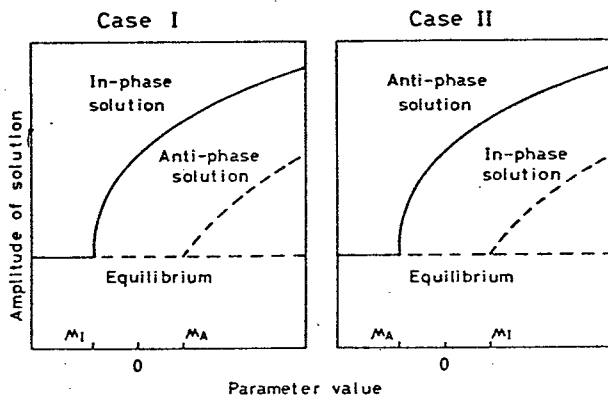


FIG. 12 Bifurcation diagram of the general two-oscillator system. A solid line shows a stable solution, and a dashed line shows an unstable solution. μ_I and μ_A are primary bifurcation points of the in-phase and anti-phase solutions respectively.

Proof of Theorem 2.1 When $\text{Re}\zeta(\mu)$ becomes zero (i.e. $[df(0,\mu)+\delta\cdot D(v)]$ becomes unstable), the in-phase solution bifurcates from the origin. Let μ_I denote the parameter value μ at which the in-phase solution bifurcates. As δ is small, μ_I is close to zero. Since $f(x,\mu)$ and $g(\xi,\eta,\nu)$ are regular with respect to μ and η , $\alpha(\delta,\mu,\nu)$ and $\beta(\delta,\mu,\nu)$ have regularities with respect to μ and ν . As $\partial\alpha(\delta,\mu,\nu)/\partial\delta|_{(0,0,\nu)}$ is positive, $\partial\alpha(\delta,\mu,\nu)/\partial\delta|_{(0,\mu_I,\nu)}$

is also positive. So, $\alpha(\delta, \mu_I, \nu)$ is positive for small positive δ because $\alpha(0, \mu_I, \nu) = 0$. Because $\text{Re}\zeta(\mu_I) = 0$ implies that $\text{Re}\lambda(\mu_I) = -\alpha(\delta, \mu_I, \nu) < 0$, μ_I is negative.

Similarly let μ_A denote μ at which the bifurcation of the anti-phase solution from the origin occurs. Because $\alpha(-\delta, \mu_A, \nu)$ is negative, $\text{Re}\lambda(\mu_A) = -\alpha(-\delta, \mu_A, \nu) > 0$ [i.e. $\text{Re}\gamma(\mu_A) = 0$]. So, μ_A is positive.

In order to analyze stabilities of the in-phase and the anti-phase solutions, we must examine characteristic (Floquet) exponents of them. $(2n-2)$ characteristic exponents out of $(2n-1)$ exponents of the in-phase solution are close to $[\zeta_3(\mu_I), \dots, \zeta_n(\mu_I), \overline{\gamma(\mu_I)}, \gamma_3(\mu_I), \dots, \gamma_n(\mu_I)]$ multiplied by $\exp(\tau_I^C)$ at $\mu \sim \mu_I$, where τ_I^C is a period of the in-phase solution. Real parts of all these $(2n-2)$ characteristic exponents are negative. First $\text{Re}\zeta_i(\mu_I)$ and $\text{Re}\gamma_i(\mu_I)$ ($i=3, \dots, n$) are negative as μ_I is small. Second $\text{Re}\gamma(\mu_I) = \text{Re}\lambda(\mu_I) + \alpha(-\delta, \mu_I, \nu) = -\alpha(\delta, \mu_I, \nu) + \alpha(-\delta, \mu_I, \nu)$ is negative. The rest one characteristic exponent is negative if the bifurcation is supercritical. It is positive if direction of the bifurcation is subcritical. So, in the supercritical case the in-phase solution is stable.

$(2n-2)$ characteristic exponents of the anti-phase solution are close to $\{\zeta(\mu_A), \overline{\zeta(\mu_A)}, \zeta_3(\mu_A), \dots, \zeta_n(\mu_A), \gamma_3(\mu_A), \dots, \gamma_n(\mu_A)\}$ multiplied by $\exp(\tau_A^C)$. τ_A^C is a period of the anti-phase solution. Because $\text{Re}\zeta(\mu_A) = \text{Re}\lambda(\mu_A) + \alpha(\delta, \mu_A, \nu) = -\alpha(-\delta, \mu_A, \nu) + \alpha(\delta, \mu_A, \nu) > 0$, the anti-phase solution is always unstable near the bifurcation point (i.e. $\mu \sim \mu_A$) regardless of direction of bifurcation.

The proof of Theorem 2.2 is the same as that of Theorem 2.1. Consequently, there are two cases for sequence of bifurcations and stability of the two solutions. Case II is quite contrary to Case I. In Fig. 12 we illustrate an amplitude of asymptotic solutions of (2.3) as a function of the bifurcation

parameter μ . If a decrease of the light intensity in Hoffman's experiment corresponds to decreasing $\partial\alpha(\delta, \mu, \nu)/\partial\delta|_{(0,0,\nu)}$ via changing the environmental parameter ν , then our general model roughly explains Hoffman's experiment. Concerning the coexistence of the stable in-phase and anti-phase solutions at the medium light intensity, the following can be expected. The bifurcation points μ_I and μ_A are continuous functions of δ . $\mu_I < \mu_A$ for ν of Case I, and $\mu_I > \mu_A$ for ν of Case II. By the theorem of intermediate value, there exists ν such that the two bifurcation points collapse. Since "multiple eigenvalues lead to secondary bifurcation" (Bauer, Keller and Reiss, 1975) we expect secondary bifurcations of the anti-phase solution in Case I and the in-phase solution in Case II and their stability changes. Rigorous proof of this and study of the hysteresis phenomena need a more concrete model, so in the succeeding sections we analyze a specific model.

2. 4 Two coupled neural oscillator model

Although for many animals it was revealed that anatomical loci of circadian pacemakers are parts of central nervous systems, whether the pacemaker consists of a population of neurons, a single neuron or part of a neuron remains unknown. Taking account of these possibilities, we use the following system of differential equations as a model of a single oscillator:

$$\begin{aligned} dx/dt &= (\mu+1)x - x^3 - y \\ dy/dt &= 2x - y, \end{aligned} \tag{2.9}$$

μ is an environmental parameter.

Equation (2.9) is a simplified version of either the Wilson-Cowan

equations, FitzHugh's BVP equation or Nagumo's equation (Wilson and Cowan, 1972; FitzHugh, 1961; Nagumo, Arimoto and Yoshizawa, 1962). Wilson and Cowan derived the coupled non-linear differential equations for the dynamics of spatially localized populations containing both excitatory and inhibitory neurons. We reduce their equations to (2.9) by some simplification. Physiological implications of the simplification were discussed by Nogawa et al. (1976). Let $E(t)$ [$I(t)$] denote the proportion of excitatory (inhibitory) cells firing per unit time at the instant t . In the transformation of the original Wilson-Cowan equation into (2.9), we set $x(t) = k_1 E(t) + k_2$, $y(t) = k_3 I(t) + k_4$ ($k_1, k_3 > 0$). So $x(t)$ and $y(t)$ may be negative. It is known that the Wilson-Cowan equation has a stable limit cycle for appropriate parameter values. Ermentrout and Cowan (1979) showed that the stable limit cycle arises from an equilibrium point via Hopf bifurcation with changing some parameter. The BVP model and Nagumo's equation are considered as a simplified version of the Hodgkin-Huxley equation (Hodgkin and Huxley, 1952). We can further reduce them to (2.9) by some change of variables and parameters. In this case x of (2.9) is the membrane potential of a neuron and y is a quantity of refractoriness. The BVP equation has a stable limit cycle for an appropriate stimulus current. Hadel, an der Heiden and Schumacher (1976) showed that the stable limit cycle appears as a result of the Hopf bifurcation.

System (2.9) has an equilibrium point $(0,0)$ for all μ . For $\mu < 1$, there is no other equilibrium point. Hereafter we deal with only the parameter range $\mu < 1$. We define for any $\alpha > 0$ a rectangle $R_\alpha = \{(x,y) : |x| < \alpha, |y| < 2\alpha\}$. Let $\alpha > \sqrt{\mu + 3}$. Then all trajectories of system (2.9) enter the rectangle R_α . Two eigenvalues of a linearized matrix around the origin $(0,0)$ of (2.9) are given as follows:

$$\lambda(\mu), \bar{\lambda}(\mu) = [\mu \pm \sqrt{\mu^2 - 4(1-\mu)}] / 2$$

Consequently, the origin is stable for $\mu < 0$ and unstable for $\mu > 0$. For $0 < \mu < 1$, Poincare-Bendixon's theorem asserts that there exists at least one stable limit cycle in R_α because R_α ($\alpha > \sqrt{\mu+3}$) is invariant and the unique equilibrium point $(0,0)$ is unstable. The Hopf bifurcation theorem tells us much about the stable limit cycle. The periodic solution whose expansion is given in Kawato and Suzuki (1980) bifurcates from the origin at $\mu=0$. It is stable and exists for $\mu > 0$ (supercritical bifurcation). A period of the oscillator, τ^u , is almost 2π for $\mu \approx 0$. For $\mu < 0$ there is no periodic solution and this corresponds to the fact that organisms do not show circadian rhythm under some environment.

Consequently (2.9) can be regarded as a model of either a neural network oscillator or a single cell oscillator. However, it is highly doubtful whether (2.9) is a good model for the single constituent circadian oscillator because the Wilson-Cowan equation, the BVP equation and Nagumo's equation were derived for neural rhythms with much shorter periods than 24h. However, in the absence of information regarding the state variables relevant to circadian pacemakers, we use the abstract model (2.9).

We study the two identical neural oscillators which are coupled to each other in a linear form. Quantities of the oscillator 1 are denoted by a suffix 1 and those of the oscillator 2 are denoted by a suffix 2. Our specific two-oscillator model is described by the following equation.

$$\begin{aligned}
 dx_1/dt &= (\mu+1)x_1 - x_1^3 - y_1 + \delta \cdot x_2 - a \cdot y_2 \\
 dy_1/dt &= 2x_1 - y_1 + b \cdot x_2 - v\delta \cdot y_2 \\
 dx_2/dt &= (\mu+1)x_2 - x_2^3 - y_2 + \delta \cdot x_1 - a \cdot y_1 \\
 dy_2/dt &= 2x_2 - y_2 + b \cdot x_1 - v\delta \cdot y_1
 \end{aligned}
 \tag{2.10}$$

x_1, y_1, x_2 and y_2 are scalar values. δ, a and b are small positive constants. v is a positive constant of order 1. The parameters μ and v depend on environmental conditions. Equation (2.10) satisfies the five assumptions in section 3.2.

In the interpretation of (2.9) as a simplified Wilson-Cowan equation, δ is coupling strength of excitatory synaptic connection from an excitatory subpopulation of one oscillator to an excitatory subpopulation of another oscillator. a is that of inhibitory synaptic connection from an inhibitory subpopulation of one oscillator to an excitatory subpopulation of another oscillator. b is that from an excitatory subpopulation to an inhibitory subpopulation. $v\delta$ is that from inhibitory one to inhibitory one (see Fig. 13). In the interpretation of (2.9) as a simplified BVP equation or a Nagumo's equation, physical mechanism of the linear coupling is obscure. However, δ is strength of interaction from the quantity of excitation (membrane potential) of one oscillator to the quantity of excitation of another oscillator. b is

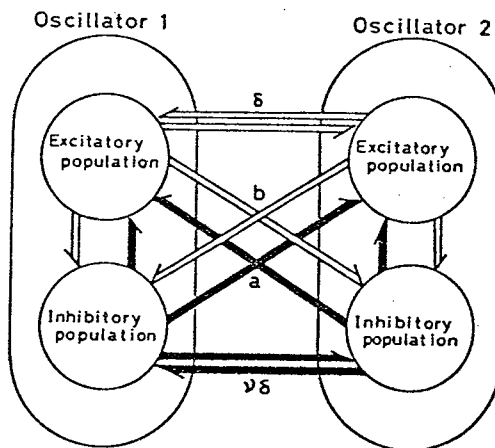


FIG.13 Schematic diagram of the two-nucleus oscillators which are coupled to each other by excitatory and inhibitory synaptic connections. Each oscillator contains the excitatory subpopulation and the inhibitory subpopulation.

that from excitation to inhibition, and $v\delta$ is that from inhibition to inhibition.

2.5 Primary and secondary bifurcations of the neural model

In order to study the in-phase and anti-phase solutions of (2.10), we make the following change of variables as in section 2.3:

$$p = (x_1 + x_2)/2,$$

$$q = (y_1 + y_2)/2,$$

$$r = (x_1 - x_2)/2,$$

$$s = (y_1 - y_2)/2.$$

For convenience of calculations, we further transform (2.10) into a canonical form by the following change of variables,

$$\begin{pmatrix} x \\ y \\ z \\ w \end{pmatrix} = \begin{pmatrix} 1 & 0 & 0 & 0 \\ (1+v\delta)/(1+a) & -\Omega_I/(1+a) & 0 & 0 \\ 0 & 0 & 1 & 0 \\ 0 & 0 & (1-v\delta)/(1+a) & -\Omega_A/(1+a) \end{pmatrix}^{-1} \begin{pmatrix} p \\ q \\ r \\ s \end{pmatrix}$$

where

$$\Omega_I = \sqrt{1 - 2v\delta - v^2\delta^2 + 2a + b + ab},$$

$$\Omega_A = \sqrt{1 + 2v\delta - v^2\delta^2 - 2a - b + ab}.$$

In the new co-ordinates (2.10) becomes,

$$\frac{d}{dt} \begin{pmatrix} x \\ y \\ z \\ w \end{pmatrix} = \begin{pmatrix} \mu + (1-\nu)\delta & \Omega_I & 0 & 0 \\ \Omega_I^*(\mu) & 0 & 0 & 0 \\ 0 & 0 & \mu + (\nu-1)\delta & \Omega_A \\ 0 & 0 & -\Omega_A^*(\mu) & 0 \end{pmatrix} \begin{pmatrix} x \\ y \\ z \\ w \end{pmatrix} \quad (2.11)$$

$$+ \begin{pmatrix} -x(3z^2+x^2) \\ -(1+\nu\delta)/\Omega_I \cdot x(3z^2+x^2) \\ -z(3x^2+z^2) \\ -(1-\nu\delta)/\Omega_A \cdot z(3x^2+z^2) \end{pmatrix}$$

where

$$\Omega_I^*(\mu) = [(1+a)(2+b) - (1+\nu\delta)(\mu+1+\delta)]/\Omega_I,$$

$$\Omega_A^*(\mu) = [(1-a)(2-b) - (1-\nu\delta)(\mu+1-\delta)]/\Omega_A.$$

Note that $\Omega_I^*[(\nu-1)\delta] = \Omega_I$ and $\Omega_A^*[(1-\nu)\delta] = \Omega_A$. The origin $(0,0,0,0)$ is an equilibrium point of (2.11). Four eigenvalues of a linearized matrix around the origin of the system (2.11) are,

$$\zeta(\mu), \overline{\zeta(\mu)} = \{ [\mu + (1-\nu)\delta] \pm \sqrt{[\mu + (1-\nu)\delta]^2 - 4\Omega_I \cdot \Omega_I^*(\mu)} \} / 2,$$

$$\gamma(\mu), \overline{\gamma(\mu)} = \{ [\mu + (\nu-1)\delta] \pm \sqrt{[\mu + (\nu-1)\delta]^2 - 4\Omega_A \cdot \Omega_A^*(\mu)} \} / 2.$$

$\zeta(\mu)$ and $\overline{\zeta(\mu)}$ correspond to the in-phase component (x,y) . $\gamma(\mu)$ and $\overline{\gamma(\mu)}$ correspond to the anti-phase component (z,w) . The function $\alpha(\delta,\mu,\nu)$ in section 2.3 is

$$\alpha(\delta,\mu,\nu) = (1-\nu)\delta$$

in this case. The in-phase solution of a frequency Ω_I bifurcates at $\mu_I = (\nu-1)\delta$ from the origin and the anti-phase solution of a frequency Ω_A bifurcates at $\mu_A = (1-\nu)\delta$ from the origin. The bifurcating in-phase and anti-phase solutions $[X_I(t) \text{ and } X_A(t)]$ can be expanded into the convergent analytical series by standard perturbation procedure when μ is sufficiently close to μ_I and μ_A respectively. They are given in Kawato and Suzuki (1980). Both bifurcations are supercritical. According to the classification in section 2.3, there are two cases.

Case I. If $\nu < 1$ [i.e. $\partial\alpha(\delta, \mu, \nu)/\partial\delta|_{(0,0,\nu)} = (1-\nu) > 0$ in section 2.3], with increasing μ , first the stable in-phase solution bifurcates at negative μ_I and next the unstable anti-phase solution bifurcates at positive μ_A . One characteristic exponent of the anti-phase solution is negative because the bifurcation is supercritical. Other two complex conjugate exponents [which are close to $\zeta(\mu_A)$ and $\overline{\zeta(\mu_A)}$ multiplied by $\exp(\tau_A^C)$] are positive near the primary bifurcation point $(\mu \sim \mu_A)$. τ_A^C is a period of the anti-phase solution.

Case II. If $\nu > 1$ [i.e. $\partial\alpha(\delta, \mu, \nu)/\partial\delta|_{(0,0,\nu)} = (1-\nu) < 0$], the anti-phase solution bifurcating at negative μ_A is stable and the in-phase solution bifurcating at positive μ_I is unstable.

From bifurcation theory we know that only the first bifurcating solution (the in-phase in Case I and the anti-phase in Case II) is stable. However, one may wonder whether a stability change of the unstable bifurcating solution (the anti-phase in Case I and the in-phase in Case II) can take place leading to a stable solution. In the present case a stability change of these solutions can particularly be expected to appear through the two complex-conjugate characteristic exponents.

The purpose of this section is to develop an analytical approach to the secondary bifurcations of the in-phase and the anti-phase solutions in the limit where the interaction coefficient δ is small. The basic idea of

our approach is following the works of Bauer, Keller and Reiss (1975) and Erneux and Herschkowitz-Kaufman (1979), to relate the problem of secondary stability changes to the coalescence of the two primary bifurcation points. In our problem, one way to relate $\mu_I = (\nu-1)\delta$ and $\mu_A = (1-\nu)\delta$ in a same bifurcation point is to take $\delta=0$. Because of assumption (iii) in section 2.2, we can assume that δ is small. Secondary bifurcation, from the primary bifurcating branch X_I or X_A , can occur only for values of $\mu = \mu_I^S(\epsilon)$ or $\mu = \mu_A^S(\epsilon)$ at which the linearized problem about X_I or X_A has non-trivial solution. Here, ϵ is an expansion parameter of the primary bifurcating branch. Hereafter we use s as the suffix which indicates the secondary bifurcation point. We consider the linearized problem as an eigenvalue problem in ϵ and solve it by a perturbation expansion in δ . This perturbation procedure is given in Kawato and Suzuki (1980). We omit this because a quite similar procedure is given in chapter 3. Results of the analysis are stated separately in the two cases.

Case I. If $\nu < 1$, there is a secondary bifurcation point on the unstable anti-phase solution. One sees that it is effectively possible to have the stable anti-phase solution for $\mu > \mu_A^S$. At the second order of the perturbation scheme there are no secondary bifurcation points on the stable in-phase solution.

The fact that real parts of the two complex conjugate characteristic exponents of the anti-phase solution change their signs at $\mu = \mu_A^S$ means that Hopf bifurcation of a Poincaré map of the anti-phase solution occurs at $\mu = \mu_A^S$. The Hopf bifurcation theorem for diffeomorphisms poses two possibilities. First, if the Hopf bifurcation of the Poincaré map is supercritical, there exists a stable invariant torus for $\mu < \mu_A^S$. Second, if the bifurcation is subcritical, an unstable invariant torus exists for $\mu > \mu_A^S$. We illustrate

Supercritical case Subcritical case

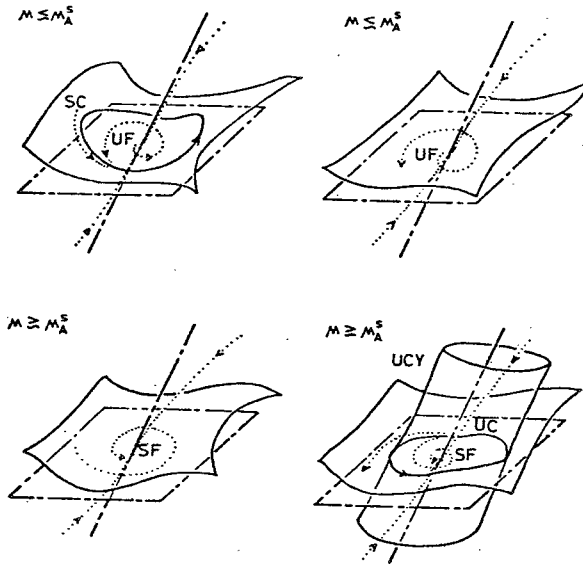


FIG.14 Phase spaces of the Poincaré map of the anti-phase solution. SF and UF are stable and unstable fixed points of the Poincaré map. SC and UC are stable and unstable invariant circles. UCY is the unstable invariant cylinder which is a stable manifold of the unstable circle. As the phase space of (10) is four-dimensional, a phase space of the Poincaré map is three-dimensional. A horizontal plane is the eigenplane of a linearization of the Poincaré map corresponding to the two complex conjugate characteristic exponents. The line which crosses the eigenplane at a fixed point is an eigenline corresponding to one negative characteristic exponent. The fixed point of the Poincaré map corresponds to the anti-phase solution and an invariant circle corresponds to the invariant torus of (10).

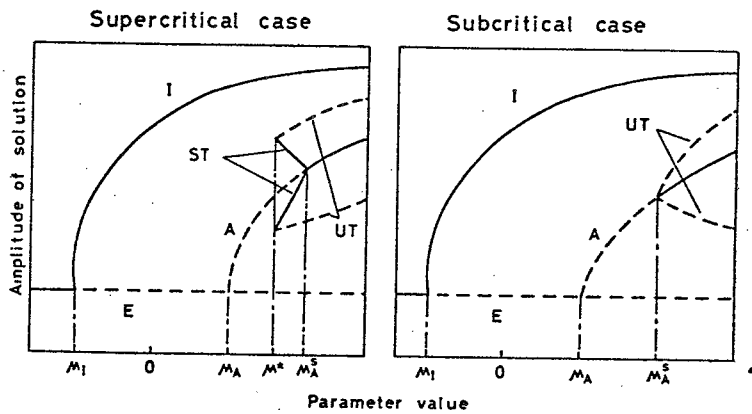


FIG.15 Bifurcation diagrams of the specific two-oscillator model (10) in Case I. There are two cases according to the direction of the Hopf bifurcation of the Poincaré map. In both cases, the in-phase and anti-phase solutions are stable simultaneously for $\mu > \mu_A^s$. I, A, E, ST and UT are the in-phase solution, the anti-phase solution, the equilibrium point, the stable invariant torus and the unstable invariant torus.

these two cases by the Poincaré maps and bifurcation diagrams in Figs 14 and 15 respectively. In the subcritical case, $\{\text{invariant cylinder}\} \times S^1 = \{\text{invariant circle}\} \times R^1 \times S^1 = \{\text{invariant torus}\} \times R^1$ may constitute a frontier between two stable manifolds (regions of attraction) of the in-phase and anti-phase solutions. As both the in-phase and anti-phase solutions are stable for $\mu > \mu_A^S$, in the supercritical case we expect the invariant torus to switch its stability at some $\mu = \mu^* < \mu_A^S$ (see supercritical case in Fig. 15) and $\{\text{resulting unstable invariant torus}\} \times R^1$ to constitute a frontier between the two stable manifolds.

Case II. If $\nu > 1$, there is a secondary bifurcation point on the unstable in-phase solution, but there are no secondary bifurcation points on the stable anti-phase solution. Bifurcation diagrams in Case II are illustrated in Fig. 16.

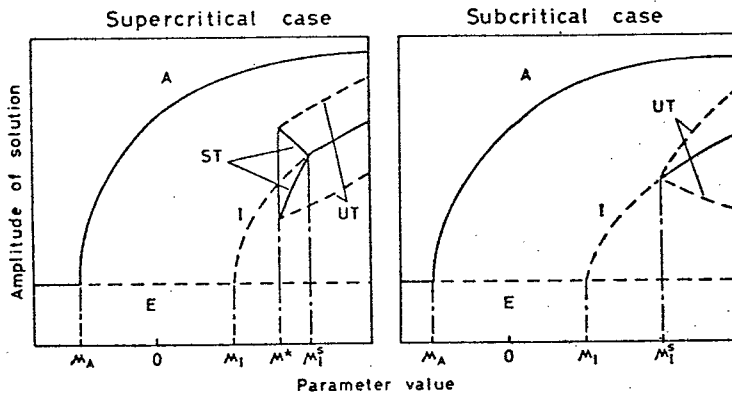


FIG. 16. Bifurcation diagrams of (10) in Case II. The two periodic solutions are stable for $\mu > \mu_1^S$. The abbreviations are the same as in Fig. 5.

2.6 Discussion and conclusions

Let us summarize the results of section 2.5 in Fig. 17. There are two environmental parameters μ and ν ; μ represents the effect of light on the constituent two oscillators and ν represents that on their coupling. Primary and secondary bifurcation points of the in-phase and anti-phase solutions were given as follows.

$$\begin{aligned} \mu_I(\nu) &= (\nu-1)\delta & \mu_I^S(\nu) &\sim 2\mu_I(\nu) \\ \mu_A(\nu) &= (1-\nu)\delta & \mu_A^S(\nu) &\sim 2\mu_A(\nu) \end{aligned} \quad (2.12)$$

For $\nu < 1$, the in-phase solution is stable for $\mu > \mu_I(\nu)$ and the anti-phase solution is stable for $\mu > \mu_A^S(\nu)$. For $\nu > 1$, the anti-phase solution is stable for $\mu > \mu_A(\nu)$ and the in-phase solution is stable for $\mu > \mu_I^S(\nu)$. Consequently, only the in-phase solution is stable in a striped region of the (μ, ν) -plane in Fig. 17. In a cross-striped region, both the in-phase and the anti-phase

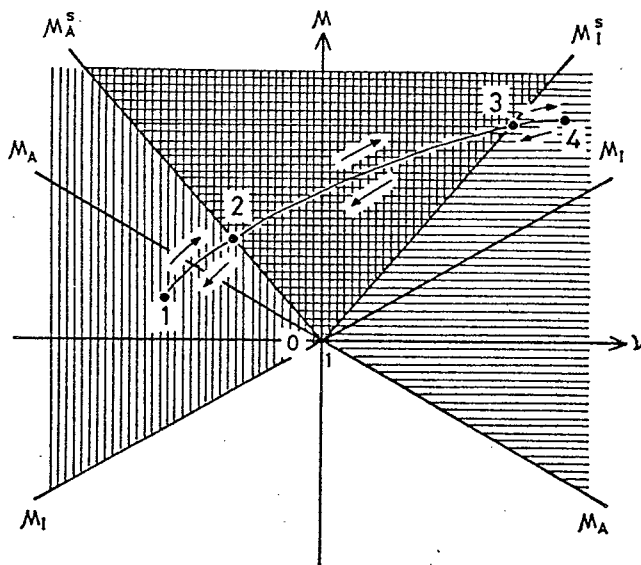


FIG. 17. Partition of the parameter plane (μ, ν) according to asymptotic behavior of the system (10).

solutions are stable. In a laterally striped region, only the anti-phase solution is stable. There exists no periodic solution in a white region. In order to explain the hysteresis phenomena, let us change parameter values (μ, ν) along a solid curve in Fig. 17 in the sequence of $(1 \rightarrow 2 \rightarrow 3 \rightarrow 4 \rightarrow 3 \rightarrow 2 \rightarrow 1)$. When the parameter values are on point 1, the phase difference between the two oscillators is 0° . The phase difference remains to be 0° until the parameter values reach point 3. At point 3, the phase difference changes dramatically to 180° . The phase difference 180° is preserved until the parameter point reaches point 2 again. Then a drastic change of the phase difference from 180° to 0° occurs. These are remarkable hysteresis phenomena. If, for example, point 1 corresponds to 1000 lux of the light intensity, point 2 corresponds to 100 lux, point 3 to 1 lux and point 4 to 0.01 lux, then the hysteresis phenomenon in Tupaia is fully explained. Note that ν must be a decreasing function of the light intensity but the increase of the light intensity does not necessarily imply increase or decrease of the μ -value. So, in our model, the light intensity in free-running conditions must effect the coupling between the two oscillators in order to cause splitting. Here, we assumed that the bifurcation of the Poincaré map is subcritical for simplicity of explanation.

The period of the uncoupled constituent oscillator τ^u , the period of the coupled oscillator system in the in-phase state τ_I^c and the period of the coupled oscillator system in the anti-phase state τ_A^c are given as follows:

$$\begin{aligned}
 \tau^u &= 2\pi, \\
 \tau_I^c &= 2\pi / \sqrt{1 - 2\nu\delta - \nu^2\delta^2 + 2a + b + ab}, \\
 \tau_A^c &= 2\pi / \sqrt{1 + 2\nu\delta - \nu^2\delta^2 - 2a - b + ab}.
 \end{aligned}
 \tag{2.13}$$

Since parameters δ , a , b and ν are positive, a and b are small and δ is very small, the following inequalities hold

$$\tau_A^c > \tau^u > \tau_I^c.$$

This is in agreement with the data in Tupaia but not with the data in hamster (Hoffman, 1971; Pittendrigh and Daan, 1976). The possible reasons for the disagreement with the hamster's data are our assumptions (i), (ii), (iv) and (v). Assumption (i) seems to be the most probable reason for the discrepancy. In other words, the two constituent oscillators of Tupaia may be nearly identical. In the study of the activity rhythms of cockroaches, Page (1978) uncoupled the two oscillators by surgical lesion and found that $\tau^u > \tau_I^c$. This is in agreement with our results.

Regarding the after-effect or the non-monotonic transients, one can explain them by the characteristic exponents of the stable in-phase solution. Since the phase space is four-dimensional, there are three characteristic exponents. One real exponent is almost the same as that of the limit cycle of the single uncoupled oscillator. So, the absolute value of one exponent is large and the stability in this direction is strong. But the absolute value of the real part of the other two exponents is small because the coupling is weak. When the environmental parameters are changed, a new stable in-phase periodic solution is formed instantaneously in a location different from that of an old solution. We expect the after effect since it takes many cycles (ie. the transient periods) for the state point to approach the new limit cycle because of the weak stability. One can assay a period of the circadian oscillator only by measuring the timing events which are controlled by the oscillator (e.g. emergence of fruit flies, onset of locomotor activity in rodents). We define an "event surface" in chapter 1. Generally, a stable manifold of the point where the event surface meets the limit cycle is

different from the event surface. So, an apparent period in the transient periods is different from the period of the new limit cycle. Sometimes, the event surface and the stable manifold meet each other several times (see Fig. 2). In this case the non-monotonic transient is observed.

Rössler (1976) found non-periodic oscillation ("chaos" or "turbulence") in a diffusion-coupled two-oscillator system. The general system (2.3) may have such solutions for some types of coupling. Pittendrigh and Daan (1976) found aperiodic activity pattern of a hamster in LL and explained it by asynchrony of a much larger number of constituent components than the two. But it can be explained also by the two-oscillator system which exhibits chaotic behavior.

Mutual excitation and lateral inhibition between neural oscillators were studied in our paper (Inui, Kawato and Suzuki, 1978) also.

CHAPTER 3

SYNERGISM AND ANTAGONISM OF NEURONS CAUSED BY AN ELECTRICAL SYNAPSE

3.1 Introduction

Electrical junctions are often found in the invertebrate nervous system (Kennedy and Davis, 1977). In the vertebrate nervous system, electrical synapses exist between fish motor neurons, pacemaker cells in the heart, inferior olive neurons and so on (Bennett, 1977; Llinas et al., 1974). Though there are many electrical junctions in the nervous system, they have attracted much less attention than chemical junctions. One of the reasons is because electrical junctions are considered to bring coupled neurons in an equal state. Only these equalizing functions have been investigated theoretically (Torre, 1976). If electrical coupling has only these functions, it is improbable that it plays an important role in the delicate functioning of the nervous system.

Taking account of the passage of large molecules through a gap junction (Kanno and Loewenstein, 1966), we study a model system consisting of two neurons electrically coupled. We investigated the model system by the theory of Hopf bifurcation and numerical integration (Kawato, Sokabe and Suzuki, 1979). The general model system has two types of periodic solutions. One is the solution where two neurons oscillate in phase synchrony (in-phase solution). The other is where the two are excited 180° out of phase. Especially for two BVP-model neurons coupled by diffusion, numerical integration showed the simultaneous stability of the two alternative solutions for a specific set of parameters. Because the anti-phase solution is unstable when it bifurcates, there must be its secondary bifurcation. We study the stability change of the two solutions by the secondary bifurcation method (Bauer, Keller and Reiss, 1975). The necessary condition of parameters for

simultaneous stability of the two alternative solutions is obtained. Moreover, we ascertain that the secondary bifurcation of the anti-phase solution really occurs using a computer algorithm by Kawakami, Matsumura and Kobayashi (1978).

3. 2 A general model system consisting of two neurons electrically coupled
 In a simple model system, the role of electrical junctions in the nervous system is examined. The model system consists of two nearly identical neurons electrically coupled (see Fig. 18). We assume that each neuron discharges a train of impulses or bursts either spontaneously or under the stimulus of chemical synapses.

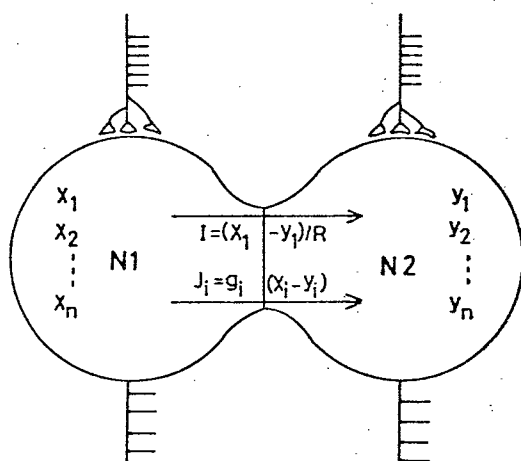


Fig.18A model system consisting of two electrically coupled, nearly identical, neurons, N1 and N2

We call the left neuron N1 and the right N2. If there is no electrical junction between two neurons, N1 and N2 discharge trains of impulses or bursts with different intervals. We want to investigate what effect electrical junction has on the time structure of impulses or bursts of two neurons. Especially, we deal with the case where the stimulus strength, such as the

magnitude of a stimulating electric current, is constant to the time. In such cases the time structure of the input impulses has no effect on that of the output of the neuron.

To describe the model system mathematically, let us examine electrical synapses first. It is known that not only an electric current but also chemical substances with 1000 molecular weight can pass through the junction of electrical synapses (gap junction) (Kanno and Loewenstein, 1966). For simplicity, we assume that the characteristics of both electric resistance and permeability for chemical substances of the gap junction are constant (i.e. independent of the inner states of neurons, such as membrane potential). Membrane potential of N1 is denoted by x_1 . Concentration of the i -th chemical substance in N1 is denoted by x_i ($i \geq 2$). Membrane potential and i -th concentration of N2 are denoted by y_1 and y_i respectively. R represents the electric resistance of the junction and g_i represents permeability of the i -th chemical substance through the gap junction. I and J_i stand for the magnitude of electric current, and the flow of the i -th chemical substance from N1 to N2 through the gap junction respectively. From the above discussion $I = (x_1 - y_1)/R$ and $J_i = g_i (x_i - y_i)$ hold.

Secondly, we express a single neuron mathematically. As the stimulus strength is constant, only the expression of a spike initiation zone is necessary. Like axons, the spike initiation zone may be described by the Hodgkin-Huxley equation (Hodgkin and Huxley, 1952) or by FitzHugh's BVP equation (FitzHugh, 1961). But here, we do not assume that the spike initiation zone is described by a peculiar equation. We assume that the dynamics of internal states (x_1, x_2, \dots, x_n) of a neuron is expressed by the following system of ordinary differential equations.

$$\frac{dx_i}{dt} = F_i(x_1, x_2, \dots, x_n, \mu), \quad i=1, 2, \dots, n$$

In vector notation this is

$$\frac{dx}{dt} = F(x, \mu). \quad (3.1)$$

Where $x = (x_1, x_2, \dots, x_n)$, and x_1 is membrane potential. $F(x, \mu)$ is a n -dimensional function. μ represents the stimulus strength, such as the magnitude of a stimulating electric current or the hormonal state of a neuron.

We use the suffix 1 for quantities of N1 and 2 for quantities of N2. x stands for internal states of N1 and y for that of N2. Consequently our model system is described by the following equation,

$$\begin{aligned} \frac{dx}{dt} &= F_1(x, \mu_1) + D^1(y-x) \\ \frac{dy}{dt} &= F_2(y, \mu_2) + D^2(x-y). \end{aligned} \quad (3.2)$$

Where D^1 and D^2 are $n \times n$ diagonal matrices and $D^j = \text{diag}(d_{11}^j, d_{22}^j, \dots, d_{nn}^j)$ ($j=1, 2$). The second term of the right-hand side of (3.2) represents the influence of an electric current and the diffusion flow of chemical substances on membrane potential and chemical concentration of neurons. Because two neurons are not completely identical, generally $d_{ii}^1 \neq d_{ii}^2$ ($i=1, \dots, n$). d_{ii}^j ($j=1, 2; i=1, 2, \dots, n$) is non-negative, but it may be 0 for $i \neq 1$. For example, if x_i and y_i represent quantities connected with channels of the membrane, then $d_{ii}^j = 0$ ($j=1, 2$). If the gap junction does not pass the i -th chemical substance, then $d_{ii}^j = 0$ ($j=1, 2$).

Now, we study (3.2) to examine relationship between the time structure of N1 and N2's discharges. When there is no electrical junction, N1 and N2 are excited with different intervals. We want to know the following. Are the discharge-periods of N1 and N2 synchronized by electrical junction? Are

they excited in phase synchrony, if discharge-periods are the same? What is the difference of phase between N1 and N2, if the two are excited asynchronously?

To investigate these matters, instead of examining (3.2) we only have to study the following system (3.3) where N1 and N2 are perfectly identical. This comes from structural stability of (3.3).

$$\begin{aligned} dx/dt &= F(x, \mu) + D(y-x) \\ dy/dt &= F(y, \mu) + D(x-y). \end{aligned} \tag{3.3}$$

We call (3.1) an individual system, (3.2) a model system, and (3.3) a coupled system hereafter. If (3.1) has a periodic solution $u(t)$, then (3.3) apparently has a periodic solution $(u(t), u(t))$ where N1 and N2 oscillate perfectly in phase. We call this solution a perfect in-phase solution. Regarding this, Torre proved that the stability of the solution $(u(t), u(t))$ of (3.3) is equivalent to the stability of some non-autonomous linear differential equations containing $u(t)$ explicitly, when $u(t)$ is a stable limit cycle of a 2-dimensional system (3.1) (Torre, 1975). He investigated the synchronization of electrically coupled pacemaker cells in the heart by the same method (Torre, 1976). But determination of stability of the nonautonomous system is difficult.

Neurons have a stable equilibrium state for small stimulus strength μ , and discharge trains of impulses or bursts for large μ . Taking account of this, we use the theory of Hopf bifurcation for the analysis of (3.1)-(3.3), especially for determination of the stability of the perfect in-phase solution of (3.3).

3.3 Stability of a perfect in-phase solution and the existence of an anti-phase solution

We assume that Hopf bifurcation occurs at the critical stimulus magnitude in the system of differential equations describing a neuron. It is known that the BVP equation and Hodgkin-Huxley equation have bifurcating periodic solutions according to the magnitude of an electric current as a bifurcation parameter (Hadelar et al., 1976; Hassard, 1978).

We assume that (3.1) satisfies assumptions of Hopf's theorem at $\mu=0$.

Let $u_\mu(t)$ denote the bifurcating solutions of (3.1). Then the following theorem can be proved.

Theorem 3.1. If the matrix $dF(0,0)-2D$ is stable, then bifurcation of perfect in-phase solutions $(u_\mu(t), u_\mu(t))$ takes place at $\mu=0$ for (3.3). If $u_\mu(t)$ is supercritical, $(u_\mu(t), u_\mu(t))$ is also supercritical. If $u_\mu(t)$ is subcritical, $(u_\mu(t), u_\mu(t))$ is subcritical.

Proof. By making a change of coordinates as $z=(x+y)/2$ and $w=(x-y)/2$, we get the following system,

$$\begin{aligned} dz/dt &= dF(0, \mu)z + G_1(z, w, \mu) \\ dw/dt &= (dF(0, \mu) - 2D)w + G_2(z, w, \mu). \end{aligned} \tag{3.3'}$$

Where, G_1 and G_2 contain only higher order terms than the second order.

(3.3'), accordingly (3.3) satisfies the conditions of the Hopf's theorem because of the assumption of the theorem, so periodic solutions bifurcate at $\mu=0$. Let $v_\mu(t)$ be this bifurcating solution of (3.3). Hopf's theorem asserts the existence of a neighborhood U of the origin in R^{2n+1} . Because

$(u_\mu(t), u_\mu(t), \mu) \subset U$ holds for small μ , $v_\mu(t)$ is $(u_\mu(t), u_\mu(t))$. (n-1) characteristic exponents of $v_\mu(t)$ coincide with (n-1) exponents of $u_\mu(t)$

and the rest n characteristic exponents of $v_\mu(t)$ are close to n eigenvalues of $(dF(0, \mu) - 2D)$ multiplied by a period of the solution. The part concerning the stability of $v_\mu(t)$ in the Theorem follows from this.

Corollary 3. 1. *On the same hypothesis of Theorem 3.1, a model system (3.2) has a stable in-phase periodic solution if the difference of two neurons is small and the bifurcation of (3.1) is supercritical.*

Proof. Small difference of two neurons implies the existence of small positive ϵ, δ such that

$$\begin{aligned} \left\| F_j(x, \mu_j) - F(x, \mu) \right\| < \epsilon \\ |D_j - D| < \delta \end{aligned} \quad (j=1,2)$$

hold for $F(x, \mu)$ and D in Theorem 3.1. Where $\| \cdot \|_1$ is a C^1 norm and $| \cdot |$ is a matrix norm. Because perfect in-phase solution of (3.3) is hyperbolic and stable from Theorem 3.1, it follows that (3.2) has a stable limit cycle near this perfect in-phase solution from the continuance of a periodic attractor under perturbation of vector fields (Hirsch and Smale, 1974). This means that N_1 and N_2 oscillate almost in phase synchrony.

Even when an electric current and flows of chemicals are different from diffusion, the existence of a phase synchronous periodic solution for the model system can be proved, as in Corollary 3.1, if the difference between the real flow and diffusion is small.

Another generalization of Theorem 3.1 is the following Corollary 3.2, concerning the system consisting of m same neurons coupled via diffusion. The proof of Corollary 3.2 is the same as that of Theorem 3.1, so is omitted.

Corollary 3. 2. *Let us consider a ring system consisting of the m same individual systems (3.1), coupled to two neighbors by diffusion, with a diffusion matrix D . If the bifurcation occurs supercritically at $\mu=0$ for the individual system (3.1) and the matrix $dF(0,0)-2D(1-\cos 2\pi j/m)$ is stable for each $j=1, \dots, m-1$, then the perfect synchronous solution, where all m systems oscillate synchronously, is stable.*

A similar result holds for the system consisting of many individual systems (3.1) which are arranged on the torus and are coupled to four neighboring systems by diffusion.

The variable z denotes the mean of states of N_1 and N_2 and w denotes difference in (3.3'). When the matrix $dF(0,\mu)$ corresponding to z loses its stability, the synchronous periodic solution appears. What happens when the matrix $dF(0,\mu)-2D$ corresponding to w loses its stability?

Proposition 3. 1. *If the two complex conjugate eigenvalues of $dF(0,\mu)-2D$ cross the imaginary axis at $\mu=\mu_C$ and the coupled system (3.3) satisfies the condition of Hopf's theorem, then the bifurcation of an anti-phase solution where N_1 and N_2 oscillate 180° out of phase takes place.*

Proof. As $\text{tr}(dF(0,0))=0$ and $\text{tr}D>0$, μ_C is positive. Bifurcation of the periodic solution takes place at $\mu=\mu_C$ for (3.3) from Hopf's theorem. Because N_1 is equal to N_2 , (3.3) has symmetry. From this symmetry and the uniqueness

of the bifurcating periodic solution for each μ , the bifurcating solution is either an in-phase solution or a 180° out of phase solution. As an invariant manifold which contains bifurcating solutions is tangent to the w -hyperplane, bifurcating solutions are not in-phase because of their continuity with respect to μ . Therefore, the bifurcating solution is anti-phase.

The anti-phase bifurcating solution is unstable for $\mu < \mu_c$ because $dF(0, \mu_c)$ is unstable, and the n characteristic exponents out of $(2n-1)$ are close to n eigenvalues of $dF(0, \mu_c)$ multiplied by a period of the solution. Being interested in the physiological phenomena, we want to know whether this anti-phase solution becomes stable at $\mu > \mu_c$. We also want to know the concrete conditions on the diffusion coefficients imposed by the assumption of Theorem 3.1 or Proposition 3.1. So, in the following section concrete analysis and computer simulation are carried out, with a single neuron being described by the BVP model.

3. 4 Two BVP model neurons coupled by diffusion

We use FitzHugh's BVP equation (1961) for a model of a single oscillator.

$$\begin{aligned} dx/dt &= C(y+x-x^3/3+I), \\ dy/dt &= -(x-A+By)/C, \end{aligned} \tag{3.4}$$

$$0 < B < 1, \quad C > 0, \quad B < C^2, \quad 1 - 2B/3 < A < 1,$$

where x is the minus quantity of membrane potential, y is the quantity of refractoriness and I is magnitude of a stimulating current. System (3.4) has an unique equilibrium point for all I . This equilibrium point is unstable for

$I_- < I < I_+$, where $I_{\pm} = -A/B \pm \sqrt{1 - B/C^2 \{1/B - 2/3 - B/(3C^2)\}}$. As Hadeler et al. showed (1976), system (3.4) has a stable limit cycle for some range of I . It corresponds to the repeated excitation of the neuron. The limit cycle bifurcates from the equilibrium point at $I = I_+$. The bifurcation is supercritical or subcritical for $C^2(2B-1) - B^2 < 0$ or > 0 respectively. Although the method of Hopf bifurcation tells us about the periodic solutions only for $I \sim I_+$, we can get the bifurcation diagrams in Fig. 19 by combining Hopf bifurcation results and Poincare-Bendixon's theorem with computer simulation.

Let us consider the system of differential equations which describes the two electrically coupled neurons. For simplicity, we assume that the characteristics of both electric resistance and permeability for chemical substances of the gap junction are constant. Let D denote the conductance of the electrical junction and θD denote the permeability of the junction for the quantity of refractoriness. For identical two neurons we get the following equation.

$$\begin{aligned}
 dx_1/dt &= C(y_1 + x_1 - x_1^3/3 + I) + D(x_2 - x_1) \\
 dy_1/dt &= -(x_1 - A + By_1)/C + \theta D(y_2 - y_1) \\
 dx_2/dt &= C(y_2 + x_2 - x_2^3/3 + I) + D(x_1 - x_2) \\
 dy_2/dt &= -(x_2 - A + By_2)/C + \theta D(y_1 - y_2),
 \end{aligned}
 \tag{3.5}$$

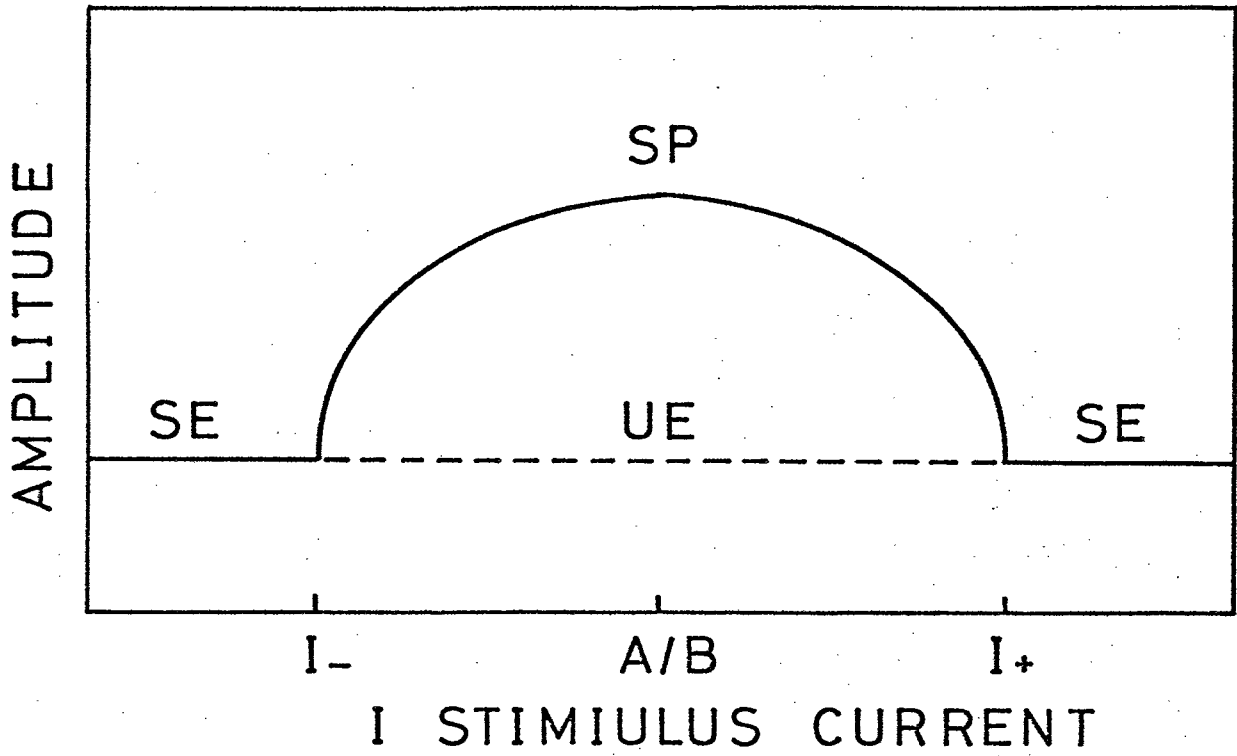
where quantities of the oscillator 1 are denoted by a suffix 1 and those of the oscillator 2 are denoted by a suffix 2.

3.5 Primary bifurcation

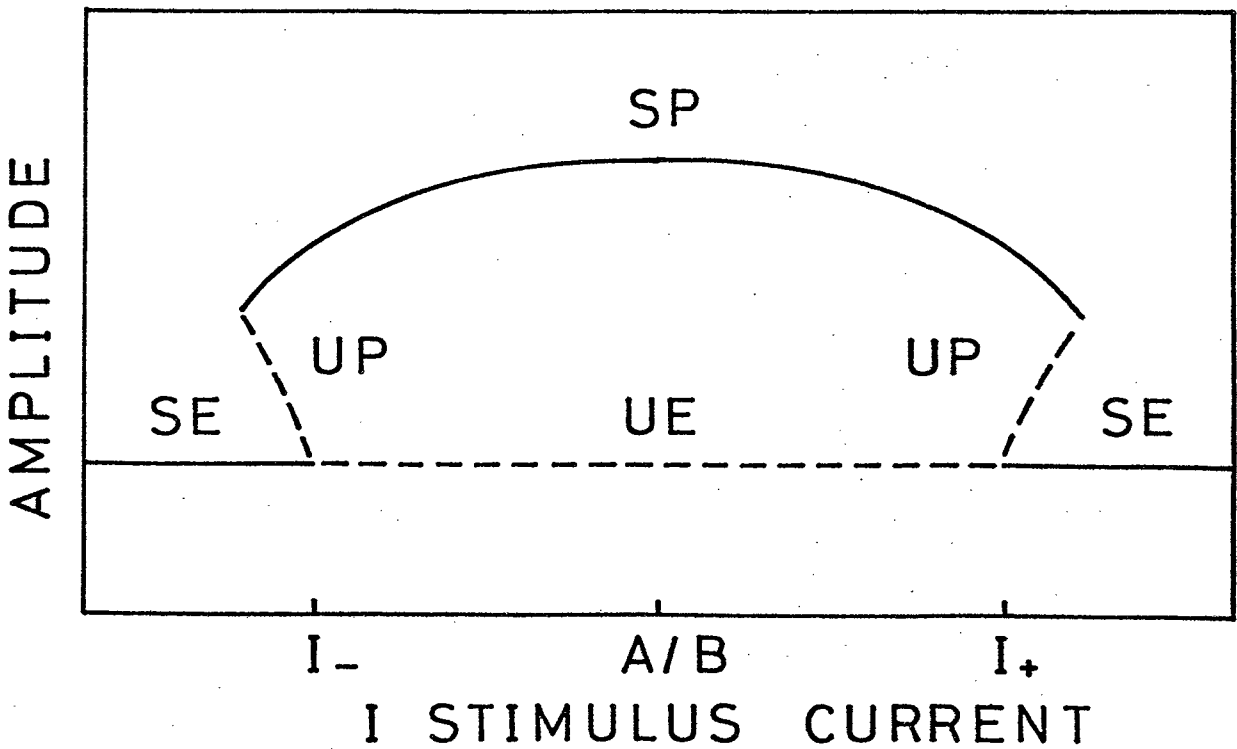
Let the unique equilibrium point of (3.4) depending on I be denoted by $(x_e(I),$

Fig. 19

a



b



$y_e(I)$). That is, the following holds.

$$y_e(I) = A/B - x_e(I)/B$$

$$x_e(I)^3/3 + (1/B-1)x_e(I) - A/B = I$$

Because B is less than 1, $x_e(I)$ is an increasing function of I . We define a bifurcation parameter μ as

$$\mu = 1 - B/C^2 - x_e(I)^2,$$

so that the equilibrium point becomes unstable at $\mu=0$. Because $x_e(-A/B)=0$, μ is an increasing function of I for $I < -A/B$ and a decreasing function for $I > -A/B$. For convenience of calculations, we make the following change of parameters

$$Ct = t',$$

$$B/C^2 = a,$$

$$1/C^2 = b,$$

$$0 < a < 1, \quad b > 0, \quad a < b$$

We denote t' by t again. We change the coordinates so that the origin is an equilibrium point.

$$\tilde{x}_1 = x_1 - x_e,$$

$$\tilde{y}_1 = y_1 - y_e,$$

$$\tilde{x}_2 = x_2 - x_e,$$

$$\tilde{y}_2 = y_2 - y_e.$$

In order to study the in-phase and anti-phase solutions which bifurcate from the equilibrium point, we make the following change of variables.

$$p = (\bar{x}_1 + \bar{x}_2)/2,$$

$$q = (\bar{y}_1 + \bar{y}_2)/2,$$

$$r = (\bar{x}_1 - \bar{x}_2)/2,$$

$$s = (\bar{y}_1 - \bar{y}_2)/2.$$

(p,q) is a mean of states of the two oscillators and (r,s) is their difference.

For convenience of calculations, we further transform (3.5) into a canonical form by the following change of variables.

$$\begin{pmatrix} x \\ y \\ z \\ w \end{pmatrix} = \begin{pmatrix} 1 & 0 & 0 \\ -a & \zeta & 0 \\ 0 & 0 & 1 \\ 0 & 0 & -(a+2\theta D) \end{pmatrix} \begin{pmatrix} 0 \\ 0 \\ 0 \\ \nu \end{pmatrix}^{-1} \begin{pmatrix} p \\ q \\ r \\ s \end{pmatrix},$$

where $\zeta = \sqrt{b-a^2},$

$$\nu = \sqrt{b-a^2 - 4a\theta D - 4\theta^2 D^2}.$$

In the new co-ordinates (3.5) becomes,

$$\frac{d}{dt} \begin{pmatrix} x \\ y \\ z \\ w \end{pmatrix} = \begin{pmatrix} \mu & \zeta & 0 \\ -\zeta + a\mu/\zeta & 0 & 0 \\ 0 & 0 & \mu - 2(1+\theta)D \\ 0 & 0 & -\nu + (a+2\theta D)\{\mu - 2(1+\theta)D\}/\nu \end{pmatrix} \begin{pmatrix} x \\ y \\ z \\ w \end{pmatrix}$$

$$-\sqrt{1-a-\mu} \begin{pmatrix} (x^2+z^2) \\ a(x^2+z^2)/\zeta \\ 2xz \\ 2(a+2\theta D)xz/\nu \end{pmatrix} -1/3 \begin{pmatrix} x(x^2+3z^2) \\ ax(x^2+3z^2)/\zeta \\ z(3x^2+z^2) \\ (a+2\theta D)z(3x^2+z^2)/\nu \end{pmatrix} . \quad (3.6)$$

(x,y) is the in-phase component and (z,w) is the anti-phase component of the system. The origin $(0,0,0,0)$ is an equilibrium point of (3.6). As we can see from the linear part of (3.6), the in-phase periodic solution of a frequency ζ bifurcates at $\mu_I = 0$ from the origin (see Marsden and McCracken, 1976). Let $W_2(\mu)$ denote the matrix

$$\begin{pmatrix} \mu - 2(1+\theta)D & \nu \\ -\nu + (a+2\theta D)\{\mu - 2(1+\theta)D\}/\nu & 0 \end{pmatrix} ,$$

which is the part of the linearized matrix for (3.6). The in-phase solution is stable near the bifurcation point if its bifurcation is supercritical and the matrix $W_2(0)$ is stable. For, its two characteristic exponents out of four are close to two eigenvalues of $W_2(0)$ multiplied by its period, $2\pi/\zeta$. The condition that $W_2(0)$ is stable is as follows.

$$4\theta D^2 - 2a\theta D + 2aD + b - a^2 > 0$$

Next, another periodic solution of a frequency ν bifurcates at $\mu_A = 2(1+\theta)D > 0$ from the origin. This is the anti-phase solution because of the symmetry of (3.6) and the uniqueness of the bifurcating periodic solution. The anti-phase solution is always unstable near its bifurcation point because its two characteristic exponents are close to two eigenvalues of

$$W_1(\mu) = \begin{pmatrix} \mu & \zeta \\ -\zeta + a\mu/\zeta & 0 \end{pmatrix},$$

multiplied by its period, $2\pi/\nu$. θ and D must satisfy following two conditions in order that the anti-phase soliton bifurcates.

$$\begin{aligned} \det W_1(\mu) > 0 & \quad \text{that is, } \theta D < (\sqrt{b-a})/2 \\ \mu_A < 1-a & \quad \text{that is, } (1+\theta)D < (1-a)/2. \end{aligned}$$

μ is less than $1-a$ from its definition. We want to know whether the in-phase solution becomes unstable as μ departs from $\mu_I = 0$ and whether the anti-phase solution becomes stable as μ departs from $\mu_A = 2(1+\theta)D$. We study this in the next section using the secondary bifurcation method. For this computation the two primary bifurcating solutions need to be expanded into the convergent analytical series.

For μ sufficiently close to zero, the in-phase solution $X_I(t)$ can be expanded as follows:

$$X_I(t) = \begin{pmatrix} x_I \\ y_I \\ z_I \\ w_I \end{pmatrix} = \epsilon X_I^0(t) + \epsilon^2 X_I^1(t) + \dots \quad (3.7a)$$

$$\mu = \epsilon \gamma_1 + \epsilon^2 \gamma_2 + \dots \quad (3.7b)$$

$$\omega_I - \zeta = \epsilon \omega_1 + \epsilon^2 \omega_2 + \dots \quad (3.7c)$$

X_I^k are $2\pi/\omega_I$ -periodic functions of t . The standard perturbation procedure up to the third order of ϵ determines the detailed expression for X_I as follows:

$$X_I^0 = \begin{pmatrix} \cos \omega_I t \\ -\sin \omega_I t \\ 0 \\ 0 \end{pmatrix}$$

$$X_I^1 = \begin{pmatrix} -a\sqrt{1-a}/(2\zeta^2) + a\sqrt{1-a}/(6\zeta^2) \cos 2\omega_I t - \sqrt{1-a}/(3\zeta) \sin 2\omega_I t \\ \sqrt{1-a}/(2\zeta) - \sqrt{1-a}/(6\zeta) \cos 2\omega_I t - a\sqrt{1-a}/(3\zeta^2) \sin 2\omega_I t \\ 0 \\ 0 \end{pmatrix} \quad (3.8a)$$

$$\gamma_1 = 0, \quad \gamma_2 = (1/2 - a(1-a)/\zeta^2)/2 \quad (3.8b)$$

$$\omega_1 = 0, \quad \omega_2 = (a-1)(\zeta^2 + a^2)/(6\zeta^3). \quad (3.8c)$$

Of course, the direction of the bifurcation is as same as that of the single BVP model.

The anti-phase solution can be expanded similarly by the following series.

$$X_A(t) = \begin{pmatrix} x_A \\ y_A \\ z_A \\ w_A \end{pmatrix} = \epsilon X_A^0(t) + \epsilon^2 X_A^1(t) + \dots \quad (3.9a)$$

$$\mu^{-2}(1+\theta)D = \epsilon \gamma_1 + \epsilon^2 \gamma_2 + \dots \quad (3.9b)$$

$$\omega_A^{-1} = \epsilon \omega_1 + \epsilon^2 \omega_2 + \dots \quad (3.9c)$$

$$X_A^0 = \begin{pmatrix} 0 \\ 0 \\ \cos \omega_A t \\ -\sin \omega_A t \end{pmatrix}, \quad X_A^1 = \begin{pmatrix} L+R \cos 2\omega_A t - I \sin 2\omega_A t \\ M+Q \cos 2\omega_A t - J \sin 2\omega_A t \\ 0 \\ 0 \end{pmatrix} \quad (3.10a)$$

$$L = \frac{a\kappa}{2(2a(1+\theta)D - \zeta^2)},$$

$$R = \frac{\kappa [a\{4v^2 - \zeta^2 + 2a(1+\theta)D\} + 8(1+\theta)v^2D]}{2[\{4v^2 - \zeta^2 + 2a(1+\theta)D\}^2 + 16(1+\theta)^2D^2v^2]},$$

$$I = \frac{\kappa [v\{4v^2 - \zeta^2 + 2a(1+\theta)D\} - 2a(1+\theta)Dv]}{\{4v^2 - \zeta^2 + 2a(1+\theta)D\}^2 + 16(1+\theta)^2D^2v^2},$$

$$\kappa = \sqrt{1 - a - 2(1+\theta)D}.$$

$$\gamma_1 = 0, \quad \gamma_2 = 1/4 + \kappa\{2L + R + (a + 2\theta D)I/2v\} \quad (3.10b)$$

$$\omega_1 = 0, \quad \omega_2 = -\kappa I\{2v^2 + (a + 2\theta D)^2\}/(4v^2) \quad (3.10c)$$

If γ_2 is positive, the bifurcation of the anti-phase solution is supercritical.

It is subcritical if $\gamma_2 < 0$. For small D , γ_2 is evaluated as follows.

$$\lim_{D \rightarrow 0} \gamma_2 = (3\zeta^2 - 8a(1-a))/(12\zeta^2).$$

Consequently for small D , we get the following conditions for parameters B , C regarding the direction of bifurcation.

$$\begin{aligned} C^2(8B-3) - 5B^2 &< 0 && \text{supercritical} \\ &> 0 && \text{subcritical} \end{aligned} \quad (3.11)$$

3.6 Computation of secondary bifurcation by perturbation method

In this section we develop an analytical approach to the stability changes of the in-phase and the anti-phase solutions in the limit where the conductance and the permeability of the gap junction are very low, that is D is very small. The basic idea of our approach is following the works of Bauer, Keller and Reiss (1975), Erneux and Herschkowitz-Kaufman (1979) and Kawato and Suzuki

(1980), to relate the problem of secondary stability changes to the coalescence of the two primary bifurcation points. In our problem, the way to relate $\mu_I=0$ and $\mu_A=2(1+\theta)D$ in a same bifurcation point is to take $D=0$. If there is an secondary bifurcation point, which is related to the multiple bifurcation point, on the in-phase or the anti-phase solution, this point also coalesces into the multiple bifurcation point as $D \rightarrow 0$. Consequently, if there exists such an secondary bifurcation point, it is on the primary bifurcation branch of small amplitude for small D . So we can use the series expansion in section 3.5 in order to make a variational system of (3.6) corresponding to the primary bifurcating solutions. When a real part of the characteristic exponent, which is obtained from the variational system, becomes zero, the secondary bifurcation occurs. The secondary bifurcation occurs at small amplitude ϵ_s for small D . Moreover, ϵ_s tends to zero as D tends to zero. Consequently we consider an eigenvalue problem in ϵ and solve it by a perturbation expansion in D . Hereafter we use s as the suffix which indicates the secondary bifurcation point.

3. 6. 1 Stability change of the in-phase solution

In this subsection we study the secondary bifurcation of the in-phase solution. In order to analyze the linear stability of the in-phase solution

$X_I=(x_I, y_I, z_I, w_I)$ we look for the solutions

$$\begin{aligned} \tilde{u}_k &= \exp(\xi_k \tau) u_k(\tau), & u_k(\tau) &= u_k(\tau + 2\pi), \\ \tau &= \omega_I t, & k &= 1, 2, 3, \end{aligned}$$

of the linearized equations of motion around the in-phase solution X_I :

$$\xi_k^u + \omega_k \partial u / \partial \tau = M u, \quad (3.12)$$

where M is an Jacobi matrix of (3.6) around X_I . A stability change of the in-phase solution can be expected to appear through the two complex-conjugate characteristic exponents. They become purely imaginary,

$$\xi_s, \bar{\xi}_s = \pm i\sigma \quad (\sigma \text{ real}) \text{ at } \mu = \mu_I^s.$$

μ_I^s is the secondary bifurcation point of the in-phase solution. We want to know if there exists some critical value of $\epsilon_s (\neq 0)$ where two of the characteristic exponents become purely imaginary. ϵ_s is related to μ by (3.7b). For some ϵ_s small we develop the following perturbation expansion for ϵ_s, ξ_s and u_s valid for D sufficiently small,

$$\epsilon_s = D^{1/2} \eta_1 + D \eta_2 + \dots \quad (3.13a)$$

$$\xi_s = i(\sigma_0 + D^{1/2} \sigma_1 + D \sigma_2 + \dots) \quad (3.13b)$$

$$u_s = u_0 + D^{1/2} u_1 + D u_2 + \dots \quad (3.13c)$$

Now, we introduce (3.13a) into (3.7b), (3.7c), (3.8b) and (3.8c) and develop ω_I^s, μ_I^s and X_I^s in powers of D .

$$\omega_I^s(D) = \zeta + D \omega_2 \eta_1^2 + O(D^{3/2}) \quad (3.13d)$$

$$\mu_I^s(D) = D \gamma_2 \eta_1^2 + O(D^{3/2}) \quad (3.13e)$$

$$X_I^s(D) = (D^{1/2} \eta_1 + D \eta_2) X_I^0 + D \eta_1^2 X_I^1 + O(D^{3/2}) \\ = D^{1/2} X_{I0}^s + D X_{I1}^s + O(D^{3/2}), \quad (3.13f)$$

where X_I^0 and X_I^1 are given in (3.8a). For simplicity of computation, M is

decomposed into powers of D. Here we use various relations such as

$$v = \zeta - 2\theta D / \zeta + O(D^2).$$

$$M = \begin{pmatrix} 0 & \zeta & 0 & 0 \\ -\zeta & 0 & 0 & 0 \\ 0 & 0 & 0 & \zeta \\ 0 & 0 & -\zeta & 0 \end{pmatrix} + \mu \begin{pmatrix} 1 & 0 & 0 & 0 \\ a/\zeta & 0 & 0 & 0 \\ 0 & 0 & 1 & 0 \\ 0 & 0 & a/\zeta & 0 \end{pmatrix}$$

$$+ D \begin{pmatrix} 0 & 0 & 0 & 0 \\ 0 & 0 & 0 & 0 \\ 0 & 0 & -2(1+\theta) & -2\theta/\zeta \\ 0 & 0 & -2a(1+\theta)/\zeta + 2\theta/\zeta & 0 \end{pmatrix}$$

$$+ \begin{pmatrix} -2\sqrt{1-ax_I} - (x_I^2 + z_I^2) & 0 & -2\sqrt{1-az_I} - 2x_I z_I & 0 \\ -2a\sqrt{1-a}/\zeta \cdot x_I - a/\zeta \cdot (x_I^2 + z_I^2) & 0 & -2a\sqrt{1-a}/\zeta \cdot z_I - 2ax_I z_I & 0 \\ -2\sqrt{1-az_I} - 2x_I z_I & 0 & -2\sqrt{1-ax_I} - (x_I^2 + z_I^2) & 0 \\ -2a\sqrt{1-a}/\zeta \cdot z_I - 2a/\zeta \cdot x_I z_I & 0 & -2a\sqrt{1-a}/\zeta \cdot x_I - a/\zeta \cdot (x_I^2 + z_I^2) & 0 \end{pmatrix}$$

$$+ O(D^2) + \mu O(D) + O(D) \cdot N_2(X_I)$$

$$= T + \mu T_1 + DL + N_1(X_I) + O(D^2) + \mu O(D) + O(D) N_2(X_I)$$

By inserting (3.13a)~(3.13f) into (3.12) and equating to zero the coefficients of each power of $D^{1/2}$, we obtain the following systems of equations to solve successively,

$$\zeta \partial u_0 / \partial \tau + i \sigma_0 u_0 - T u_0 = 0 \tag{3.14a}$$

$$\zeta \frac{\partial u_1}{\partial \tau} + i \sigma_{01} u_1 - \tau u_1 = -i \sigma_{10} u_1 + N_1(X^S, u) = f_1 \quad (3.14b)$$

$$\zeta \frac{\partial u_2}{\partial \tau} + i \sigma_{02} u_2 - \tau u_2 = -i \sigma_{11} u_1 - i \sigma_{20} u_2 - \omega_{21} \frac{\partial u_1}{\partial \tau} + \gamma_{21} \frac{\partial u_2}{\partial \tau} + \tau u_2 + L u_2 + N_2(X^S, u; X^S, u; X^S, u) = f_2 \quad (3.14c)$$

and in general

$$\zeta \frac{\partial u_n}{\partial \tau} + i \sigma_{0n} u_n - \tau u_n = f_n, \quad n=1,2, \dots \quad (3.14d)$$

The homogeneous system of equations (3.14a) admits two eigenfunctions associated with $\sigma_0 = 0$,

$$u_{01} = \begin{pmatrix} \cos \tau \\ -\sin \tau \\ 0 \\ 0 \end{pmatrix}, \quad u_{02} = \begin{pmatrix} 0 \\ 0 \\ \cos \tau \\ -\sin \tau \end{pmatrix}.$$

The general solution for u_0 of (3.14a) can be written as follows,

$$u_0 = \beta_1 u_{01} + \beta_2 u_{02}. \quad (3.15)$$

Either β_1 or β_2 is not zero. Because (3.14a) is a self-adjoint system, the two solutions of the adjoint system of (3.14a), u_1^* and u_2^* , are as same as u_{01} and u_{02} . The inhomogeneous system of equations (3.14b)~(3.14d) have solutions if and only if each f_n satisfies the following orthogonality conditions (non-resonance condition).

$$\int_0^{2\pi} d\tau (f_n \cdot u_j^*) = 0 \quad (j=1,2) \quad (3.16)$$

In general orthogonality conditions (3.16) will be satisfied only for particular values of the unknown parameters η_1 , σ_1 , σ_2 , β_1 and β_2 defined by (3.13a), (3.13b) and (3.15). At the first order in $D^{1/2}$, the orthogonality conditions of f_2 give

$$\sigma_1 \beta_1 = 0, \quad (3.17a)$$

$$\sigma_1 \beta_2 = 0. \quad (3.17b)$$

Since both β_1 and β_2 are not zero, we have

$$\sigma_1 = 0. \quad (3.18)$$

At the second-order in $D^{1/2}$, the orthogonality conditions of f_2 give:

$$\beta_1 \eta_1^2 G = 0, \quad (3.19a)$$

$$\beta_2 \{ \eta_1^2 G - (1+\theta) \} = 0, \quad (3.19b)$$

$$G = -1/4 + a(1-a)/(b-a^2) \quad (3.19c)$$

Since $0 < a < 1$ and $a^2 < b$, G is negative. Because both β_1 and β_2 are not zero, we have

$$\eta_1 = 0. \quad (3.20)$$

At the second-order of the perturbation scheme there are thus no secondary bifurcation points which may be related to a purely imaginary characteristic exponent.

3. 5. 2 Stability change of the anti-phase solution

A similar procedure is applicable to the stability change of the anti-phase solution. We use the exactly same notation as in the previous subsection without fear of confusion. We present only the results because the computation is quite similar. At the first order in $D^{1/2}$, the orthogonality conditions of f_1 give

$$\sigma_1 = 0. \quad (3.21)$$

At the second-order in $D^{1/2}$, the orthogonality conditions of f_2 give:

$$\beta_1 \{ H \eta_1^2 + (1+\theta) \} = 0, \quad (3.22a)$$

$$\beta_1 H \eta_1^2 = 0, \quad (3.22b)$$

$$H = \gamma_2 / 2 - 3/8 + a(1-a) / (2\zeta^2) - \sqrt{1-a(aI/2\zeta + L + R/2)}, \quad (3.22c)$$

where I , L and R are given in (3.10a). If H is positive, η_1 must be zero because either β_1 or β_2 is not zero. That is, at the second-order of the perturbation scheme there are no secondary bifurcation points on the anti-phase solution. If H is negative (3.22a) and (3.22b) yield,

$$\beta_1 \neq 0, \quad (3.23a)$$

$$\beta_2 = 0, \quad (3.23b)$$

$$\eta_1^2 = -(1+\theta)/H. \quad (3.23c)$$

That is, the secondary bifurcation occurs on the anti-phase solution at

$$\mu_A^S = D \{ \eta_1^2 \gamma_2 + 2(1+\theta) \} + O(D^{3/2}). \quad (3.24)$$

For infinitely small D, the sign of H is evaluated as follows.

$$\begin{array}{ll} C^2(5B-3)-2B^2 < 0; & H < 0 \\ & H > 0 \\ & > 0; \end{array}$$

3. 7 Bifurcation diagram of the coupled system

The coupled system (3.5) has six parameters A, B, C, I, θ and D. We got several conditions for parameter B, C by the primary and the secondary bifurcation analysis in the preceding sections. First, the direction of bifurcation for the in-phase solution is supercritical, if

$$C^2(2B-1)-B^2 < 0. \tag{3.25a}$$

Second, for small D the bifurcation of the anti-phase solution is supercritical when

$$C^2(8B-3)-5B^2 < 0. \tag{3.25b}$$

Third, for small D the secondary bifurcation occurs on the anti-phase solution if

$$C^2(5B-3)-2B^2 < 0. \tag{3.25c}$$

These three conditions divide (B,C)-plane into four regions I, II, III, IV according to the asymptotic behavior of (3.5) (see Fig. 20). For example, the bifurcation diagram of the system (3.5) for the parameters in region I is such as in Fig. 21 I, because the parameter region I satisfies the three

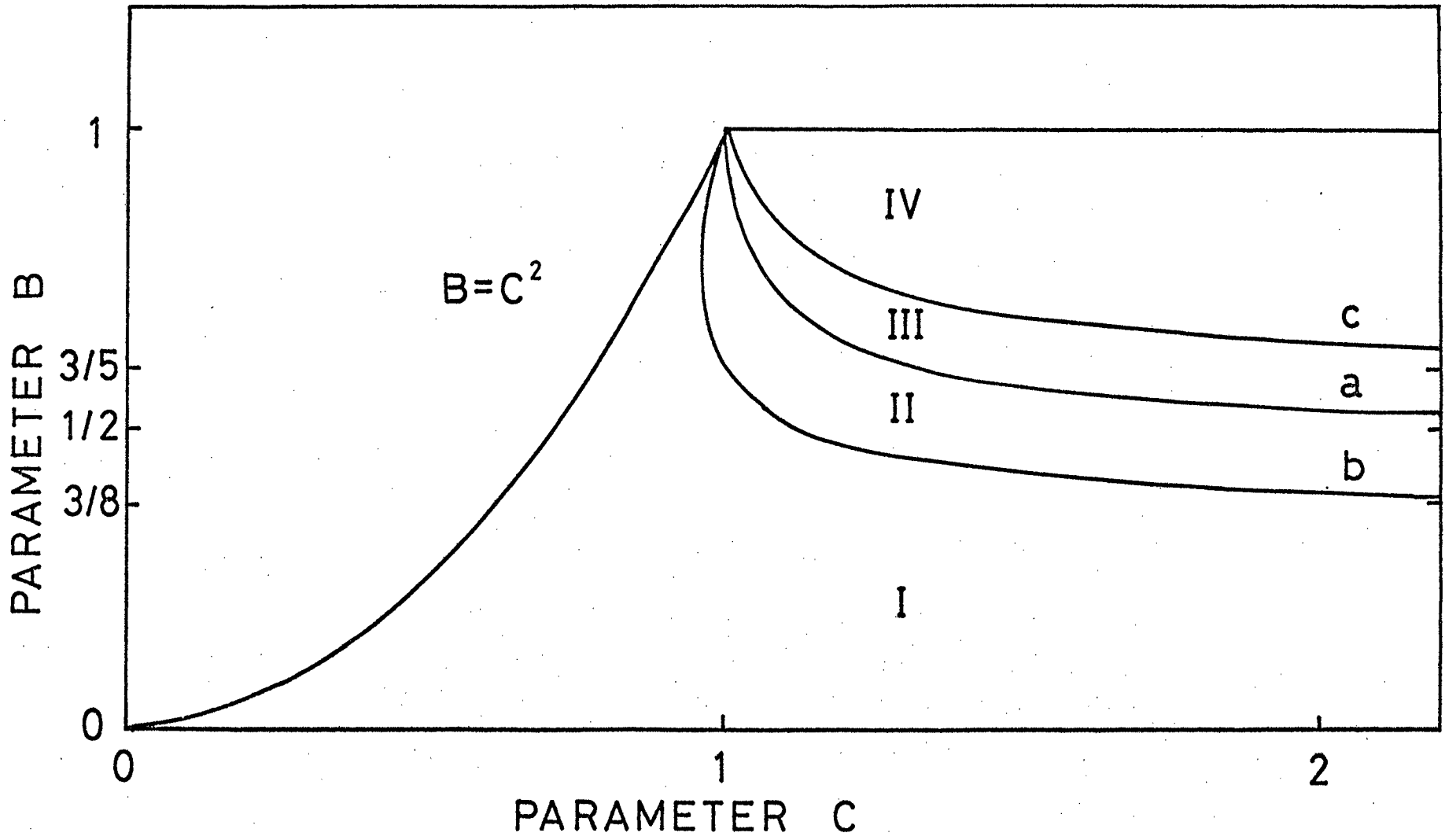


Fig. 20

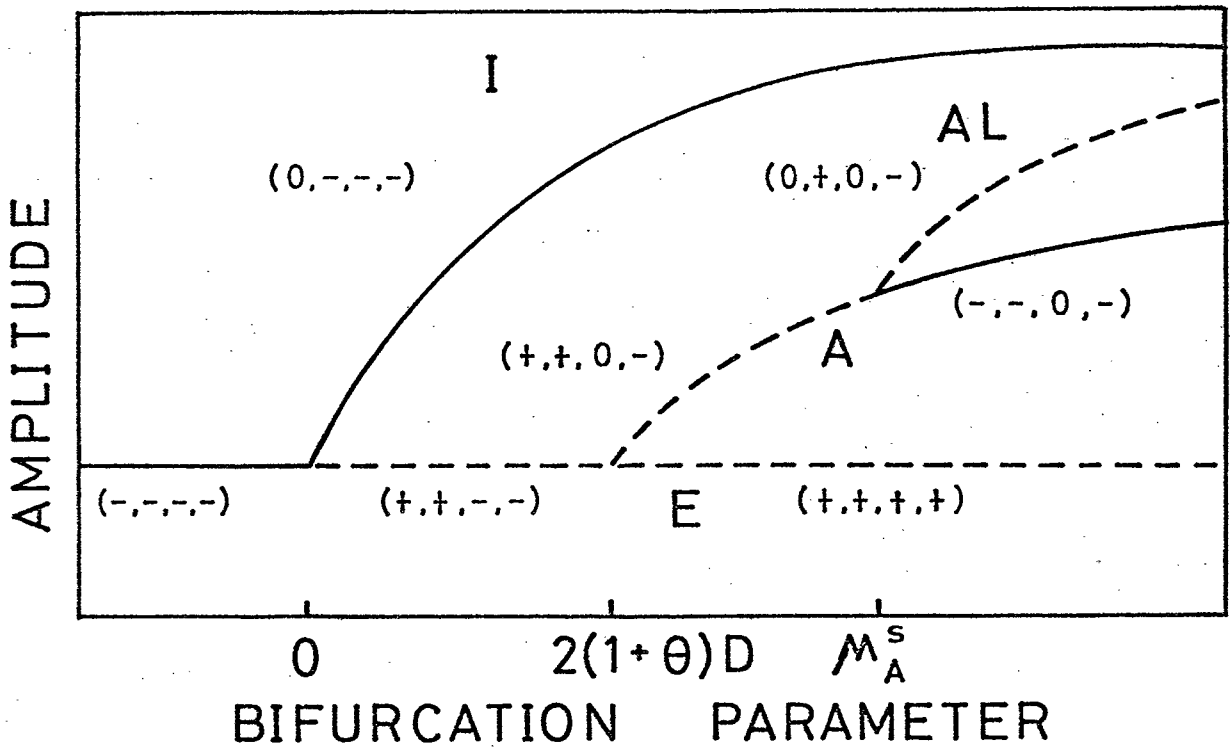
conditions (3.25a), (3.25b) and (3.25c). We attach four signs to various solutions in Fig. 21. If the solution is an equilibrium point, these are signs of real parts of four eigenvalues for a linearized system around the equilibrium point. If the solution is a periodic orbit, these are signs of real parts of four characteristic exponents associated with the periodic orbit. The solution which bifurcates secondarily from the anti-phase solution is an almost periodic solution (invariant torus). As (3.23a) in the preceding section shows, the almost periodic solution is the anti-phase solution plus the in-phase solution of small amplitude near the secondary bifurcation point. We must develop a perturbation procedure for the almost periodic solution around $\mu = \mu_A^S$ in order to know whether the almost periodic solution exists for $\mu < \mu_A^S$ and is stable (supercritical) or exists for $\mu > \mu_A^S$ and is unstable (subcritical). This is one of our future problems. However, Fig. 21 shows the subcritical case because we cannot find a stable almost periodic solution by computer simulation. In Fig. 21 II, III and IV the bifurcation diagrams of the in-phase and anti-phase solutions are bent. This implies that bifurcations of birth and death type occur. This is also a conjecture inferred from computer simulation.

3. 8 Discussions

The secondary bifurcation method in sections and 3.7 is valid only for small D . Although the results summarized in section 3.7 is independent of θ (the proportion of conductance to permeability of the gap junction), we have got a different result by numerical integration of (3.5) using an ordinary Runge-Kutta method. For only large θ the two alternative solutions seem to be stable at the same time (Kawato, Sokabe and Suzuki, 1979; see

Fig. 21 I & II

I



II

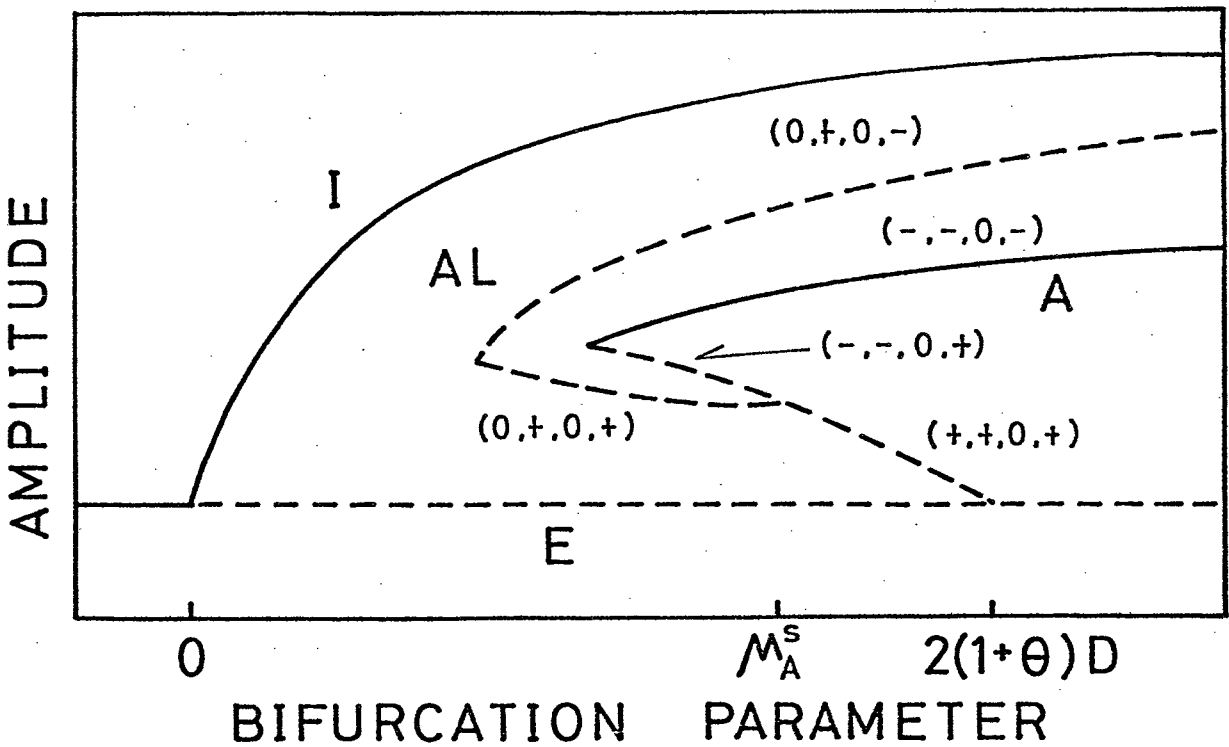
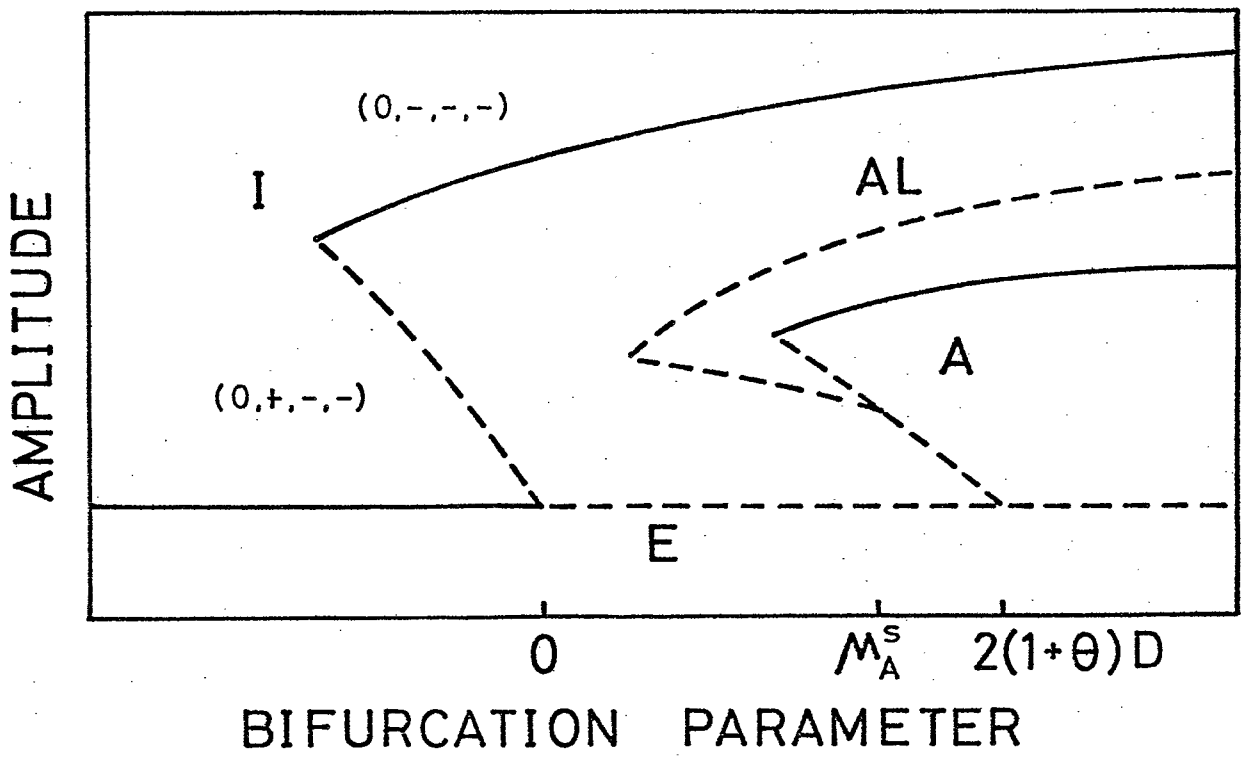
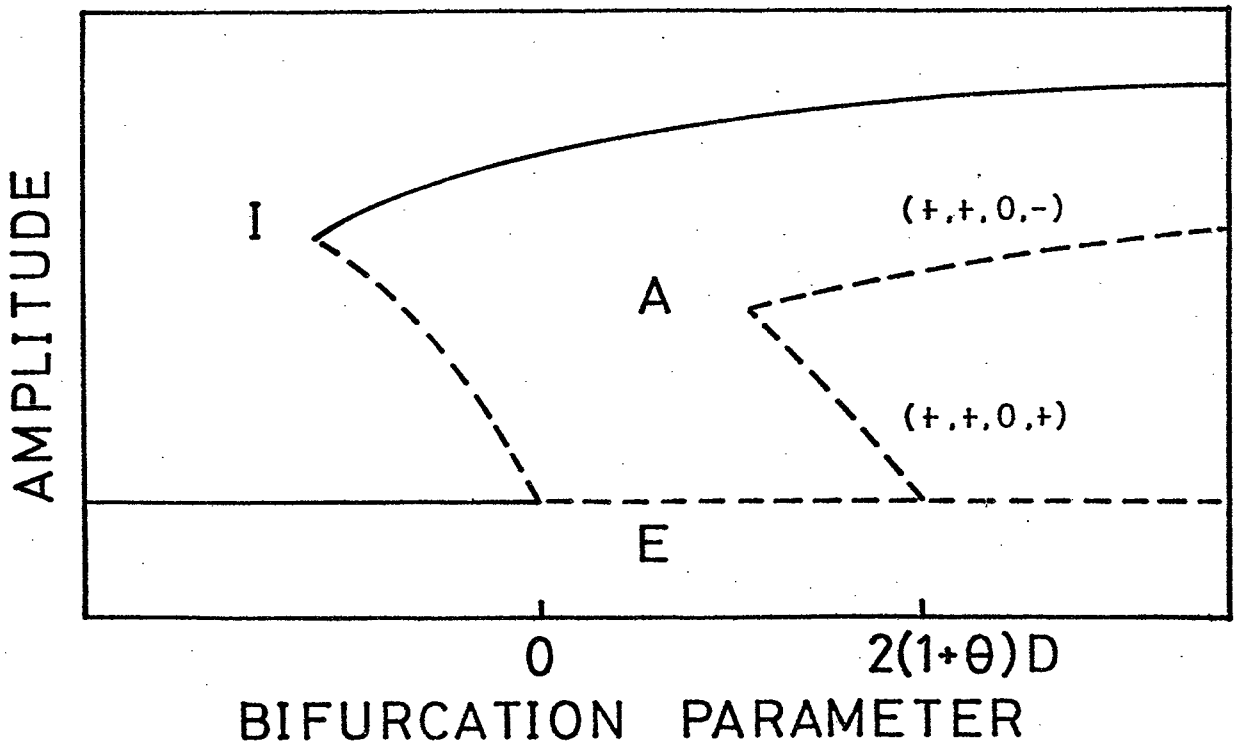


Fig. 21 III & IV

III



IV



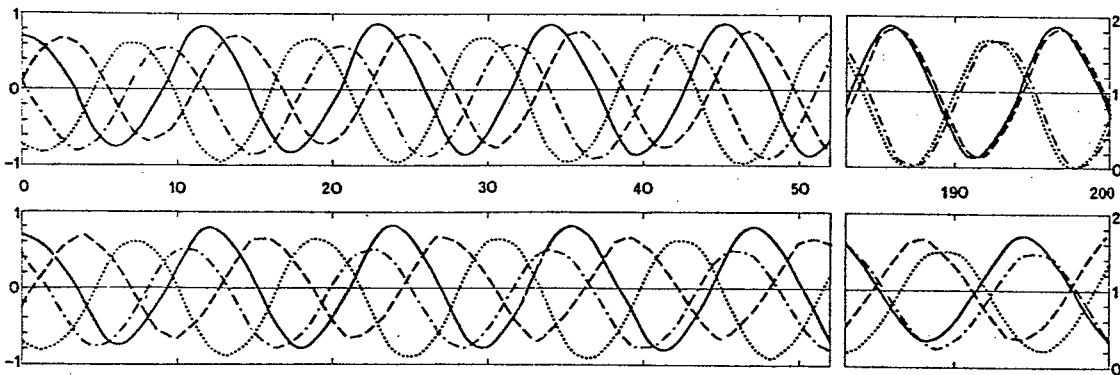


Fig. 22 Numerically integrated solutions of (5) which approach either the in-phase solution (upper) or the anti-phase solution (lower). A solid line, a broken line, a dotted line and an alternate long and short dash line are $x_1(t)$, $y_1(t)$, $x_2(t)$, and $y_2(t)$, respectively. The abscissa is the time. The left ordinate scales membrane potential (x_1, y_1) and the right ordinate scales refractoriness (x_2, y_2)

Fig. 22). However this is an ambiguous result because the numerical integration cannot determine the stability of the periodic solution rigorously. In order to compute a hyperbolic periodic solution numerically we need a new method. Kawakami, Matsumura and Kobayashi found an algorithm to obtain the hyperbolic periodic solutions on autonomous dynamical system (1978). The algorithm is a newton method to obtain a fixed point of a Poincaré map of the required periodic solution. Conveniently we can compute characteristic multipliers of the periodic solution by this algorithm at the same time. We examine the secondary bifurcation of the anti-phase solution using this algorithm. The computer calculation revealed the following results. First, the secondary bifurcation of the anti-phase solution really occurs. Fig. 23 is the bifurcation diagram of the anti-phase solution which is obtained for parameters $B=0.8$, $C=1.0$, $D=0.01$ and $\theta=3.0$. Fig. 24 shows the movement of three characteristic multipliers of the anti-phase solution with the change of the bifurcation parameter μ for the same set of parameters. When the two complex conjugate characteristic multipliers cross the unit circle at $\mu=0.17$,

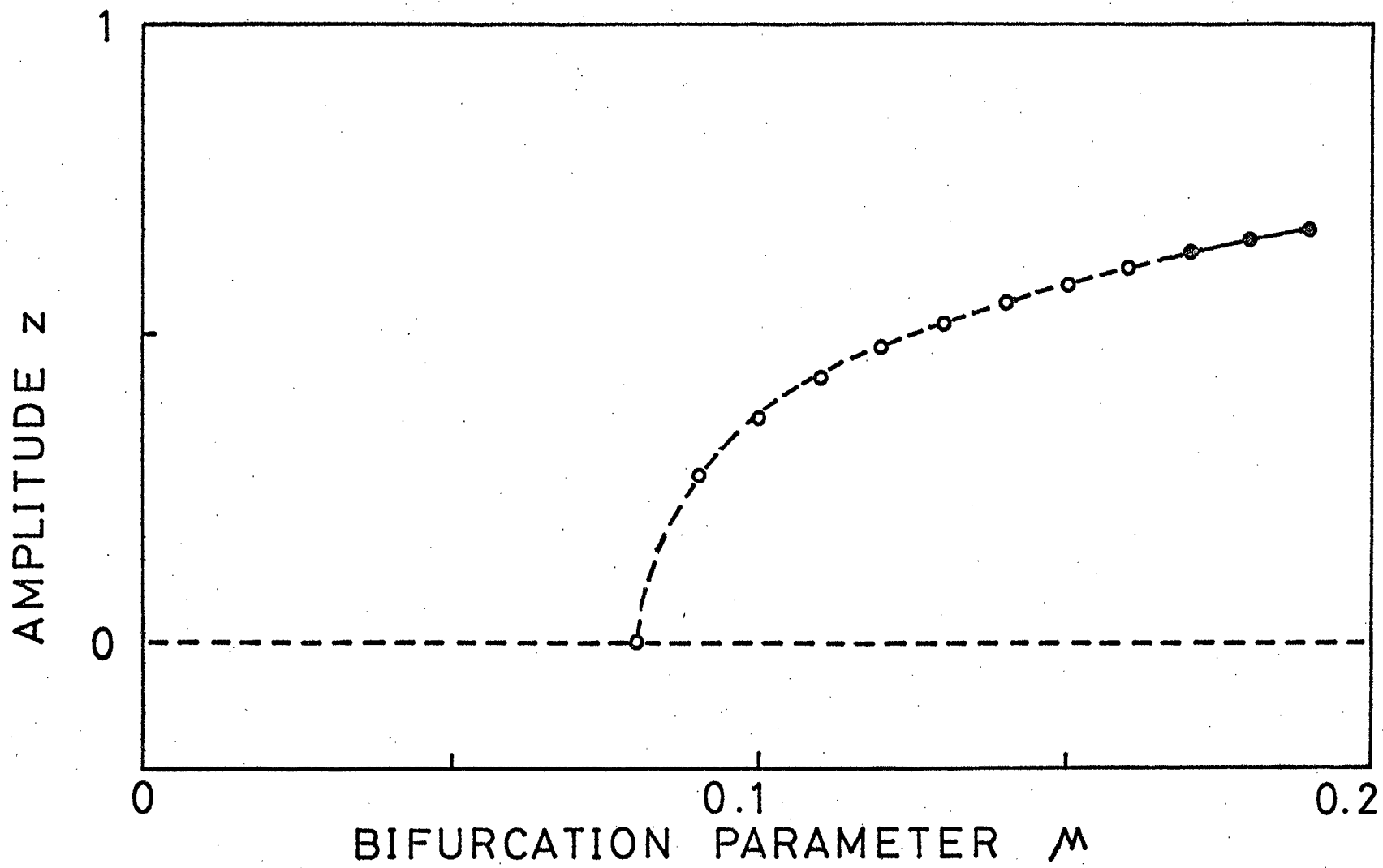


Fig. 23

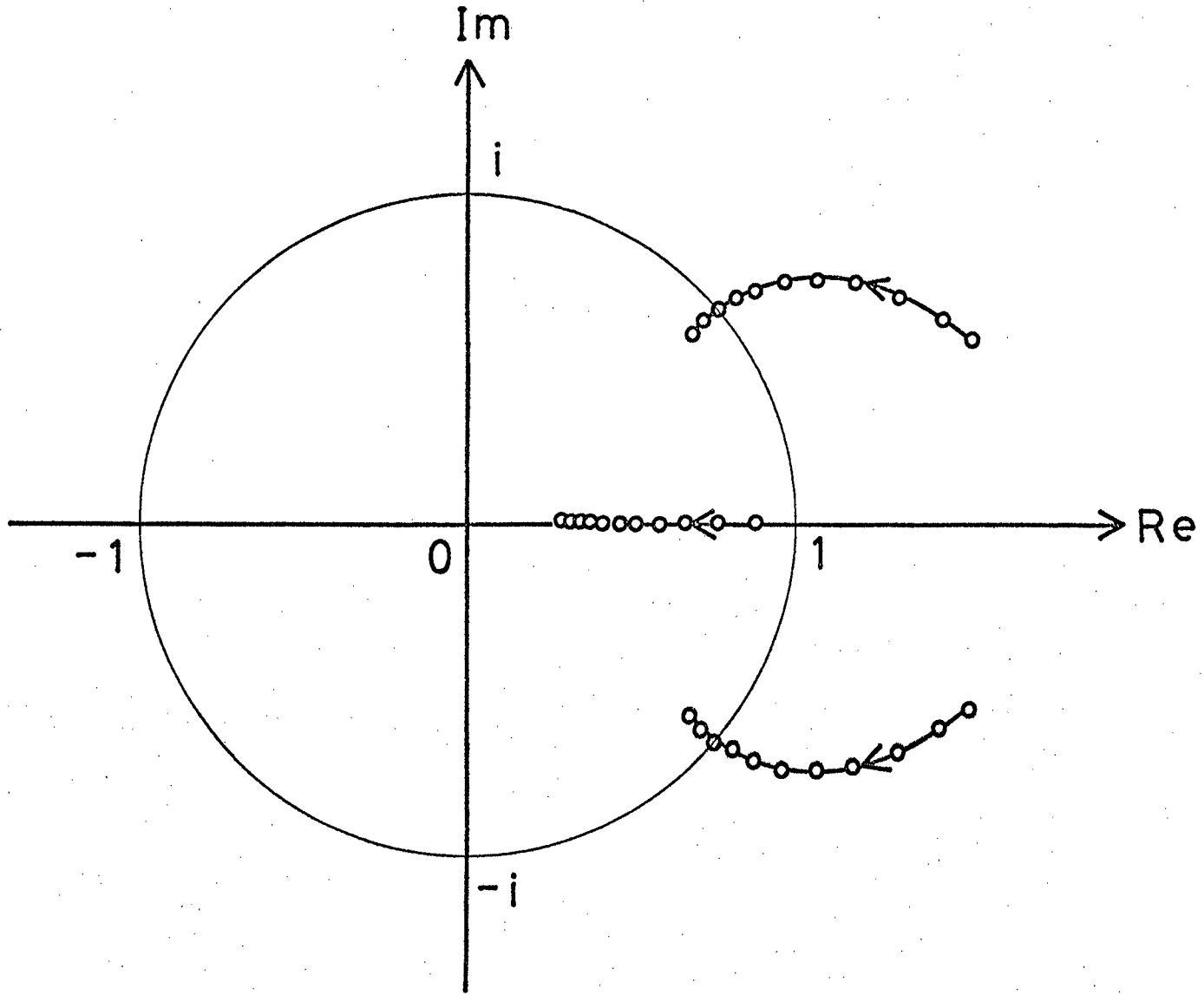


Fig. 24

the secondary bifurcation occurs. Second, the direction of bifurcation and whether the stability change occurs or not depend on D and θ . Table 1 summarizes the result of computer simulation. Although the parameter set ($B=0.8$, $C=1.0$) lies in the parameter region II (that is, γ_2 of the anti-phase solution is evaluated as negative for small D), γ_2 of (3.10b) is positive for $\theta > 1$. This effect of θ and D is not predicted by the analytical discussion. Similarly the stability change occurs for $\theta > 1$ but it does not occur for $\theta = 1$. In Fig. 25 we illustrate the movement of three characteristic multipliers for parameters $B=0.8$, $C=1.0$, $D=0.01$ and $\theta=1.0$ where there is other kind of secondary bifurcation point. As μ increases, the two complex conjugate characteristic multipliers collide with each other on the real axis and two real characteristic multipliers appear. One of them increases and the other decreases. When the smaller multiplier crosses the unit circle at $\mu=0.06$, the secondary bifurcation occurs on the anti-phase solution. However it does not imply the stability change of the anti-phase solution. Consequently, there are no secondary bifurcation points which are related to a purely imaginary characteristic exponent. In section 3.6 we assume that the stability change can be expected to appear through the two complex-conjugate characteristic exponents. However this assumption does not hold always.

Hitherto, we dealt with diffusion of refractoriness θD . The refractoriness of the BVP model correspond to $(n-h)$ of the Hodgkin Huxley equation (FitzHugh, 1961). n represents the activation of g_K and corresponds to relative refractoriness. $-h$ denotes the inactivation of g_{Na} and corresponds to absolute refractoriness. According to Hodgkin-Huxley's theory (1952), n and h are one of the parameters of the K channel and the Na channel respectively. So it is hardly probable that these quantities pass through the junctions of

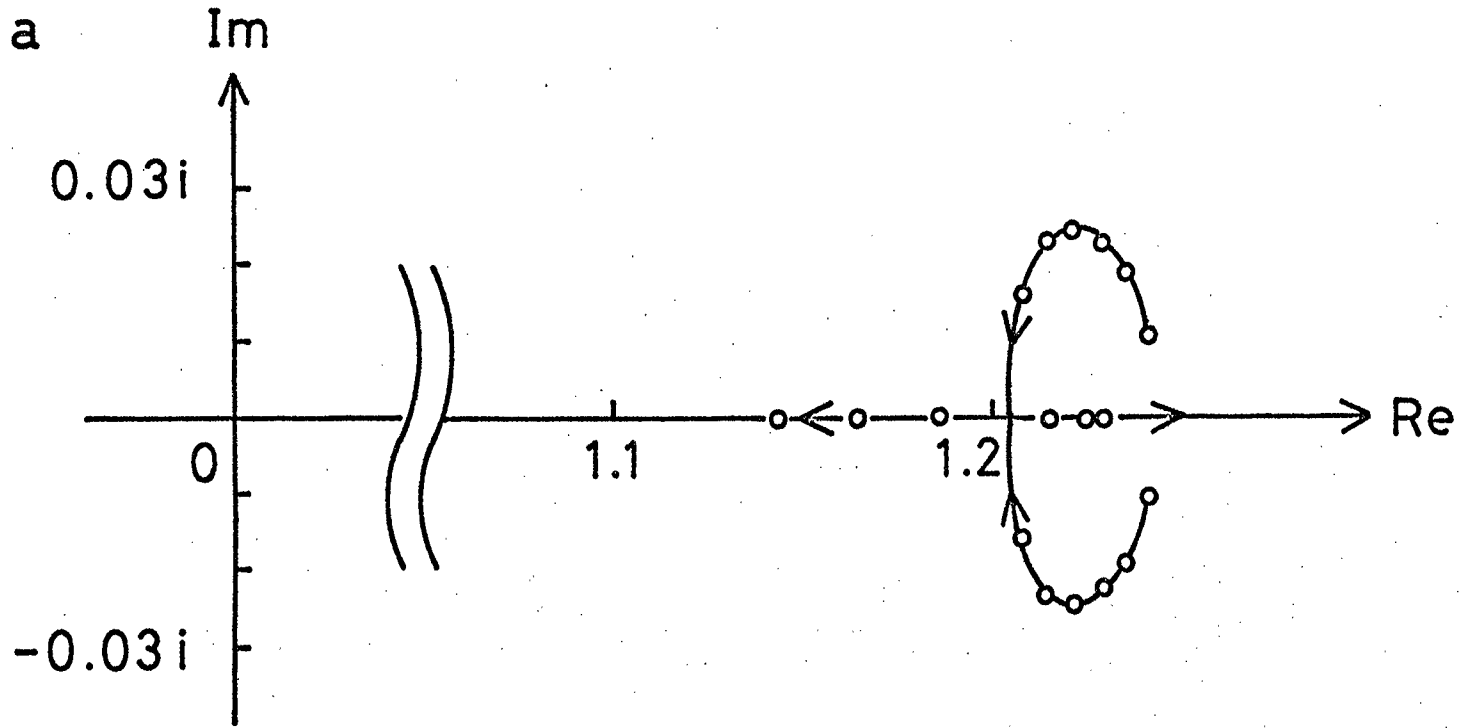


Fig. 25a

b

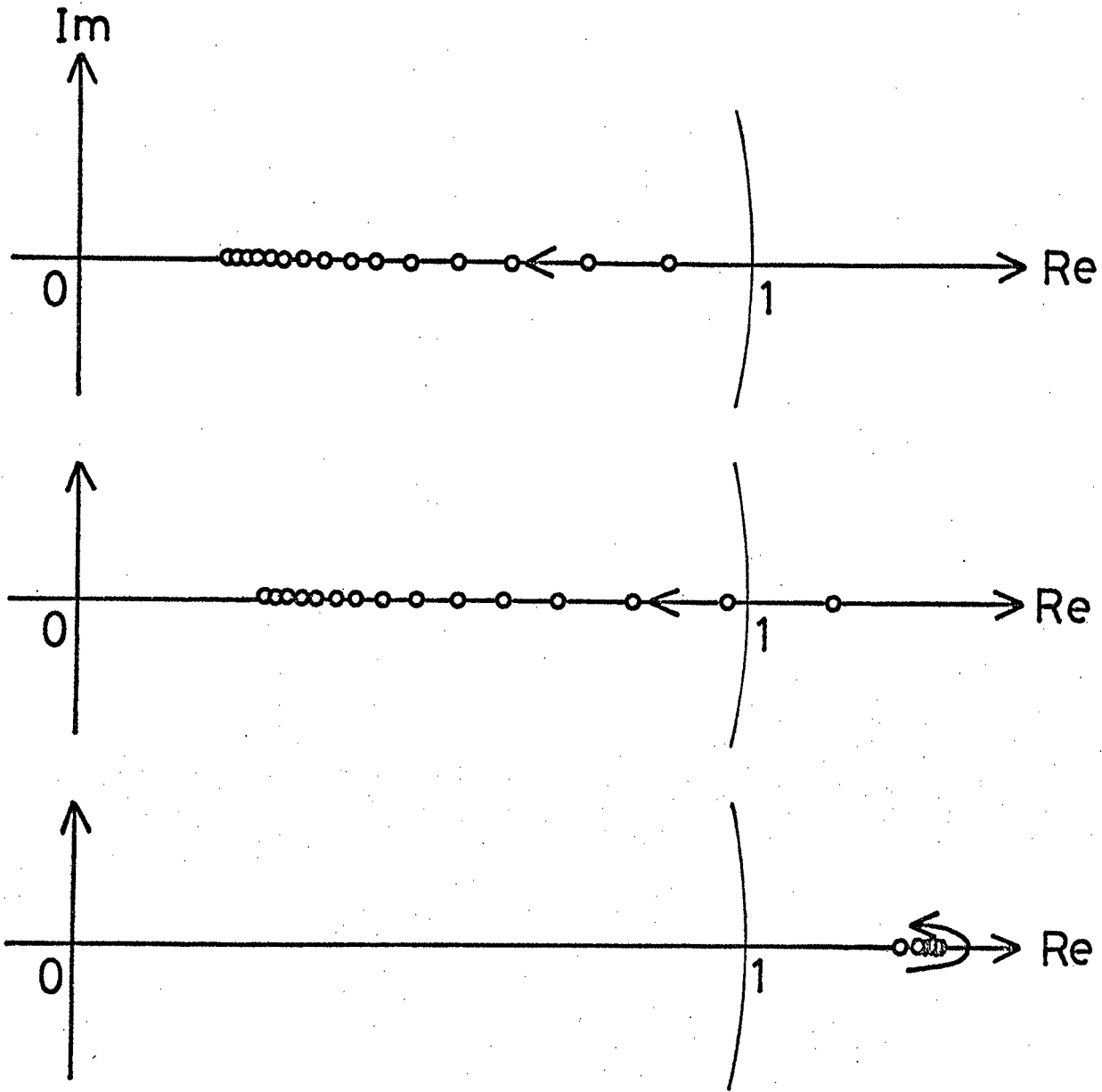


Fig. 25b

electrical synapses. It implies $\theta \sim 0$. Therefore, the computer simulation in this section reveals that the electrical synapses have only the role of synchronizations of action potentials in case of firing. An electrically coupled system of pacemaker neurons in the heart is an example of this case.

Next, let us examine the electrically coupled system of neurons with long excitation periods, such as burster neurons whose EPSP (or IPSP) undergoes the long period oscillation, or burster neurons whose Na-pumps are periodically activated. Generally excitation rhythms of long periods are determined by the dynamics of quantities with long time constants, such as chemical reactions or the activities of ion-pumps, rather than the quantities related to channels of the membrane. So, it is probable that the passage of chemical substance through the electric junctions plays an essential role in the electrically coupled neurons of long excitation periods. Because this implies that θ is not small, the electrically coupled system of burster neurons has a stable anti-phase periodic solution. That is, it is possible that electrical synapses play a role in antagonism of slow potentials.

Our model system is regarded as an endogenous pattern generating circuit which discharges periodic motor-control patterns. When θ (the proportion of conductance to permeability of the gap junction) is not small, the electrically coupled system can generate both the in-phase output pattern and the anti-phase pattern stably. This implies that one neural mechanism can generate two output patterns as Harmon (1964) and Suzuki et al. (1971) have found in a neural network consisting of reciprocally inhibiting neurons.

BIBLIOGRAPHY

- Ashkenazi, M., Othmer, H.G.: Spatial patterns in coupled biochemical oscillations. *J. Math. Biol.* 5, 305-350 (1978)
- Bauer, L., Keller, H.B., Reiss, E.L.: Multiple eigenvalues lead to secondary bifurcation. *SIAM Review* 17, 101-122 (1975)
- Bennett, M.V.L.: Electrical transmission. In *Handbook of physiology*, Vol. 1, pp. 357-416, Kandel, E.R., (ed.). Bethesda, Maryland: American Physiological Society 1977
- Daan, S., Berde, C.: Two coupled oscillators: Simulations of the circadian pacemaker in mammalian activity rhythms. *J. theor. Biol.* 70, 297-313 (1978)
- Ermentrout, G.B., Cowan, J.D.: Temporal oscillations in neuronal nets. *J. Math. Biol.* 7, 265-280 (1979)
- Erneux, T., Herschkowitz-Kaufman, M.: Bifurcation diagram of a model chemical reaction- I. Stability changes of time-periodic solutions. *Bull. Math. Biol.* 41, 21-38 (1979)
- FitzHugh, R.: Impulses and physiological states in theoretical models of nerve membrane. *Biophys. J.* 1, 445-466 (1961)
- Guckenheimer, J.: Isochrons and phaseless sets. *J. Math. Biol.* 1, 259-273 (1975)
- Hadeler, K.P., an der Heiden, U., Schumacher, K.: Generation of the nervous impulse and periodic oscillations. *Biol. Cybern.* 23, 211-218 (1976)
- Harmon, L.D.: Neuromimes; action of a reciprocally inhibiting pair. *Science* 146, 1323-1325 (1964)
- Harth, E., Lewis, N.S., Csermely, T.J.: The escape of tritonia: Dynamics of a neuromuscular control mechanism. *J. theor. Biol.* 55, 201-228 (1975)
- Hassard, B.: Bifurcation of periodic solutions of the Hodgkin-Huxley model for the squid giant axon. *J. theor. Biol.* 71, 401-420 (1978)
- Hirsch, M.W., Smale, S.: *Differential equations, dynamical systems, and linear algebra*. New York: Academic Press 1974
- Hodgkin, A.L., Huxley, A.F.: A quantitative description of membrane current and its application to conduction and excitation in nerve. *J. Physiol.* 117, 500-544 (1952)

- Hoffman, K.: Splitting of the circadian rhythm as a function of light intensity. In: *Biochronometry*, pp. 134-148. Menaker, M., (ed.). Washington, D.C.: Nat. Acad. Sciences 1971
- Hudson, D.J., Lickey, M.E.: Weak negative coupling between the eyes of *Aplysia*. In: *Society for Neuroscience Abstracts Vol. III* pp. 179. Anaheim, 1977
- Ibuka, N., Kawamura, H.: Loss of circadian rhythm in sleep-wakefulness cycle in the rat by suprachiasmatic nucleus lesions. *Brain Research* 96, 76-81 (1975)
- Inouye, S.T. and Kawamura, H.: Persistence of circadian rhythmicity in a mammalian hypothalamic "island" containing suprachiasmatic nucleus. *Proc. natn. Acad. Sci. U.S.A.* 76, 5962-5966 (1979)
- Inui, T., Kawato, M., Suzuki, R.: The mechanism of mental scanning in foveal vision. *Biol. Cybern.* 30, 147-155 (1978)
- Kanno, Y., Loewenstein, W.R.: Cell-to-cell passage of large molecules. *Nature* 212, 629-630 (1966)
- Kaus, P.: Possible adaptive values of the resonant slave in biological clocks. *J. theor. Biol.* 61, 249-265 (1976)
- Kawakami, H., Matsumura, T., Kobayashi, K.: An algorithm to obtain the periodic solutions on autonomous systems. *Trans. IECE Japan* 61, 1051-1053 (1978)
- Kawato, M.: Transient and steady state phase response curves of limit cycle oscillators. *J. Math. Biol.* in press (1981a)
- Kawato, M.: Secondary bifurcation of electrotonically coupled two neurons. *J. Math. Biol.* to be submitted (1981b)
- Kawato, M., Sokabe, M., Suzuki, R.: Synergism and antagonism of neurons caused by an electrical synapse. *Biol. Cybern.* 34, 81-89 (1979)
- Kawato, M., Suzuki, R.: Biological oscillators can be stopped- Topological study of a phase response curve. *Biol. Cybern.* 30, 241-248 (1978)
- Kawato, M., Suzuki, R.: Two coupled neural oscillators as a model of the circadian pacemaker. *J. theor. Biol.* 86, 547-575 (1980)
- Kawato, M., Suzuki, R.: Analysis of entrainment of circadian oscillators by skeleton photoperiods using phase transition curves. *Biol. Cybern.* in press (1981)

- Kennedy, D., Davis, W.J.: Organization of invertebrate motor systems. In Handbook of physiology, Vol. 1, pp. 1023-1087. Kandel, E.R. (ed.). Bethesda, Maryland: American Physiological Society 1977
- Levinson, N.: Small periodic perturbations of an autonomous system with a stable orbit. *Annals Math.* 52, 727-738 (1950)
- Linkens, D.A.: The stability of entrainment conditions for RLC coupled Van der Pol oscillators used as a model for intestinal electrical rhythms. *Bull. Math. Biol.* 39, 359-372 (1977)
- Llinas, R., Baker, R., Sotelo, C.: Electrotonic coupling between neurons in cat inferior olive. *J. Neurophysiol.* 37, 560-571 (1974)
- Marsden, J.E., McCracken, M.: The Hopf bifurcation and its applications. New York: Springer-Verlag 1976
- Moore, R.Y., Eichler, V.B.: Loss of a circadian corticosterone rhythm following suprachiasmatic lesions in the rat. *Brain Res.* 42, 201-206 (1972)
- Nagumo, J., Arimoto, S., Yoshizawa, S.: An active pulse transmission line simulating nerve axon. *PIRE* 50, 2061-2067 (1962)
- Nishiitsutsuji-Uwo, J., Pittendrigh, C.S.: Central nervous system control of circadian rhythmicity in the cockroach. III. The optic lobes, locus of the driving oscillation? *Z. vergl. Physiol.* 58, 14-46 (1968)
- Nogawa, T., Katayama, K., Tabata, Y., Ohshio, T., Kawahara, T.: Proceedings of the 11th Int. Conf. on Med. & Biol. Eng., Ottawa
- Page, T.L.: Interactions between bilaterally paired components of the cockroach circadian system. *J. comp. Physiol.* 124, 225-236 (1978)
- Page, T.L., Caldarola, P.C., Pittendrigh, C.S.: Mutual entrainment of bilaterally distributed circadian pacemakers. *Proc. Natl. Acad. Sci. USA* 74, 1277-1281 (1977)
- Pavlidis, T.: Biological oscillators: Their mathematical analysis. New York and London: Academic Press 1973
- Pavlidis, T.: What do mathematical models tell us about circadian clocks? *Bull. Math. Biol.* 40, 625-635 (1978)

- Perkel, D.H., Schulman, J.H., Bullock, T.H., Moore, G.P., Segundo, J.P.: Pacemaker neurons: effects of regularly spaced synaptic input. *Science* 145, 61-63 (1964)
- Pinsker, H.M.: Aplysia bursting neurons as endogenous oscillators. I. Phase response curves for pulsed inhibitory synaptic input. *J. Neurophysiol.* 40, 527-543 (1977)
- Pittendrigh, C.S.: Circadian rhythms and the circadian organization of living systems. *Cold Spr. Harb. Symp. quant. Biol.* 25, 155-184 (1960)
- Pittendrigh, C.S.: On the mechanism of the entrainment of a circadian rhythm by light cycles. In *circadian clocks*. pp. 277-297 Aschoff, (ed.). 1965
- Pittendrigh, C.S.: Circadian oscillations in cells and the circadian organization of multicellular systems. In *The neurosciences: Third study program*. pp. 437-458 Schmitt, F.O., Worden, F.G. (eds.). Cambridge Mass.: MIT Press 1974
- Pittendrigh, C.S., Bruce, V.G.: An oscillator model for biological clocks. In *Rhythmic and synthetic processes in growth*. pp. 75-109 D. Rudnick (ed.). Princeton: Princeton Univ. Press 1957
- Pittendrigh, C.S., Bruce, V.G.: Daily rhythms as coupled oscillator systems and their relation to thermoperiodism and photoperiodism. In *Photoperiodism and related phenomena in plants and animals*. pp. 475-505 Washington: A.A.A.S. 1959
- Pittendrigh, C.S., Bruce, V., Kaus, P.: On the significance of transients in daily rhythms. *Proc. nat. Acad. Sci.* 44, 965-973 (1958)
- Pittendrigh, C.S., Daan, S.: V. Pacemaker structure: A clock for all seasons. *J. comp. Physiol.* 106, 333-355 (1976)
- Pittendrigh, C.S., Minis, D.H.: The entrainment of circadian oscillations by light and their role as photoperiodic clocks. *The American Naturalist* 98, 261-294 (1964)
- Rosen, R.: Some comments on the physico-chemical description of biological activity. *J. theor. Biol.* 18, 380-386 (1968)
- Rosen, R.: *Dynamical system theory in biology. Vol. 1 Stability and its applications*. New York: John Wiley & Sons 1970

- Rössler, O.E.:Chemical turbulence:Chaos in a simple reaction-diffusion system. *Z. Naturforsch.* 31a, 1168-1172 (1976)
- Ruelle, D.:Some comments on chemical oscillations. *Trans. N. Y. Acad. Sci.* 70, 66-71 (1973)
- Stein, P.S.G.:Neural control of interappendage phase during locomotion. *Amer. Zool.* 14, 1003-1016 (1974)
- Suzuki, R., Katsuno, I., Matano, K.:Dynamics of "neron ring". *Kybernetik* 8, 39-45 (1971)
- Torre, V.:Synchronization of non-linear biochemical oscillators coupled by diffusion. *Biol. Cybern.* 17, 137-144 (1975)
- Torre, V.:A theory of synchronization of heart pace-maker cells. *J. theor. Biol.* 61, 55-71 (1976)
- Truman, J.W.:The role of the brain in the ecdysis rhythm of silkmoths:Comparison with the termination of diapause. In *Biochronometry*, pp. 483-504 Washington, D.C.: Nat. Acad. Sci. 1971
- Tyson, J., Kauffman, S.:Control of mitosis by a continuous biochemical oscillation: Synchronization; Spatially inhomogeneous oscillations. *J. Math. Biol.* 1, 289-310 (1975)
- Wilson, H.R., Cowan, J.D.:Excitatory and inhibitory interactions in localized populations of model neurons. *Biophys. J.* 12, 1-24 (1972)
- Winfree, A.T.:Biological rhythms and the behavior of populations of coupled oscillators. *J. theor. Biol.* 16, 15-42 (1967)
- Winfree, A.T.:Integrated view of resetting a circadian clock. *J. theor. Biol.* 28, 327-374 (1970)
- Winfree, A.T.:The investigation of oscillatory processes by perturbation experiments. In *biological and biochemical oscillators*. pp. 461-501 Chance, B., Pye, E., Ghosh, A., Hess., B. (eds.). New York:Academic Press 1973a
- Winfree, A.T.:Resetting the amplitude of *Drosophila*'s circadian chronometer. *J. comp. Physiol.* 85, 105-140 (1973)
- Winfree, A.T.:Resetting biological clocks. *Physics Today* 28, 34-39 (1975)

Yamanishi, J., Kawato, M., Suzuki, R.: Studies on human finger tapping neural networks by phase transition curves. Biol. Cybern. 33, 199-208 (1979)

Yamanishi, J., Kawato, M., Suzuki, R.: Two coupled oscillators as a model for the coordinated finger tapping by both hands. Biol. Cybern. 37, 219-225 (1980)

